Universitat de Lleida

Determination of free metal ion concentrations with the speciation techniques agnes and DMT

Mireia Lao Martínez

DOCTORAL THESIS

DETERMINATION OF FREE METAL ION CONCENTRATIONS WITH THE SPECIATION TECHNIQUES AGNES AND DMT

Mireia Lao Martinez

Report presented to opt for the Doctorate degree by the University of Lleida
Doctorate program “Electroquímica. Ciencia y Tecnología”

Supervisors
Josep Galceran
Encarnació Companys

Lleida, June 2019

To the memory of

my beloved mother

Agraïments

Aquesta tesi és el resultat d'anys de treball i esforços que finalment es veuen recompensats i plasmats en aquests fulls. Durant aquest temps he viscut moments de tot tipus bons i dolents, però en cadascun d'ells m'he sentit sempre acompanyada per gent que van començar sent companys de feina i han acabat deixant una empremta en la meva vida.

Per començar, voldria agrair tant a la Universitat de Lleida com al Ministerio de Ciencia e Innovación per la concessió de la beca per a la Formació de Personal Investigador (FPI) a través de la qual ha estat possible la realització d'aquesta tesis doctoral.

Als Doctors Josep Galceran i Encarna Companys, els meus directors i les persones que m'han guiat al llarg d'aquesta aventura, per les seves aportacions acadèmiques, per la seva gran ajuda i paciència especialment en aquells moments més complicats i per la seva gran estima que tant he sentit en aquells moments on tot era realment difícil. Gràcies de tot cor.

Als Doctors Jaume Puy i José Salvador per la seva col·laboració i la seva ajuda que sempre han estat presents quan les he necessitat, contribuint a la gran formació que he pogut rebre.

Als membres del departament de Química Analítica de la Universitat de Barcelona (la Dra Àngela Dago, la Dra Núria Serrano, la Dra Cristina Ariño així com la resta del grup d'investigació) per les seves aportacions i coneixements que han culminat amb una col·laboració conjunta.

A la Doctora Liping Weng del Department of Soil Quality de la Universitat de Wageningen pels seus coneixements i ajuda en el treball amb la tècnica DMT.

A la resta de membres del grup pel seu suport i companyia en els diferents moments d'aquests anys que hem compartit junts: al Calin, la Sandrine, la Diana, el David, la Sara i el Ramiro, les persones amb les que he compartit més hores en el laboratori, gràcies per la vostra ajuda i les vostres paraules d'alè que tant m'han ajudat. A la Marjan, el Martin i l'Alexandra que tot i que ens vam conèixer en el meu últim any a Lleida els agrairé sempre el seu suport en tot moment. I a la resta de gent amb qui hem compartit grans moments que m'han ajudat a tirar endavant aquest projecte: la

Mayela, la Daniela, el Carlos, el Ferran, la Gemma, l'Albert, la Mireia, la Sílvia López, la Olalla, el Pau, l'Edinson, el Toni, l'Alexis, la Remei, la Silvia Galitó, la Montse, la Maria, a tots moltes gràcies.

A la meva família que sempre ha cregut i confiat en mi: als meus tres fills (l'Arnau, l'Oriol i l'Aleix) que són el motor de la meva vida i al seu pare l'Oriol que junts em donen les forces per tirar endavant. Així com el meu pare i germà per sempre estar al meu cantó.

I per últim, a la meva estimada mare, que tot i que ens va deixar abans de temps després de mesos de lluita, el seu exemple de força i superació i les últimes converses que vam poder compartir (i que guardaré per sempre a la meva memòria) són les que m'han donat les forces per poder arribar al final. Mare allà on siguis gràcies per haver-me ajudat a ser la dona que avui en dia sóc, sé que he tingut el millor exemple que la vida em podia donar.

A totes i tots moltes gràcies.

Summary

Since many years ago, heavy metals have been associated with contamination and potential toxicity. They can be found in the environment in different chemical forms, but the scientific community agrees that their toxic effects are usually dependent on the concentrations of their free form. So, proper techniques to quantify them are required. This thesis focuses on the determination of free metal concentrations in synthetic or natural samples using the analytical techniques AGNES (Absence of Gradients and Nernstian Equilibrium Stripping) and DMT (Donnan Membrane Technique).

In the first part of this work, a possible impact from electrodic adsorption on the electroanalytical technique AGNES has been evaluated through several systems with induced adsorption (Pb-Xylenol Orange, Cd- Polyacrilic Acid and Cd-Iodide among others). It has been confirmed that, when the special AGNES equilibrium situation at the end of the first stage is reached, the existence of other equilibria processes (such as adsorption) does not disturb the analytical signal in any of the AGNES variants. Also, for the assayed systems, the required time to reach the equilibrium state did not need to be extended.

In the second part, AGNES has been applied to study the system Zn-Glutathione, first in synthetic samples and later on in root extracts of *Hordeum Vulgare*, considering different complexation models. In the synthetic samples determination, it has been checked that the theoretical results of two of the models agree with AGNES determinations. With the root extracts, the experimentally determined free Zn concentration was much lower than the predicted one, suggesting the presence of other ligands (such as other phytochelatins) apart from Glutathione.

In the third part, the inorganic speciation in wine was studied with AGNES and with the non-electroanalytical technique DMT. Determinations of free metal ion concentrations in synthetic wine were consistent with the predicted ones, but the required time to reach equilibrium with DMT was longer. When working with real wine, it required even longer times. For free Zn concentration, DMT results, using K and Na as reference ions, (1.76 μmol L^{-1}) agreed with the corresponding ones using AGNES (1.7 μmol L^{-1}). The DMT technique has also be used to determine the metal concentrations of Fe, Mg and Ca.

Resum

Des de fa molts anys, els metalls pesants s'han associat amb la contaminació i la toxicitat. Els podem trobar en el medi sota diferents formes químiques, però la comunitat científica coincideix en què els efectes tòxics que provoquen bàsicament depenen de la seva concentració lliure. Per això és important disposar de les tècniques adequades per quantificar-los. Aquesta tesi està centrada en la determinació de la concentració de metall lliure en mostres sintètiques i naturals mitjançant les tècniques analítiques d'AGNES (Absence of Gradients and Nernstian Equilibrium Stripping) i DMT (Donnan Membrane Technique).

En la primera part d'aquest treball, s'ha estudiat el possible impacte en la tècnica electroanalítica AGNES degut a l'adsorció electròdica a través de diferents sistemes (Pb-taronja de xilenol, Cd- àcid poliacrílic i Cd-iodur entre d'altres). S'ha pogut confirmar que quan s'arriba a la situació especial d'equilibri d'AGNES al final de la primera etapa, l'existència d'altres processos d'equilibri (com l'adsorció) no afecta el senyal analític en cap de les variants d'AGNES. També, pels sistemes estudiats, els temps necessaris per arribar a l'estat d'equilibri no es veuen augmentats.

En la segona part, AGNES s'ha aplicat a l'estudi del sistema Zn-glutatió, primer en mostres sintètiques i després en extractes de l'arrel de la planta *Hordeum Vulgare*, considerant diferents models de complexació. En la determinació en mostres sintètiques, s'ha vist que els resultats teòrics de dos dels models coincideixen amb les determinacions d'AGNES. En el cas de les arrels, la concentració lliure de Zn determinada experimentalment ha estat bastant inferior que la predita teòricament, suggerint per tant la presència d'altres lligands (com altres fitoquelatines) apart del glutatió.

En la tercera part, s'ha estudiat la especiació inorgànica en el vi amb les tècniques AGNES i DMT. Les concentracions de metall lliure determinades en les mostres sintètiques de vi han sigut consistents amb les prediccions teòriques, però el temps necessari per arribar a l'equilibri DMT s'ha vist augmentat. En treballar amb les mostres de vi reals, aquest temps s'incrementa encara més. Pel que fa a la concentració lliure de Zn, els resultats obtinguts amb DMT, utilitzant K i Na com a ions de referència, (1.76 μmol L^{-1}) coincideixen amb els corresponents obtinguts amb AGNES (1.7 μmol L^{-1}). La tècnica DMT s'ha utilitzat també per determinar les concentracions de Fe, Mg i Ca.

Resumen

Desde hace años, los metales pesados se han asociado con la contaminación y la toxicidad. Los podemos encontrar en el medio bajo distintas formas químicas, pero la comunidad científica coincide en que los efectos tóxicos que provocan básicamente dependen de su concentración libre. Por ello es importante disponer de las técnicas adecuadas para cuantificarlos. Esta tesis está enfocada en la determinación de la concentración de metal libre en muestras sintéticas y naturales mediante las técnicas analíticas AGNES (Absence of Gradients and Nernstian Equilibrium Stripping) y DMT (Donnan Membrane Technique).

En la primera parte de este trabajo, se ha estudiado el posible impacto en la técnica electroanalítica AGNES debido a la adsorción electródica mediante diversos sistemas (Pb-naranja de xilenol, Cd-ácido poliacrílico y Cd-yoduro entre otros). Se ha confirmado que cuando se llega a la situación especial de equilibrio de AGNES al final de la primera etapa, la existencia de otros procesos de equilibrio (como la adsorción) no afecta a la señal analítica en ninguna de las variantes de AGNES. También para estos sistemas estudiados, el tiempo necesario para llegar al estado de equilibrio no se ve aumentado.

En la segunda parte, AGNES se aplica al estudio del sistema Zn-glutatión, primero en muestras sintéticas y después en extractos de la raíz de la planta *Hordeum Vulgare*, considerando diferentes modelos de complejación. En la determinación en muestras sintéticas, se ha visto que los resultados teóricos de dos de los modelos coinciden con las determinaciones de AGNES. En el caso de las raíces, la concentración libre de Zn determinada experimentalmente ha sido bastante inferior a la predicha teóricamente, sugiriendo por tanto la presencia de otros ligandos (como otras fitoquelatinas) además del glutatión.

En la tercera parte, se ha estudiado la especiación inorgánica en el vino con las técnicas AGNES y DMT. Las concentraciones de metal libre determinadas en las muestras de vino sintético han sido consistentes con las predicciones teóricas, pero el tiempo necesario para alcanzar el equilibrio DMT se ve aumentado. Al trabajar con las muestras de vino real, este tiempo todavía se incrementa más. En relación a la concentración libre de Zn, los resultados obtenidos con DMT, utilizando K y Na como iones de referencia, (1.76 μmol L^{-1}) coinciden con los correspondientes obtenidos con AGNES (1.7 μmol L^{-1}). La técnica DMT también se ha utilizado para determinar las concentraciones de Fe, Mg y Ca.

Table of contents

Chapter 2. The impact of electrodic adsorption on Zn, Cd and Pb speciation measurements with AGNES

Chapter 3. Free Zn^{2+} determination in systems with Zn-Glutathione

Chapter 4. Speciation of Zn, Fe, Cd, and Mg in wine with the Donnan Membrane Technique

List of symbols and abbreviations

Latin Symbols

Symbol	Description	Unit
A	Electrode surface area	m^2
C	Complexing agent / Carrier	none
c^*_M	Bulk metal concentration	mol L^{-1}
$c^*_{M^0}$	Reduced metal concentration at the end of the first stage $t=t_1$	mol L^{-1}
$D_{M^{n+}}$	Diffusion coefficient of the specie M^{n+}	m^2 s^{-1}
D_{M^0}	Diffusion coefficient of the specie M^0	m^2 s^{-1}
${}_{EtOH}D_M$	Diffusion coefficient of the specie M in ethanolic medium	m^2 s^{-1}
${}_{w}D_M$	Diffusion coefficient of the specie M in aqueous medium	m^2 s^{-1}
D_m^{MC}	Diffusion coefficient of the metal-carrier complex in the membrane	m^2 s^{-1}
D_{so}^{X}	Diffusion coefficient of the specie X in the source solution	m^2 s^{-1}
ΔE	Potential jump / modulation amplitude	V
E	Potential	V
E_1	Deposition potential	V
$E_{1,a}$	Deposition potential in the first substage of AGNES 2P	V
$E_{1,b}$	Deposition potential in the second substage of AGNES 2P	V
E_2	Stripping potential	V
$E^{0'}$	Formal potential of the redox couple	V
E_d	Deposition potential	V
E_{peak}	Peak potential corresponding to a DPP	V
E_p	Peak potential corresponding in a plot dt/dE vs E	V
$E_{peak}^{\mu\geq 0.01}$	Potential peak at an ionic strength ≥0.01 M	V
F	Faraday constant	C mol^{-1}
I	Current	A
I_b	Current of a blank experiment	A
I_{cap}	Capacitative current	A
I_{fna}	Faradaic current due to the non-analyte elements	A
$I_{faradaic}$	Faradaic current	A
I_s	Stripping current	A
I_{sb}	Shifted blank current	A
I_{Ox}	Current due to other oxidant components	A
${}_{EtOH}I_{peak}$	DPP peak height in ethanolic medium	A

${}_{w}I_{peak}$	DPP peak height in aqueous medium	A
K_p	Partition coefficient of the metal between the solution and the membrane	none
K_{ML}	Stability constant of species ML^{4-}	none
K_{MHL}	Stability constant of species MHL^{3-}	none
K_{MH_2L}	Stability constant of species MH_2L^{2-}	none
K^{H}_{MHL}	Stability constant of species MHL^{3-}	none
$K^{H}_{MH_2L}$	Stability constant of species MH_2L^{2-}	none
K_{M_2L}	Stability constant of species M_2L^{2-}	none
K_{M_2HL}	Stability constant of species M_2HL^{-}	none
$K^{H}_{M_2HL}$	Stability constant of specie M_2HL^{-}	none
ℓ	Membrane thickness	m
L	Ligand	none
M	Metal	none
$[M]^0$	Concentration of reduced metal	mol L^{-1}
$\left[M^{n+}\right]$	Bulk free metal concentration	mol L^{-1}
$\left[M^{z_M}\right]_A$	Concentration of the metal M present in the acceptor side	mol L^{-1}
$\left[M^{z_M}\right]_D$	Concentration of the metal M present in the donor side	mol L^{-1}
MC	Metal complexed with a complexing agent	none
ML	Complex	none
M^{n+} / M^{z+}	Free metal ion	none
MX-	Complexed metal on the membrane surface	none
n	number of exchanged electrons	none
Q_b	Charge of a blank experiment	C
$Q_{capacitive}$	Capacitive charge	C
$Q_{faradaic}$	Faradaic stripped charge	C
$\left[R^{z_R}\right]_A$	Concentration of the reference ion present in the acceptor side	mol L^{-1}
$\left[R^{z_R}\right]_D$	Concentration of the reference ion present in the donor side	mol L^{-1}
r	Radial co-ordinate	m
r_0	Radius of the spherical electrode	m
r_{NP}	Radius of the nanoparticle	m
R	Gas constant	J $K^{-1}mol^{-1}$
T	Temperature	K
t_1	Deposition time in AGNES 1P	s

$t_{1,a}$	Deposition time in the first substage of AGNES 2P	s
$t_{1,a,w}$	Deposition time in the first substage of AGNES 2P without stirring	s
$t_{1,b}$	Deposition time in the second subtage of AGNES 2P	s
t_2	Stripping time	s
t_{dep}	Deposition time	s
t_p	Pulse time	s
t_w	Waiting time	s
X	Ligand on the membrane surface	none
Y	Concentration gain	none
$Y_{1,a}$	Concentration gain in the first substage of AGNES 2P	none
$Y_{1,b}$	Concentration gain in the second substage of AGNES 2P	none
$Y_{1,sb}$	Shifted blank gain corresponding to the first stage of AGNES	none
$Y_{2,sb}$	Shifted blank gain corresponding to the second stage of AGNES	none
${}_{w}Y$	Concentration gain in aqueous medium	none
$\left[Zn^{2+}\right]_{NP}$	Free zinc concentration in equilibrium with nanoparticles	mol L^{-1}

Greek Symbols

γ	Activity coefficient	
γ_M	Activity coefficient of the metal M	
δ_{so}	Diffusion layer thickness in the source solution	m
δ_{st}	Diffusion layer thickness in the strip solution	m
η / η_I	Proportionality factor when taking intensity as analytical signal (AGNES-I)	A L mol^{-1}
η_Q	Proportionality factor when taking charge as analytical signal (AGNES-Q, AGNES-LSV, AGNES-SCP)	C L mol^{-1}
${}_{w}\eta$	Proportionality factor in aqueous medium	A L mol^{-1}
Π	Boltzmann factor	none
τ	Transition time	s

Abbreviations

AGNES	Absence of Gradients and Nernstian Equilibrium Stripping
AGNES 1P	AGNES one pulse
AGNES 2P	AGNES two pulses
AGNES-LSV	Variant of AGNES with LSV in the second stage
AGNES-Q	Variant of AGNES determining charge from stripping current at constant re-oxidation potential
AGNES-SCP	Variant of AGNES with SCP in the second stage
ASV	Anodic Stripping Voltammetry
ATR-FTIR	Attenuated Total Reflection–Fourier Transform Infra-Red
Bi-FE	Bismuth Film Electrode
BLM	Biotic Ligand Model
CLE-AdCSV	Competitive Ligand Exchange Cathodic Stripping Voltammetry
CSV	Cathodic Stripping Voltammetry
CTA	Cellulose triacetate
DGT	Diffusion Gradients in Thin-Films
DMT	Donnan Membrane Technique
DOM	Dissolved Organic Matter
DPP	Differential Pulse Polarography
DPASV	Differential Pulse Anodic Stripping Voltammetry
EDTA	Ethylenediaminetetraacetic Acid
EPPS	3-[4-(2-hidroxietil)piperazin-1-il]propane-1-sulfonic Acid
FIAM	Free Ion Activity Model
GSH	Glutathione
HA	Humic Acid
HER	Hydrogen Evolution Reaction
HMDE	Hanging Mercury Drop Electrode
HPLC	High-Performance Liquid Chromatography
ICP-MS	Inductively Coupled Plasma Mass Spectrometry
IET	Ion Exchange Technique
ISE	Ion Selective Electrode
KHTar	Potassium hydrogentartrate
LOD	Limit of Detection
LOQ	Limit of Quantification
LSASV	Linear Sweep Anodic Stripping Voltammetry
MCR-ALS	Multivariate curve resolution method by alternating least-squares
MES	2-(N-morpholino)ethanesulfonic acid
NP	Nanoparticles
NPP	Normal Pulse Polarography
PAA	Polyacrilic Acid
PIM	Permeation Inclusion Membrane technique
PLM	Permeation Liquid Membrane technique
PSA	Potentiometric Stripping Analysis

PSS	Poly Stirenesulfonate
PVC	Polyvinyl Chloride
RPP	Reverse Pulse Polarography
S	Metal ion complexant in the strip solution
SCP	Stripping Chronopotentiometry
SPE	Screen Printed Electrode
SWASV	Square Wave Anodic Stripping Voltammetry
TFA	Trifluoroacetic acid
TRIS	Tris(hydroxymethyl)aminomethane
VGME	Vibrated Gold Microwire Electrode
XO	Xylenol Orange

CHAPTER 1

Introduction

1.1 The relevance of heavy metals in the environment

Along the history, the term heavy metal has been related to a group of metals and semimetals that have been associated with contamination and potential toxicity or ecotoxicity (Duffus, 2002). In fact, several definitions can be found in the literature. For instance: i) in terms of density, they are defined as metals with density higher than 5 g cm^{-3}, ii) in terms of atomic weight, as a group of metals with a high atomic mass that are toxic and cannot be processed by living organisms, such as lead, mercury and cadmium (Duffus, 2002), etc.

Some of them (such as zinc, copper, iron, among others) are essential because they are involved in redox-processes, acting as components of various enzymes and regulating the osmotic pressure (Bruins et al., 2000). Others, such as silver, cadmium, gold, lead and mercury do not have a known biological role and, in fact, are potentially toxic to organisms. But both, essential and non essential metals (above a certain concentration threshold), can produce harmful consequences in human health as development retardation, several types of cancer and kidney damage.

Metals are found naturally in earth localised in soils, waters, rocks, sediments, etc., so humans come into contact with them through food, air and water. But they can also be introduced into nature from other non-natural sources such as mining activity, industry, agrochemical products, etc. (see Figure 1-1).

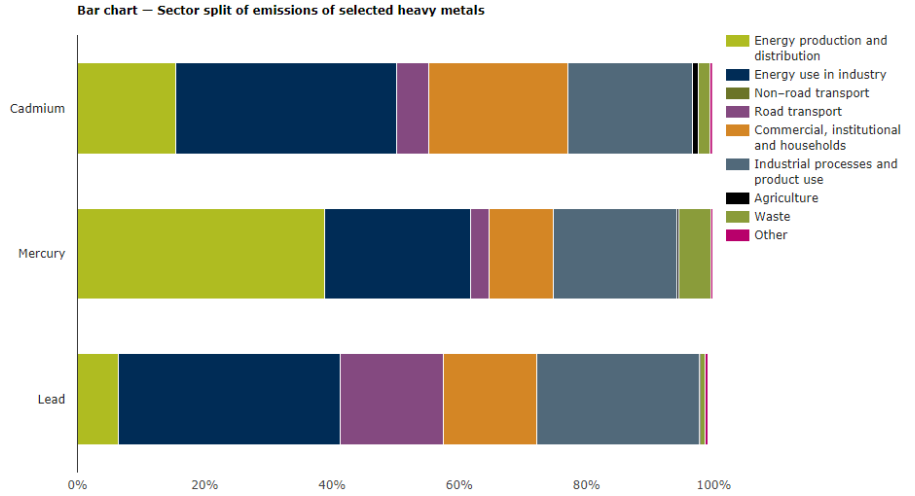

Figure 1-1. Plot of cadmium, mercury and lead emissions classified depending on the sector as reported by the European Environment Agency (https://www.eea.europa.eu/data-and-maps/indicators/eea32-heavy-metal-hm-emissions-1/assessment-8, 07/03/2018)

Pollutants in water behave in several different ways. Non-conservative materials and many microorganisms can be degraded by natural self-purification processes. So, their amount declines with time, and the rate of this reduction depends on many factors as type of pollutant, water quality, temperature and environmental factors. Other kind of pollutants, due to their nature, are not affected by this natural process and remain in the environment, so its use has to be more strictly regulated (A.S.Mohammed et al., 2011)

The effect of the emissions (arising from industrial processes, road transport and agriculture, among others) received by soils will depend on the capability of retention, which, at the same time, depends on different physicochemical properties such as mineralogy, grain size or organic matter. These metals can be present in soils in different ways: near the surface or in internal layers where they can precipitate forming sulphides, carbonates, oxides or hydroxides. Their mobility and reaction capability in soil or water play an important role in their bioavailability. So, it is important to have the suitable tools to identify and quantify them.

1.2 The importance of speciation

Metal speciation is defined as the process through which it is possible to know the chemical distribution into the different chemical species which are present in a medium. Basically, in natural aqueous samples, metals can be present as (Mota and Correia dos Santos, 1995):

- Hydratated free metal ion (M).
- Complexed with inorganic species like chlorides, sulphides, carbonates, etc. (ML)
- Complexed with organic species such as humic acids.
- Adsorbed on colloids and other surfaces.

The typically accepted bioavailability model is represented in figure 1-2:

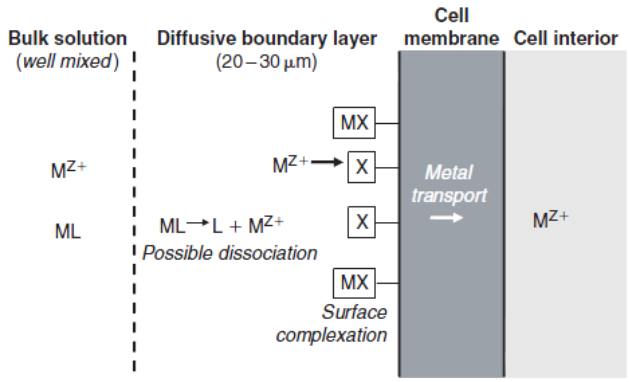

Figure 1-2. Scheme of metal bioavailability resulting from its supply and crossing through a biological membrane. M^{Z+}: free metal ion; L: ligand; ML: metal-ligand complex; MX-: metal-ligand complex on the membrane surface and X: ligand on the membrane surface (Batley et al., 2004).

Two extreme situations can happen. A) The rate of metal crossing the membrane is very slow in comparison with the metal diffusion rate from the bulk solution to the membrane surface (bioavailability under thermodynamic control). In this case, the metal reaches a pseudo-equilibrium situation along the solution, so that the concentration of M is the same in the bulk as in the surface. And B) the rate of metal

internalization through the membrane surface is faster than the diffusion process (bioavailability under kinetic control). Here, a gradient in the metal concentration profile is generated close to the membrane surface forcing the dissociation of the complexes ML to compensate the local perturbation of equilibrium (Batley et al., 2004).

Many species coexist in natural media, but in general the scientific community agrees on that the toxic effects of heavy metals, depends essentially on the free ion concentration as it is described in some toxicity models such as the Biotic Ligand Model, BLM (Paquin et al., 2002) and the Free Ion Activity Model, FIAM (Anderson et al., 1978). So, the knowledge of the free concentration is important to understand the availability and mobility of toxic metals and micronutrients in environmental and biological systems (Galceran et al., 2014).

1.3 Analytical techniques used for metal speciation

Metals present in aquatic media can take different forms, even though usually it is assumed that just one of them has a key role in terms of toxicity. Several techniques have been developed to determine the forms or fractions thought to be more relevant. In the selection of the most suitable technique it should be taken into consideration that it is better to work without the application of any pre-treatment to the sample to avoid a possible sample composition change (Tonello et al., 2011).

Speciation techniques can be classified into two different groups: electrochemical techniques and non-electrochemical techniques.

1.3.1 Electrochemical techniques

Electroanalytical techniques take advantage of the electrical properties of the analyte in solution (Skoog et al., 2001). They have several favouring circumstances such as the relative cheap equipment required and the low concentration which can be reached, among others.

Amongst the electroanalytical techniques AGNES is also present and will be extensively described in section 1.4.

1.3.1.1 The Ion Selective Electrode (ISE)

It is one of the most used techniques to determine free metal ion concentration measuring directly in the sample. It is based on the potential difference generated at the membrane (which is ion selective) when the electrode comes into contact with the sample (Bakker et al., 1997). The selective membrane, which responds to the activity of a particular ion, is placed between two aqueous phases (the sample and the internal electrolyte solution). The commercial ISE electrodes allow working in a wide range of concentration from 1 mol L^{-1} to 1×10^{-6} mol L^{-1}, but they are not suitable to work in a low concentration range as is the case of trace metal in natural samples. Despite of the existence of ISE for some ions as Cu^{2+}, Cd^{2+}, Pb^{2+}, NO_3^- among others, there is not a commercial ISE to measure some other ions such as Zn^{2+}.

1.3.1.2 Anodic Stripping Voltammetry (ASV)

In this technique, a reducing potential is applied during a specific deposition time accumulating the reduced analyte on the electrode surface or forming an amalgam (Helaluddin et al., 2016). Then, it is reoxidated with the application of more positive potentials while the current is recorded. The area below the curve (*I* vs *E*) can be measured in order to quantify the metal concentration, because the charge is proportional to the amount of metal deposited on the electrode (Batley et al., 2004) (Pesavento et al., 2009). But, unless the sample is extremely simple, ASV does not provide the free ion concentration, but a labile fraction (Pesavento et al., 2009) (Companys et al., 2018).

Depending on the sweep potential type, several variants result (Bansod et al., 2017): linear sweep anodic stripping voltammetry (LSASV), differential pulse anodic stripping voltammetry (DPASV), square wave anodic stripping voltammetry (SWASV) among others. The main advantage of this technique is the low level which can be reached (10^{-12} mol L^{-1}).

A typical ASV plot is represented in Fig 1-3.

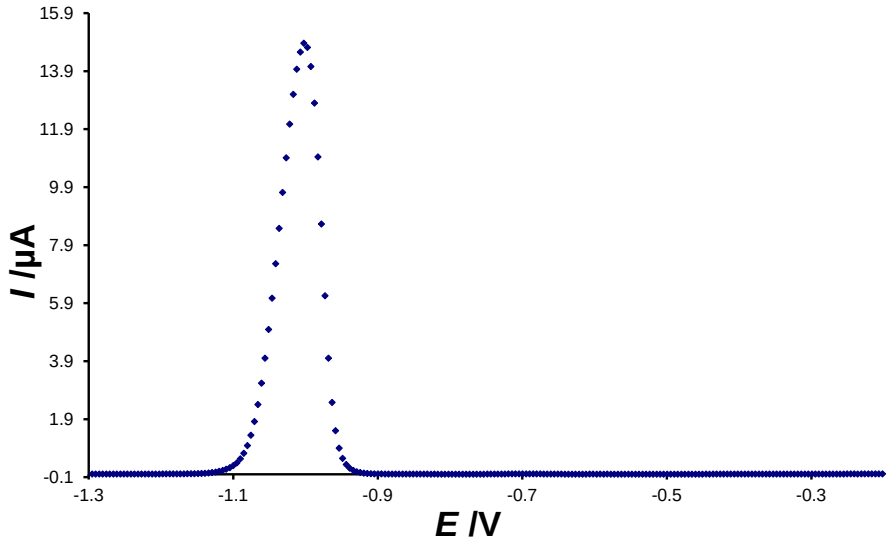

Figure 1-3. Plot of a Differential Pulse Anodic Stripping Voltammogram where E_{dep}= -1.3V and t_{dep}= 30 s in a solution with $c_{T,Zn}$= 1.14×10^{-5} mol L^{-1} and $c_{T,KNO3}$= 9.79×10^{-2} mol L^{-1} .

1.3.1.3 Stripping Chronopotentiometry

This technique, also named as Stripping Potentiometry or Potentiometric Stripping Analysis (PSA), has been used in several matrices as blood (Almestrand et al., 1987), urine (Jagner et al., 1981; Gozzo et al., 1999), wine (Froning et al., 1993), natural waters (Jagner et al., 1981; Cleven and Fokkert, 1994) among others. It has been demonstrated to be specially useful in the case of heavy metal ions due to the lower impact of adsorption on the electrode surface in the presence of a huge amount of organic matter (Jagner, 1982; Estela et al., 1995). As seen in figure 1-4, SCP is applied in two steps. In the first one (the deposition step), the metal ion is reduced as in the case of the ASV at a constant potential during a fixed time (Town and van Leeuwen, 2001). The second one is the stripping step, in which the accumulated metal is quantified generating a wave-shaped signal for each stripped species (Serrano et al., 2007a). The analytical signal used for the quantification is

the required time for reoxidation, called transition time (τ), while a constant oxidising current (stripping current I_s) is applied. The transition time is obtained by integration of the curve (d*t*/d*E* vs *E*). It has to be noticed that besides the faradaic current ($I_{faradaic}$), there exist other components which have to be taken into consideration such as the current generated by other oxidant components such as the oxygen (I_{ox}) and the capacitative current (I_{cap}) (Parat et al., 2011c). But the crucial point when applying this technique is the stripping regime (van Leeuwen and Town, 2002). It can range from semi-infinite linear diffusion ($I_s\tau^{1/2}$ constant) to complete depletion ($I_s\tau$ constant). Complete depletion is most suitable for techniques such as AGNES-SCP. This can be achieved with not too high values of I_s. At the same time, a too low value of I_s might become critical if I_{Ox} is not known with sufficient accuracy.

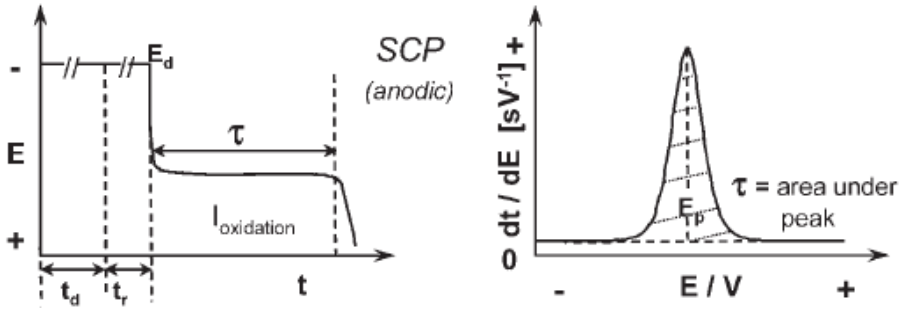

Figure 1-4. Scheme of an SCP procedure (Serrano et al., 2007a)

1.3.1.4 Cathodic Stripping Voltammetry (CSV)

This technique (which is also known as Adsorptive Stripping Voltammetry) is useful for trace level determinations of metals via formation of species that adsorb onto the working electrode surface (Ribeiro et al., 2017). It consists in the addition to the solution of an excess of a specific ligand which forms a strong adsorbing complex with the metal ion of interest (Batley et al., 2004; van Leeuwen and Town, 2007). A relatively positive potential is applied while the formed stable complex M-L is being adsorbed onto the mercury drop surface. Then, to quantify the metal, this formed M-L film is dissolved through the application of a more negative potential. Although it is mostly used to determine organic compounds (Arino et al., 2017), it is also possible to determine some metalloids as selenium, antimony or arsenic and to

determine the complexing capacity of different samples as for example sea water (van den Berg, 1991).

1.3.1.5 Differential Pulse Polarography (DPP)

In DPP (Differential Pulse Polarography), two potential pulses (differing by a constant potential jump ΔE) are applied at each mercury drop at a succession of potentials. A varying base potential is applied during each first pulse. There is a potential sweep of the base potential from a more positive potential towards a more negative one. The signal is recorded at two different moments: the first one some ms before the application of the second pulse (during the base potential) and the other, some ms before the end of the second pulse. The plotted signal is this difference of intensities in front of the potential. Typically, a peak-shaped curve is obtained.

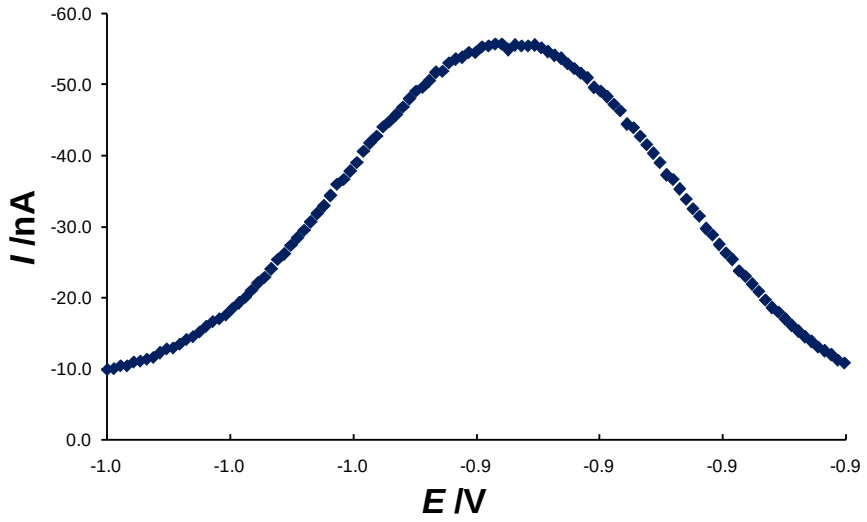

Figure 1-5 Obtained peak after the application of a DPP in a solution where $c_{T,NaNO3}$= 0.011 mol L^{-1}, $c_{T,Zn}$= 1.16×10^{-5}mol L^{-1} and pH=3.422.

1.3.2 Non-electrochemical techniques

In this group, all those techniques which do not use an electrode are included. The Donnan Membrane Technique (DMT) which belongs to this group is explained in detail in section 1.5.

1.3.2.1 The Ion-Exchange Technique (IET)

This technique, which presents a high sensitivity, uses a column filled with an ion exchanger (such as Dowex resin) to accumulate the target species, to an extent depending on their charge, chemical structures and the resulting thermodynamic stability in different media (Fortin and Campbell, 1998). The ions in the solution (analyte) can be accumulated until reaching equilibrium as a result of the ion exchanger being in contact with the solution during the pumping of the solution through the column. Depending on their nature, cations or anions can be exchanged and even both of them in case of some materials called amphoteric ion exchangers. Normally, it is a reversible process as the ion exchanger can be regenerated. For heavy metals, the ion exchanger is flushed with acid and the metal can be quantified from the eluate by Mass Spectrometry with Inductively Coupled Plasma, ICP-MS. It has been used in the determination of some metals, such as Cd, Ni and Zn among others, in synthetic and soil solutions and in natural waters (Vigneault and Campbell, 2005; Fortin et al., 2010).

More recently a field-IET, where the resin is directly equilibrated on site using dialysis cassettes, has been developed (Cremazy et al., 2015). In this case, the main advantage is the avoiding of sample manipulation which might impact on metal speciation.

1.3.2.2 Diffusion Gradients in Thin-films (DGT)

The DGT technique stands out due to its *in situ* application (Davison et al., 1994) and has been used in several research fields such as monitoring water quality, chemical speciation in solutions, soils and sediments and bioavailability in waters among others. It consists of two steps: a) accumulation step along which the metal species present in the solution move by diffusion through a porous hydrogel (previously they have passed through a filter) getting trapped in a resin. b)

quantification step (Town et al., 2009). The metal accumulated is extracted by an elution process with a known volume of acid (in the case of Chelex resin, nitric acid is the most suitable eluent) after certain time and the quantification can be done by ICP-MS. The determination of the so-called DGT concentration can be done from the knowledge of the accumulated moles, the diffusion coefficient of the metal of interest (at the working temperature), the deployment time and the area (Mongin et al., 2011).

In practice, as seen in Figure 1-6, a polypropylene device formed by two different pieces (the piston and the cap) is put in contact with the solution which contains the analyte of interest (Davison and Zhang, 2012; Mongin et al., 2013). The role of the piston is to hold the different "layers" (the filter, the hydrogel and the resin) which are put into the device. Then the piston and the layers are subjected by a tight-fitting cap, guaranteeing in this way that diffusion of the metals from the solution to the resin takes place through a certain area and a (mostly) fixed diffusion domain (Menegario et al., 2017).

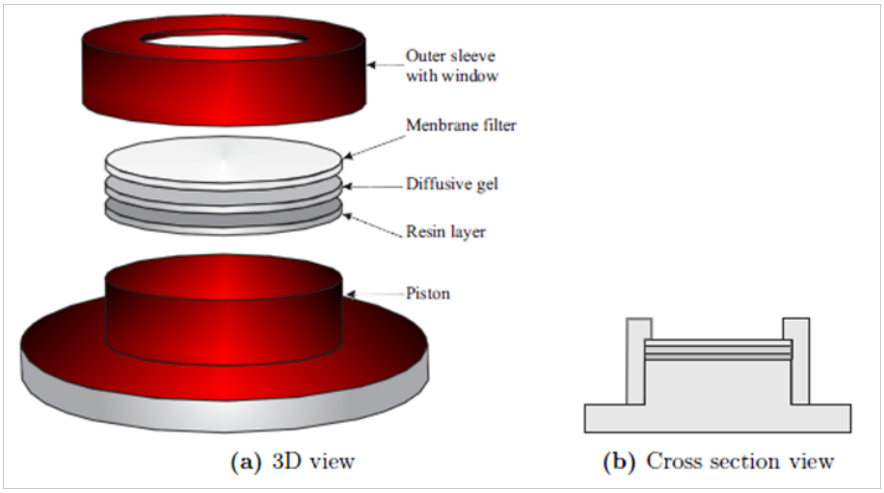

Figure 1-6. Scheme of a DGT device taken from (Uribe, 2012)

The simplest interpretation of this technique has often relied on several approximations such as: a) the transport through the different diffusion layers reaches a steady-state regime under perfect-sink conditions and can be related to the amount of moles accumulated in the resin (Galceran and Puy, 2015). b) the

complexes which cannot penetrate through the filter or hydrogel do not contribute to the flux.

A more refined framework based on the penetration of complexes in the resin disc and on the lability of the complexes has been developed (Puy et al., 2016).

1.3.2.3 Permeation Liquid Membrane Technique (PLM)

It is a useful technique to determine metal concentrations, based on the separation of the metal of interest (which could be in equilibrium with a ligand L) to a water-insoluble organic solvent which contains a complexing agent (C, carrier) selected according to the metal of interest (Batley et al., 2004) (see Figure 1-7). A chemically inert porous membrane, which is impregnated with the organic solution, is put as a "sandwich" between two aqueous solutions: one which contains the metal of interest (source solution) and another one that could be named as "acceptor or strip solution". At the interface source solution/membrane, an equilibrium is established between the metal (M) and the carrier forming the specie MC, which is able to diffuse in this organic solution towards the interface membrane/acceptor solution. Then, the metal is "captured" in this solution by a complexation process with a strong complexing agent which is present in the acceptor solution (Gunkel-Grillon and Buffle, 2008; Pesavento et al., 2009). Once the metal of interest is there, it can be quantified by several techniques as atomic absorption spectroscopy, voltammetry, ICP-MS, etc.

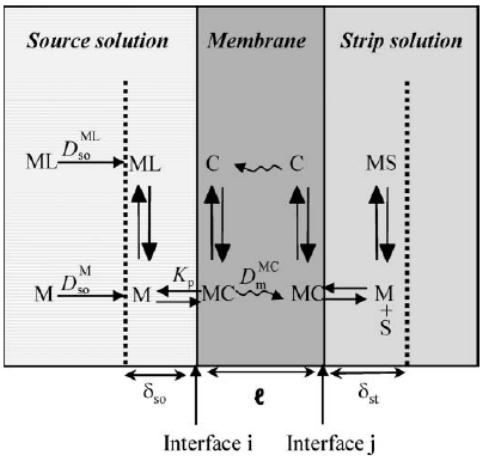

Figure 1-7. Schematic representation of the transfer of metal ion, M, through a PLM, in the presence of ligand, L, and of ML complex in the source solution. C, carrier; S, complexing agent of the acceptor solution (strip solution) (Gunkel-Grillon and Buffle, 2008).

1.3.2.4 Polymer Inclusion Membrane (PIM)

The PIM technique is similar to the PLM (described above in section 1.3.2.3) as the analyte of interest is transported through a membrane from the donor solution to the acceptor solution by a carrier (Tomaszewski et al., 2003; Gramlich et al., 2012). The difference here is in the membrane composition, since in that case it relies on a polymeric matrix commonly composed by cellulose triacetate (CTA) or polyvinyl chloride (PVC) (Vera et al., 2018). With that change, the membrane gets more mechanically resistant and if other components are necessary, they could be also added to contribute to an improvement of the elasticity. In addition, various studies have been done which show the good stability of the membrane in terms of: i) a possible decrease in the capacity of transport of it with time due to its use and ii) a possible mass loss (Vera et al., 2018). This technique has been used to determine the free zinc concentration (finding a satisfactory correlation) in solutions containing ligands such as EDTA, citrate and humic acids and in the absence of them, employing a plant nutrient solution as donor phase.

1.4 AGNES technique

AGNES (Absence of Gradients and Nernstian Equilibrium Stripping) is a useful technique developed to determine free metal ion concentrations. Among its advantages, one can highlight the low concentration level which can be reached and the possibility to perform the determination without any separation of the sample.

1.4.1 AGNES principles

AGNES (Galceran et al., 2004; Companys et al., 2017) is a stripping technique used to determine the free ion concentrations of elements such as Zn, In, Sn, Sb, Cu, Cd, among others. Although most work with AGNES has been done with mercury electrodes, it is also possible to apply this technique with other type of electrodes such as Bi or Au electrodes (Rocha et al., 2015; Domingos et al., 2016). Work with non-Hg electrodes is described in section 1.4.3.4. AGNES consists of 2 stages or conceptual stages: a) Accumulation and b) Stripping. In this section, the principles of AGNES using mercury electrodes are described through its first implementation (Galceran et al., 2004) (in a variant which -in the perspective of later developments- can be classified as 1 Pulse for the first stage, and AGNES-I for the second stage):

a) Firstly, the metal in solution, M, is reduced and dissolved in the mercury drop up to an equilibrium situation.

$$M^{n+} + ne^{-} \rightarrow M^{0}(Hg) \tag{1-1}$$

Here a sufficiently negative potential E_1 (just a few mV more negative than the standard redox potential) is applied during a long enough time t_1, see Figure 1-8. Most of the time in this first stage, the stirrer is on to reduce deposition time (because reducing the diffusion layer thickness leads to a more effective mass transport process). The deposition stage lasts until a special situation is reached: the metal flux that crosses the electrode surface ceases because the Nernstian equilibrium has been reached and the concentration profiles are flat.

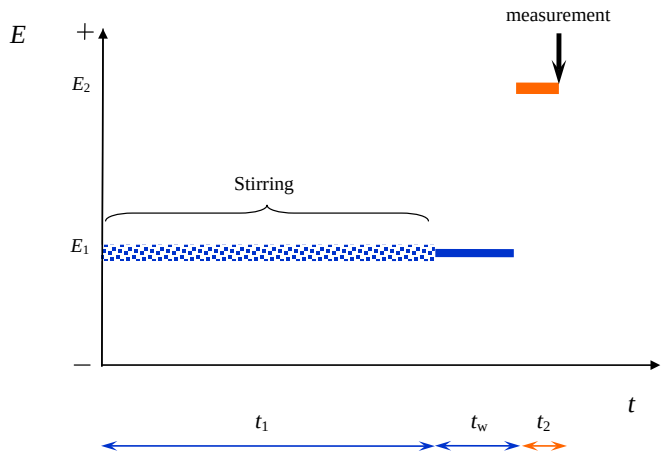

Figure 1-8. Potential program applied for AGNES 1 Pulse with quantification via the current. t_1 corresponds to the deposition time with stirring and t_w to the (deposition) waiting time (without stirring). t_2 is the stripping time when the intensity current is recorded, E_1 is the deposition potential and E_2 is the stripping potential.

The waiting time (t_w) is considered as a “safe” period to ensure that turbulences do not impact on the measuring step which follows immediately.

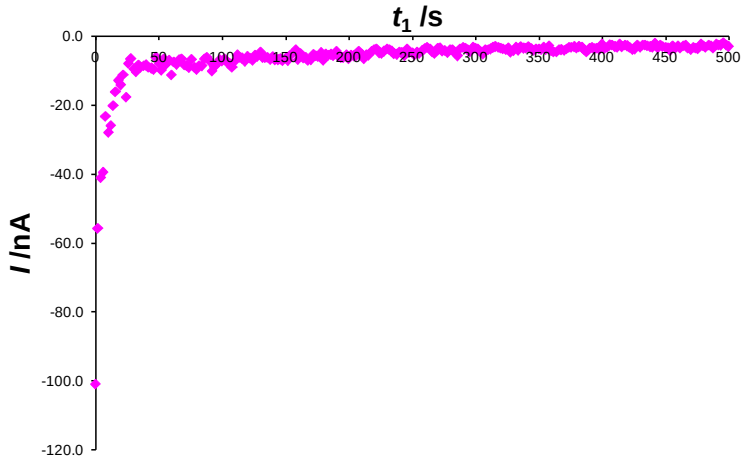

Figure 1-9. Plot of I vs t_1 in a solution with c_{KNO3}= 0.1 mol L^{-1} and $c_{T,Zn}$= 1.03×10^{-4} mol L^{-1} during the deposition stage at AGNES 1P. Y=50 and t_1= 500 s.

The ratio between the concentrations at both sides of the electrode surface at any time of the experiment (see Figure 1-10) is denoted as the gain (Y)

$$Y \equiv \frac{\left[\mathrm{M}^{0}\right]}{\left[\mathrm{M}^{n+}\right]} \tag{1-2}$$

which can be tuned through the applied potential (E_1) according to Nernst law:

$$Y = \frac{\left[\mathrm{M}^{0}\right]}{\left[\mathrm{M}^{n+}\right]} = \exp\left[-\frac{nF}{RT}\left(E_1 - E^{0'}\right)\right] \tag{1-3}$$

where $E^{0'}$ corresponds to the formal standard potential of the redox couple and $[M^0]$ to the final reduced-metal concentration in the amalgam.

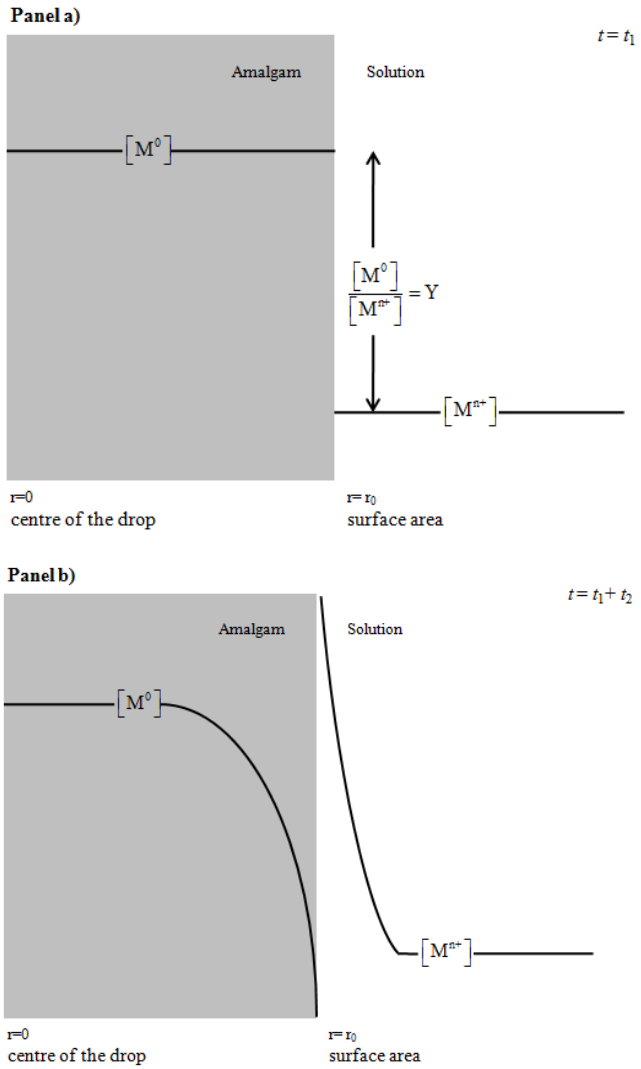

Figure 1-10. Plot of the concentration profiles of AGNES. Panel a) at the end of the first stage $t=t_1$ (corresponding to the end of the deposition time). Panel b) the second (stripping) stage of AGNES at $t=t_1+t_w+t_2$ when the intensity response is measured. Taken from (Galceran et al., 2004).

The equilibrium amalgamated concentration ($[M^0]$) depends only on the metal bulk concentration ($[M^{n+}]$) and the gain and is independent of any characteristic of the medium such as complexation.

Experimentally, to know the value of the deposition potential (E_1) corresponding to a given *Y*, it is convenient to run a DPP (Differential Pulse Polarogram) in a solution with just metal. Combining equation (1-3) with the well-known expression of DPP peak (Bard and Faulkner, 1980) one obtains:

$$Y = \sqrt{\frac{D_{M^{n+}}}{D_{M^0}}} \exp\left[-\frac{nF}{RT}\left(E_1 - E_{peak} - \frac{\Delta E}{2} \right) \right] \quad (1\text{-}4)$$

where $D_{M^{n+}}$ corresponds to the diffusion coefficient of the specie M^{n+}, D_{M^0} to the diffusion coefficient of the specie M^0, E_1 to the needed reduction potential applied to obtain the desired gain and ΔE to the modulation amplitude applied in DPP.

b) Then, at the second stage (panel b in figure 1-10) the amount of preconcentrated metal in the mercury drop is determined. With that aim, a re-oxidation potential (E_2) is applied.

$$M^0 - ne^- \rightarrow M^{n+} \quad (1\text{-}5)$$

In its first implementation, the faradaic current was taken as the response function to determine the free ion concentration (Galceran et al., 2004).

The measured current at a certain reoxidation time t_2 is the sum of different components (Galceran et al., 2007):

- The capacitive current, I_c
- The current which appears because of the reduction of oxygen, I_{O2}. Despite the nitrogen flux present at the polarographic cell, O_2 can remain in trace levels.
- The faradaic current due to non-analyte elements, I_{fna} which can be preconcentrated during the first stage of AGNES.
- The faradaic current due to the analyte, I_f.

The faradaic current of the analyte can be obtained subtracting a suitable blank experiment (see section 1.4.3.1).

It has been shown that, due to the linear nature of the diffusion equation in the amalgam (see Appendix in (Galceran et al., 2004), the measured intensity under diffusion limited conditions keeps a linear relationship with the concentration of amalgamated metal. The proportionality factor (which depends on the measuring time t_2 and also on the geometry and diffusion properties of the used mercury electrode) is called η:

$$I = \eta\left[\mathrm{M}^0\right] \tag{1-6}$$

Considering the expression of the gain (1-2), it follows, then, that the free metal concentration is directly related with the faradaic current measured.

$$I = Y\eta\left[\mathrm{M}^{n+}\right] \tag{1-7}$$

As seen in figure 1-11, t_2 was chosen to minimize the ratio between the current in a blank experiment I_b (mostly capacitive current) and the total current (Galceran et al., 2004).

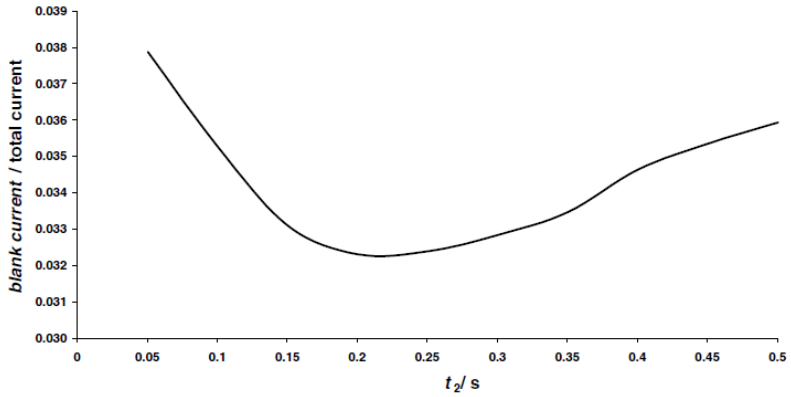

Figure 1-11. Ratio of blank (just KNO_3 in the solution) and total (with total Cd concentration 1.02×10^{-6} mol L^{-1}) currents showing the convenience of using t_2=0.2 s as suitable measuring time. Settings: t_1=260 s, t_w=100 s, E_1=-0.660 V, Y=145. Taken from (Galceran et al., 2004).

Depending on the response function in the second stage taken as analytical signal, several AGNES variants have been developed which are extensively explained in section 1.4.3.3. They could be divided in two different groups:

- Intensity current as analytical signal: AGNES-I.
- Charge as analytical signal: AGNES-Q, AGNES-LSV and AGNES-SCP.

1.4.2 Experimental implementation of AGNES

The corresponding voltammetric measurements are done with an Eco Chemie Autolab PGSTAT12, an Autolab type III potentiostat or μ-AUTOLAB type III potentiostat attached to a Metrohm 663VA Stand and to a computer by means of the GPES 4.9, the NOVA 1.7 and 1.10 (Eco Chemie) software packages. In the polarographic cell the necessary electrodes to perform the measurements are located: the working electrode (usually the mercury drop electrode, although it can be replaced with others, see section 1.4.3.4), the auxiliary electrode which is a glassy carbon one and the reference electrode which consists of an Ag/AgCl/3 mol L^{-1} KCl, encased in a 0.1 mol L^{-1} KNO_3 jacket.

For determining the free ion concentration, the first step is to obtain the proportionality factor η. With that purpose, several stages have to be followed:

- E_{peak} determination by a DPP measurement.
- AGNES calibration making additions of a standard metal solution whose free concentration is well known.
- Check of the contamination degree in the polarographic cell with ASV.
- Free metal AGNES measurement of the sample solution.

1.4.2.1 Determination of E_{peak}

As mentioned above, the first step for determining the E_{peak} value is performing a DPP (see section 1.3.1.5 for more details about the technique). This determination is done in a solution with a sufficiently high metal concentration to ensure that the peak resolution is good.

Then, once the plot I vs E is represented, the obtained E_{peak} value is applied in eq (1-4) to obtain the gain Y as seen in section 1.4.1.

1.4.2.2 AGNES calibration

Several additions of a standard solution of the metal are done to obtain known free metal concentrations in the cell (calculated with the speciation program Vminteq (Gustafsson, 2016). The usual supporting electrolyte to provide an ionic strength similar to that of the sample is KNO_3. To adjust the pH, HNO_3 or NaOH are added and the increased volume of the solution is taken into account to calculate the metal concentration. After each addition, AGNES measurements are run.

The exact free metal concentration is calculated by VMinteq in every addition and the plot I-I_b (for the variant AGNES-I) or Q-Q_b (for the variant AGNES-Q) vs the free metal ion concentration is built. Q_b is the charge of blank experiments. Dividing the slope of this plot (see Figure 1-12) by the used gain, the proportionality factor η is obtained (or η_Q in the case of the variants where the charge is the analytical signal).

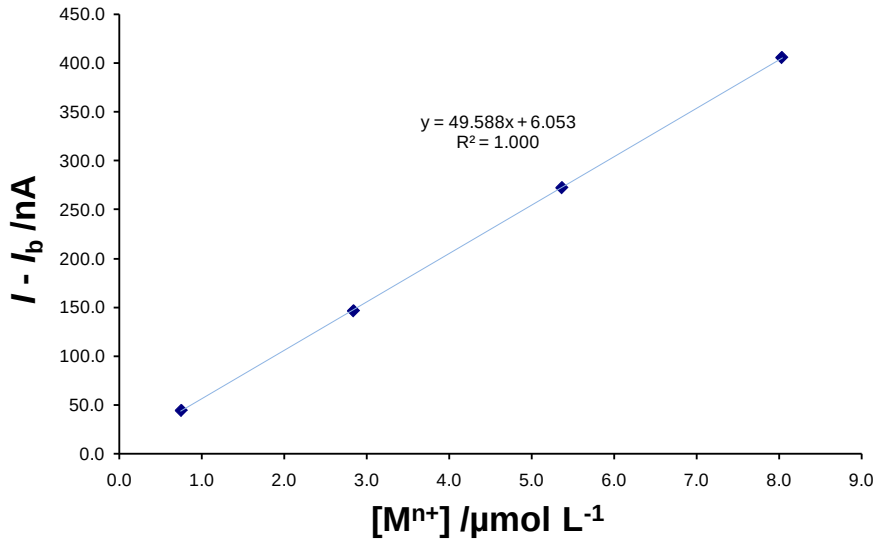

Figure 1-12. Determination of the proportionality factor η (in this case with a value of 2.48×10^{-3} A/mol L^{-1}) working with a Y=20 in a Zn calibration and in a solution with c_{KNO3}= 0.011 mol L^{-1} and T=25.0^{0}C

1.4.2.3 Check of the contamination degree

Firstly it is essential to ensure that the cell is "clean" of metal (this step is extremely important when working with natural samples where the determined free metal concentration could be very low and this contamination could lead to an incorrect determination). With this purpose, an ASV is performed by applying a deposition time of 30 s and the obtained I_{peak} is compared with 5 nA as seen in figure 1-13. For systems with lower total metal concentrations, more stringent contamination levels were required. If the threshold was surpassed, then one considers that the metal contamination of the cell could interfere in the measurement and it is necessary to clean again the cell and repeat the ASV.

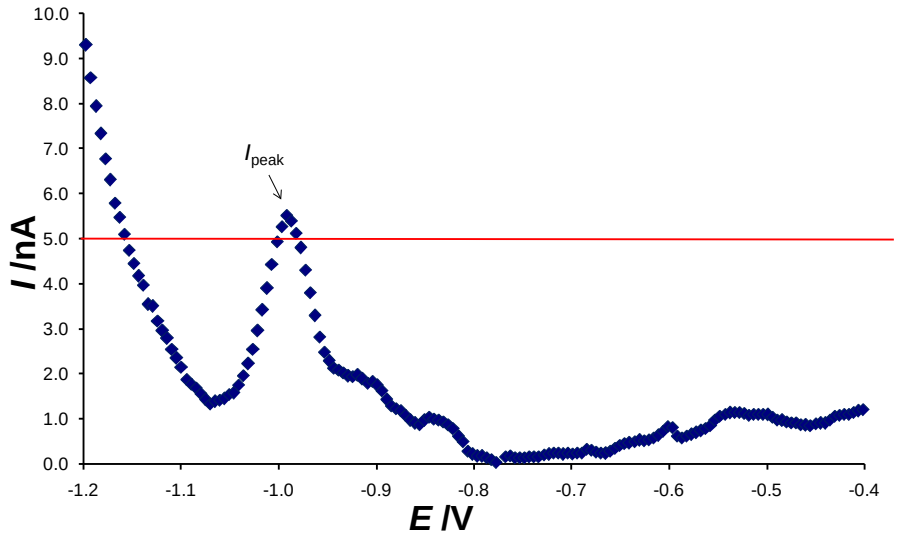

Figure1-13. Plot of an Anodic Stripping Voltammogram in a solution with $c_{T,KNO3}$= 0.1 mol L^{-1} exhibiting unacceptable initial contamination.

1.4.2.4 Free metal determination in the sample

Finally, once contamination of the cell is discarded, with the experimentally determined η and applying equation (1-7), the free metal ion concentration of any sample can be computed from the corresponding AGNES signal.

1.4.3 AGNES developments

1.4.3.1 Types of blank measurements

Several strategies have been developed to obtain the blank signal which has to be subtracted from the total current to provide AGNES measurement.

a) *Classical blank or synthetic blank (Galceran et al., 2004)*: consists in applying the same AGNES measurement to a solution with the same matrix as the sample, but without metal. The presence of traces of the metal to analyse could interfere in the signal. It might be difficult to synthetically create the same matrix as a natural sample, so other blanks were developed for complex media.

b) *Shifted blank (Galceran et al., 2007)*: with the aim of quantifying the capacitive current, the same potential difference is applied (ΔE) to the sample (where there is the analyte), but in a range of more positive potentials where there is no interference from other metals. This potential shift is always constant (i.e. the same for both E_1 and E_2). For most experiments, the value of the shifted-blank gain ($Y_{1,sb}$) is determined as:

$$\frac{Y_1}{Y_{1,sb}} = 500 \tag{1-8}$$

so, the metal accumulated in the amalgam due to $Y_{1,sb}$ will be negligible in comparison with the one at the measuring $Y=Y_1$.

To calculate the gain corresponding to the re-oxidation potential ($Y_{2,sb}$) of the blank, one applies:

$$Y_{2,sb} = Y_{sb} \times \frac{Y_2}{Y_1} \tag{1-9}$$

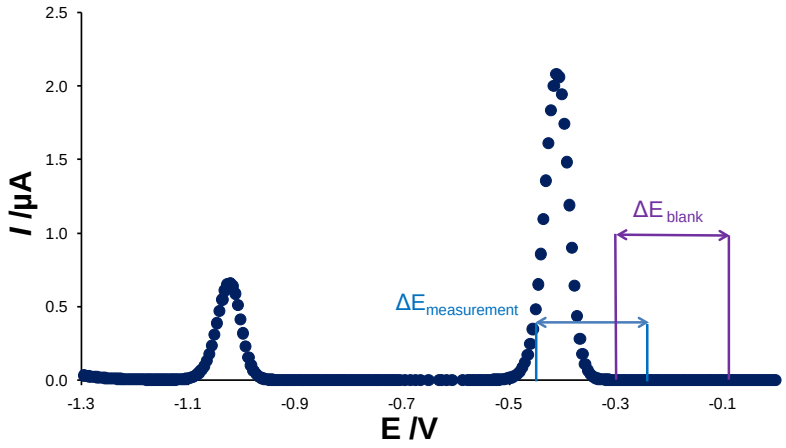

Figure 1-14 Plot of an ASV measurement in a solution with $c_{T,KNO3}$= 0.1 mol L^{-1}, $c_{T,XO}$= 8.95×10^{-7} mol L^{-1} and $c_{T,Pb}$= 4.99×10^{-6} mol L^{-1}. The difference of potential for determining the metal is represented in light blue and the potential jump is the same for determining the blank, but in a region with no interference of other metals (represented in purple).

c) *EDTA-Blank (Companys et al., 2008)*: a strong complexant agent (EDTA) is added to the solution to cut down the free metal ion concentration and then apply the same AGNES measurement as with the analyte. The reduction of the free metal ion can be followed performing an ASV. The main problem of this variant of blank is the destruction of the sample.

1.4.3.2 Reduction of the deposition time

The strategy consists in dividing the first stage of AGNES into two sub-stages (see figure 1-15), in a version called AGNES 2P (Companys et al., 2005) as alternative to the more "classical" AGNES 1P:

a) A potential corresponding to a gain called $Y_{1,a}$ (producing diffusion limited conditions for accumulation) is applied during a time $t_{1,a}$ so that most of the required metal is supplied to the electrode during this period.

b) Then, the potential corresponding to the desired gain ($Y_{1,b}$) is applied during $t_{1,b}$ so that the system reaches the prescribed equilibrium conditions. The t_w without stirring after that sub-stage is considered as an "extra" time to be on the safe side.

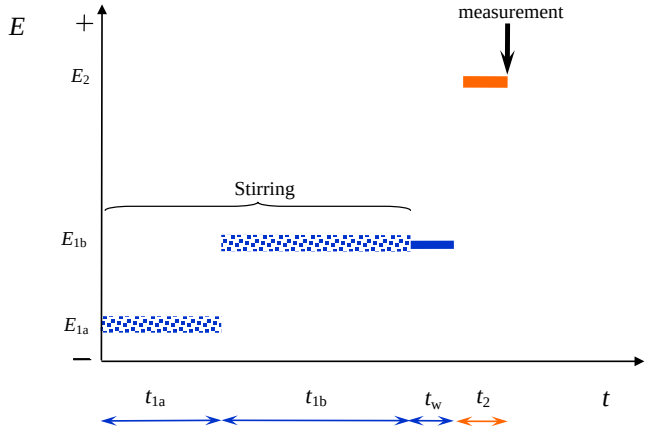

Figure 1-15. Potential program applied when the first stage of AGNES is divided into two sub-stages (AGNES 2P). In this case, the deposition time t_1 is the sum of the first sub-stage ($t_{1,a}$), the second sub-stage ($t_{1,b}$) and the waiting time (t_w).

In AGNES 2P, if the potential corresponding to $Y_{1,a}$ is applied during a too long time $t_{1,a,}$ the metal inside the mercury drop will be in excess, so we will need a longer $t_{1,b}$ to compensate for the *overshoot* (see Figure 1-16).

Conversely, if the applied potential $E_{1,a}$ was too short, a longer $t_{1,b}$ will be needed to reach the desired gain $Y_{1,b}$ (*undershoot* situation, see Figure 1-17).

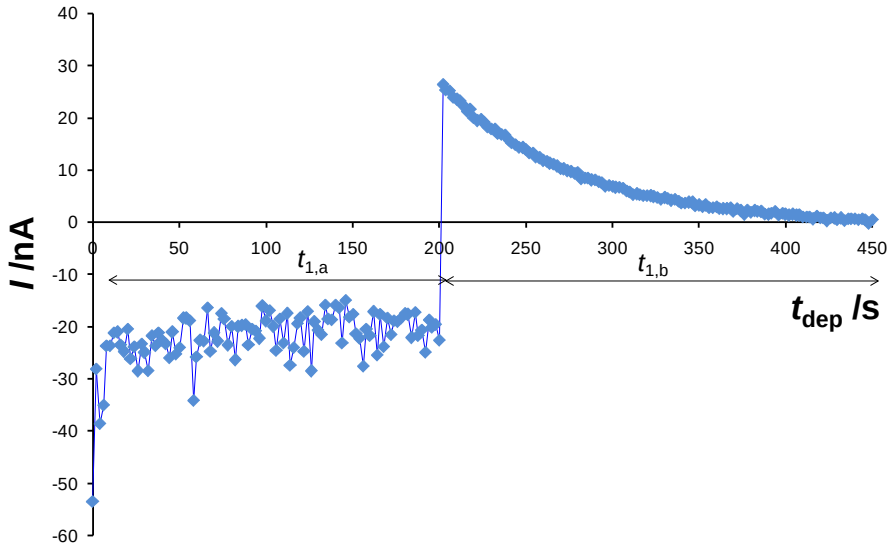

Figure 1-16. Plot of I vs time during the deposition stage of an AGNES 2P. Solution with $c_{T,KNO3}$= 0.01 mol L^{-1}, $c_{T,Zn}$= 1.05×10^{-5} mol L^{-1} and $c_{T,GSH}$= 3.50×10^{-4} mol L^{-1}. $Y_{1,a}$= 10^{10}, $t_{1,a}$= 300 s, $Y_{1,b}$= 1000 and $t_{1,b}$= 600 s. Due to the chosen conditions, an overshoot appears.

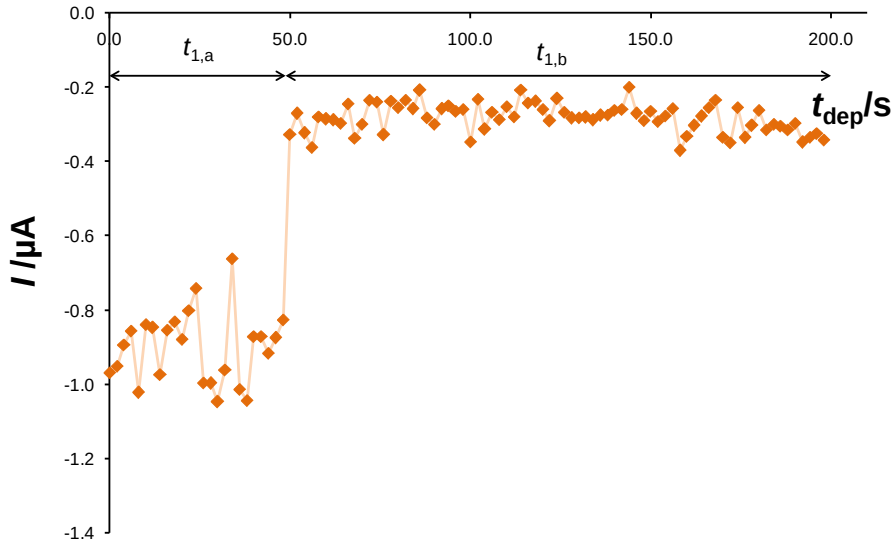

Figure 1-17. Plot of *I* vs time during the deposition stage of an AGNES 2P in wine where Zn is determined. $Y_{1,a}$= 10^{10}, $t_{1,a}$= 50 s, $Y_{1,b}$= 50 and $t_{1,b}$= 150 s. Due to the conditions, an undershoot appears

So with the aim of finding suitable gains and deposition times $t_{1,a}$, an existing flowchart (Chito, 2012) was improved:

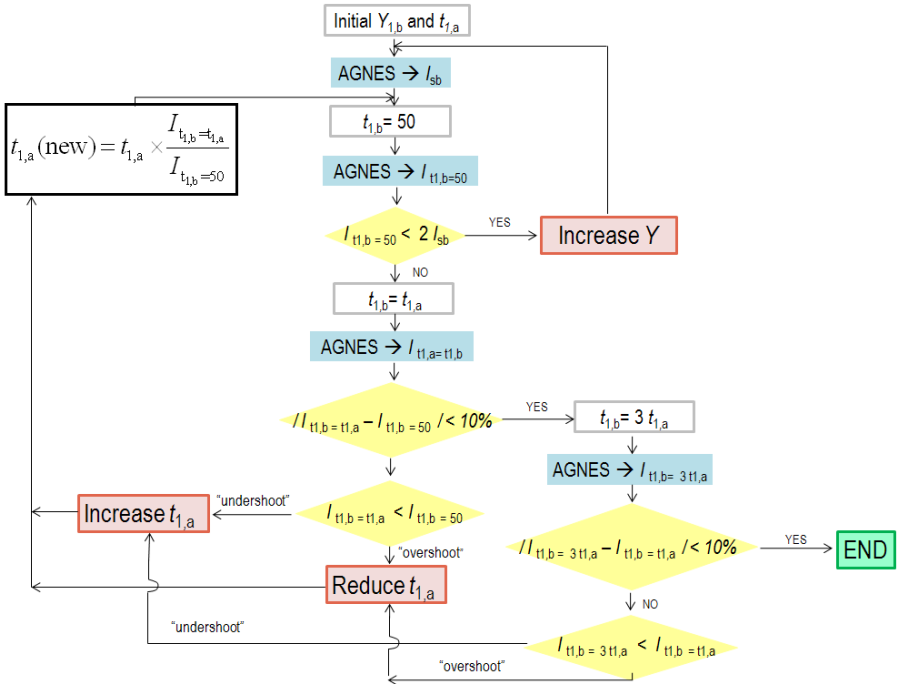

Figure 1-18. Algorithm used to optimize the gain and the deposition time (Chito, 2012)

As reflected in figure 1-18, initially AGNES is applied using certain initial parameters of $Y_{1,b}$, $t_{1,a}$ and $t_{1,b}$. The first goal is to adjust the gain ($Y_{1,b}$) in such a way that the obtained current could be high enough with respect to the corresponding blank current. So, once that "blank current" is determined, an AGNES 2P measurement is done where $t_{1,b}$= 50 s. Here if the obtained current ($I_{t1,b=50s}$) is lower than two times the current corresponding to the blank (I_{sb}), AGNES has to be repeated increasing the desired gain $Y_{1,b}$ as it means that the measurement is too close to the blank. But if not, this means that the gain that is being used ($Y_{1,b}$) is appropriate and the next parameter to be adjusted is the required deposition time. In that sense, another AGNES determination has to be done where $t_{1,b}$=$t_{1,a}$. In this occasion, if the difference between $I_{t1,b=t1,a}$ and $I_{t1,a=50s}$ is lower than 10%, the AGNES measurement is repeated, but with $t_{1,b}$=3$t_{1,a}$ as, in case of the existence of an overshoot or undershoot, this would be corrected with the taken long time (3$t_{1,a}$). And, if the difference between $I_{t1,b=3t1,a}$ and $I_{t1,b=t1,a}$ is less than 10%, the measurement is accepted and AGNES determination is finished. Otherwise, if it is greater

(indicating the appearance of an overshoot), then it is necessary to repeat AGNES reducing $t_{1,a}$. But if $I_{t1,b=t1,a}$ is greater than $I_{t1,a=50s}$ (indicating the appearance of an undershoot), AGNES is repeated again, but in this case increasing $t_{1,a}$. For new experiments, the new $t_{1,a}$ can be estimated with

$$t_{1,a}(\text{new}) = t_{1,a} \times \frac{I_{t_{1,b}=t_{1,a}}}{I_{t_{1,a}=50s}} \tag{1-10}$$

if the experiment yielding $I_{t_{1,b}=3\times t_{1,a}}$ has not been run for the old $t_{1,a}$, and with

$$t_{1,a}(\text{new}) = t_{1,a} \times \frac{I_{t_{1,b}=3\times t_{1,a}}}{I_{t_{1,a}=50s}} \tag{1-11}$$

if the value of $I_{t_{1,b}=3\times t_{1,a}}$ is available.

1.4.3.3 Signals used as response functions of AGNES

Two types of analytical signals can be taken as the response function:

a) The *intensity current under diffusion limited conditions*: in the first works on AGNES, *I* was the analytical signal taken at the stripping stage to determine the free ion concentration (now labelled as variant AGNES-I, (Galceran et al., 2014).

b) The *charge*. There are three different AGNES variants which have considered the charge as the response signal.

   b.1) AGNES-Q (Galceran et al., 2010; Galceran et al., 2014). Where the total stripped faradaic charge (*Q*) along a constant reoxidation potential step (not necessarily under diffusion limited conditions) is used to determine the concentration (see figure 1-19). From the combination of Nernst and Faraday laws, the following expression is obtained:

$$Q = nFV_{Hg}c^{*}_{M^0} = \eta_Q Y c^{*}_{M} \quad (1\text{-}12)$$

where V_{Hg} corresponds to the volume of the mercury drop.

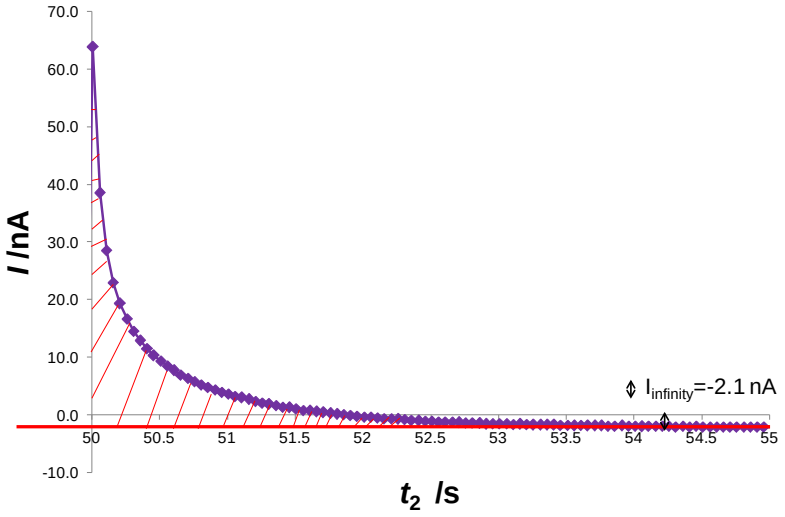

Figure 1-19. Plot of intensity vs stripping time (t_2) in a solution with $c_{T,Zn}$=2.44×10^{-5} mol L^{-1}, $c_{T,KNO3}$= 0.01 mol L^{-1}, $c_{T,MES}$= 0.001 mol L^{-1}, T=25.0 ºC and pH=4. The value of $I_{infinity}$ is represented with a double black arrow and corresponds to -2.1 nA. The shaded area under the curve represents the stripped faradaic charge.

b.2) AGNES-LSV (Galceran et al., 2010; Galceran et al., 2014; Companys et al., 2017). The potential is scanned at a sufficiently slow constant rate from the deposition potential E_1 to a less negative potential where all metal is reoxidized. In that case, Q is obtained from the area between the curve of the stripping current and the baseline (which replaces the blank) as observed in figure 1-20.

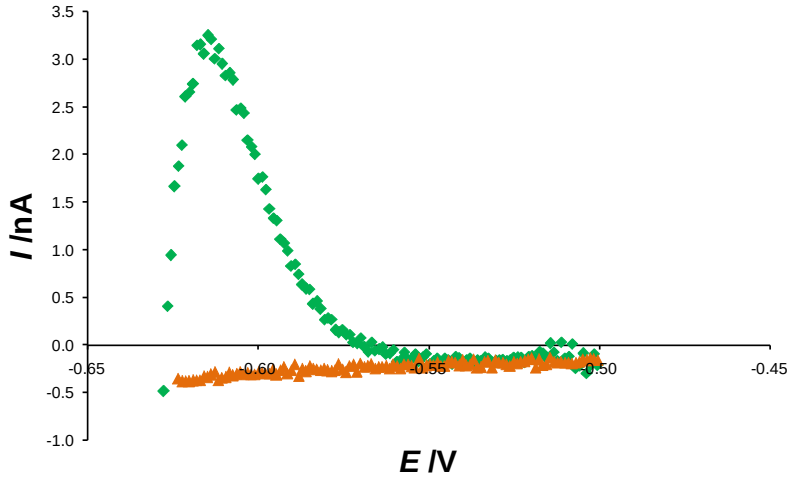

Figure 1-20. Plot of I vs E during an AGNES-LSV measurement in a solution with $c_{T,Cd}$= 5.68×10^{-6} mol L^{-1}, $c_{T,iodide}$= 9.53×10^{-2} mol L^{-1}, $c_{T,KNO3}$= 0.1 mol L^{-1}, pH=6.0 and T=25.0ºC. The green diamonds correspond to the measurements with Cd, iodide and supporting electrolyte and the orange triangles just with supporting electrolyte and which gives an idea of the baseline.

b.3) AGNES-SCP (Parat et al., 2011a; Galceran et al., 2014; Companys et al., 2017). Here at the second stage of AGNES (re-oxidation), a stripping chronopotentiometry (SCP) method is applied. A constant oxidising current or stripping current (I_s) is imposed and the evolution of the potential is recorded. The analytical signal taken as the response function is the re-oxidation time (τ), called the transition time. I_s is the sum from the signals arising from several components (e.g. other oxidants) apart from the faradaic signal. τ is determined from the area above the baseline in a plot dt/dE vs E. The charge can be computed as:

$$Q = \left(I_s - I_{Ox} \right) \tau \qquad (1\text{-}13)$$

1.4.3.4 Different kinds of electrodes

Usually, AGNES has been applied using a hanging mercury drop electrode (HMDE), but there exist other possibilities which are described here.

1.4.3.4.1 Mercury electrodes

- **Microelectrode**

  It consists of a hemispherical mercury droplet electrodeposited onto an iridium disk. In that case, the reduction of the mercury volume helps to reduce the deposition time (although the signal is reduced too) as the amount of metal needed to reach the desired gain is less (Huidobro et al., 2007). Results for the Hg-Ir microelectrode indicate that the limit of quantification has been reduced just in a factor of approximately two with respect to the one with HMDE.

- **Rotating disk electrode**

  In this kind of electrode, a thin mercury film is deposited on the rotating disk. It was observed that the thickness of the mercury film was a key point to reduce the high capacitive current present in the measurements (a thickness of 16 nm being finally established as the best option) (Rocha et al., 2010). Several rotation speeds were tested (1000 and 500 rpm). As the results were comparable, the speed chosen was 500 rpm because of the reduction of the mechanical degradation of the electrode. To check any possible falling of the small Hg drops, the same measurement is repeated several times to check it.

- **Screen printed electrodes**

  The screen printed electrodes are manually prepared on a 1 mm-thick polystyrene plates by using a commercial ink (Parat et al., 2011a). Their particular interest lies on the fact that are cheap, can be modified and easily transported, very handy when performing *in situ* measurements (Parat et al., 2011b; Parat et al., 2015).

Because of their behaviour at the stripping stage (which leads to think that even with the application of Y_2= 10^{-8}, the currents SPE are not under diffusion limited conditions, probably due to the relatively large resistance and capacitance), the intensity cannot be used as the analytical signal. So, as the charge is also proportional to the free metal ion concentration (Galceran et al., 2014), this is the analytical signal used to quantify the free metal ion concentration (i.e. the variant AGNES-Q or AGNES-SCP).

1.4.3.4.2 Non- Mercury electrodes

In recent years, there has been an increased concern about the use of Hg electrodes due to their toxicity. So, other materials have been presented as an alternative.

- **Bismuth film electrodes (Bi-FE)**

  The low toxicity of Bi and the good resolution of the stripping signals, has suggested Bi as a "green element" that could replace Hg in voltammetric measurements (Alves et al., 2017; Lu et al., 2018). Always one has to bear in mind that there exist some limitations in terms of potential range, so those elements with similar oxidation potential (i.e. Cu and Sb) will not be determined with it.

  The Bi film preparation can be done by two different methods depending on the platting method and the substrate used to coat Bi (Arino et al., 2017): a) *ex situ,* where Bi is deposited on the electrodic surface by electroplating of a solution of Bi^{3+} and, then, the modified electrode is immersed in the solution which contains the analyte of interest; b) *in situ,* where Bi^{3+} is directly added to the solution to be measured and Bi is deposited on the electrode surface during the measurement and c) *bulk method,* where there exists a precursor in the electrode surface (which is incorporated during the manufacturing of the electrode) and has to be reduced before the analysis.

  AGNES has been successfully implemented in the determination of Pb(II) (Rocha et al., 2015) in aqueous solutions with Pb(II)- PolyStirenesulfonate

and Pb(II)-IDA sytems demonstrating in this way that the Bi-FE electrode is a good alternative to the conventional Hg electrode.

- **Vibrated Gold Microwire Electrode (VGME)**

  The use of gold electrodes allow to determine several metal concentrations including Cu, which is not possible when working with Bi-FE, and there is no need to remove oxygen from the sample (Domingos et al., 2016) (which is a huge advantage when working with natural samples) as the metal reduction wave is more positive than that of oxygen. Apart from that, the new vibrated gold electrode eliminates the need of using an external stirrer, the hydrodynamic conditions produced at the surface of the electrode are much more stable and, therefore, having a better reproducibility. The flux of the species generated towards the electrodes is higher due to the smaller diffusion layer and the stripping can start just at the end of the vibration period without the need of a waiting period.

  In that case, as the electrode surface is not renewed after each AGNES experiment, a cleaning procedure has to be followed to ensure to have a reproducible surface.

  Finally, AGNES was successfully applied in Cu determinations in the systems Cu-malonic and Cu-iminodiacetic where a linear calibration plot was obtained from 4.9×10^{-9} to 9.8×10^{-7} mol L^{-1} of free Cu (Domingos et al., 2016).

1.4.4 AGNES measurements in non-synthetic samples

One of the advantages of AGNES is that the free metal determination can be done without altering the nature of the sample. Furthermore, considering that very low LOD (Limit Of Detection) and LOQ (Limit Of Quantification) can be achieved, this makes this technique really useful to work with natural samples where usually the concentration is low.

Several measurements in natural media were done with AGNES.

a) *Sea water (Galceran et al., 2007)*:

Due to the complex nature of the matrix sample where the aim was the determination of free zinc concentration, the shifted blank was developed for this case (see 1.3.2.2 section). AGNES could be applied satisfactory in this kind of sample applying the AGNES 2P strategy as the low metal concentration would have demanded too long deposition times in 1P mode. Finally the free zinc concentration determined in the sample which had been taken in the coasts of Tarragona and Barcelona was in the range of 1-3 nmol L^{-1}.

b) *River water (Zavarise et al., 2010; Chito et al., 2012; Aguilar et al., 2013b):*

In this case (when the ionic strength of the medium is low), it is necessary to take into account that the behaviour of the intensity current taken as the analytical signal did not follow the usual evolution.

Moreover, care has to be devoted not to disturb the carbonates speciation of the sample. With this purpose, a special device was designed to control N_2/CO_2 purging, because if the measurement was done under just nitrogen atmosphere, the concentration of others gases, such as CO_2, could be altered, breaking the established equilibrium between the dissolved gas and the CO_3^{2-}. Moreover, the pH of the sample could be fixed without the addition of any acid or base.

When working in low ionic strength media, the usual AGNES application of DPP to compute the gain could not be done, as it has been observed that E_{peak} at low ionic strengths could not be trusted. So, a new expression was proposed to determine the needed deposition potential:

$$E_1 = E_{\text{peak}}^{\mu \geq 0.01} + \frac{\Delta E}{2} + \frac{RT}{nF} \ln \left(\frac{\gamma_{\text{M}}}{\gamma_{\text{M}}^{\mu \geq 0.01} Y} \sqrt{\frac{D_{\text{M}}}{D_{\text{M}^0}}} \right) \qquad \text{(1-14)}$$

where E_1 is the needed deposition potential for the gain *Y*, $E_{peak}^{\mu \geq 0.01}$ is the potential peak determined by a DPP at sufficiently high ionic strength ($\mu \geq 0.01$ mol L^{-1}) and γ_M is the activity coefficient of the metal.

Then, a general methodology was proposed:

- ✓ The DPP peak is obtained in a medium with a high ionic strength ($\mu \geq 0.01$ mol L^{-1}).
- ✓ Equation (1-14) is applied to estimate the needed deposition potential E_1.
- ✓ AGNES calibration is done using solutions of known free metal concentrations at the same ionic strength of the sample.
- ✓ Finally AGNES measurement can be applied to the sample. With the measured analytical signal and the value of η_Q found in the calibration, the free metal ion concentration can be determined.

c) *Estuarine waters (Pearson et al., 2016):*

In this case, AGNES has been used to determine free zinc concentration in several samples of estuarine waters with a different salinity range as they were collected at different seasons and places of the estuary. The obtained results from the 13 estuarine studied samples were compared with those coming from the use of the Competitive Ligand Exchange Cathodic Stripping Voltammetry (CLE-AdCSV) and there was a good agreement in all samples except one.

d) *Wine (Companys et al., 2008):*

When working in an ethanolic media, some aspects have to be taken into account as the increase of viscosity (and so, the decrease of the diffusion coefficient) and the increase of the activity of the metal ions.

This reduction of the diffusion coefficient implies a reduction of the current of the DPP peak. In systems without relevant complexation, the maximum

current is proportional to the total metal concentration (which is also the free one) (Galceran et al., 2004):

$$I_{\text{peak}} = nFA\sqrt{\frac{D_{\text{M}}}{\pi t_{\text{p}}}}c_{\text{T,M}} \tag{1-15}$$

where I_{peak} is the peak current of a DPP, t_{p} is the pulse time and $c_{\text{T,M}}$ is the total metal concentration.

If equation (1-15) is applied to an ethanolic solution and to an aqueous solution, this relationship holds:

$$\frac{{}_{\text{w}}I_{\text{peak}}}{{}_{\text{EtOH}}I_{\text{peak}}} = \sqrt{\frac{{}_{\text{w}}D_{\text{M}}}{{}_{\text{EtOH}}D_{\text{M}}}} \tag{1-16}$$

where subscripts w and EtOH refer to the aqueous and ethanolic medium, respectively.

From (1-16), once the diffusion coefficient of metal in aqueous medium is known, the corresponding one for the ethanolic medium can be calculated.

Then a specific procedure was developed to determine free metal ion in wine:

- Determine the proportionality factor ${}_{\text{w}}\eta$ working with a known ${}_{\text{w}}Y$ through a calibration in an aqueous medium as described before.

- Compute the gain in an ethanolic solution. Equation (1-4) can be written as:

$${}_{\text{EtOH}}Y = \sqrt{\frac{{}_{\text{EtOH}}D_{\text{M}}}{D_{\text{M}^0}}}\exp\left[\frac{nF}{RT}\left(E_1 - {}_{\text{EtOH}}E_{\text{peak}} - \frac{\Delta E}{2}\right)\right] \tag{1-17}$$

- And then, as the fact of being in an aqueous or an ethanolic solution is not important in terms of the diffusion inside the amalgam, the proportionality factors should remain equal ($_{w}\eta = _{EtOH}\eta$). So the proportionality factor $_{w}\eta$ determined in the calibration could be used to determine the free metal concentration in wine.

Apart from determining the free metal ion concentration, AGNES has also been used to study the complexing capacity of wine (Chito et al., 2013). In that case, a correction of the ionic strength was necessary as the large change in total metal concentration during the titration implies a change too in ionic strength. The applied gain at the deposition stage would change, even when the potential was kept fixed.

Moreover, when AGNES is applied to the sample of real wine with added Zn, an unusual behaviour is observed in both the first and the second stage. During the first step of AGNES, it is observed that the intensity recorded decreases with time, instead of the typical form of increasing to more positive potential until reaching a stable value. This phenomenon is attributed to the hydrogen evolution reaction (HER effect) see Figure 1-21. On the other hand as observed in Figure 1-22 which has been extracted from (Chito, 2012) , during the reoxidation stage, when I_2 vs t_2 is represented, a minimum, which is called the DIP effect, is observed. At the same time, it is also seen that the residual current is more negative than the usual one. These difficulties could be overcome with judicious selection of AGNES parameters.

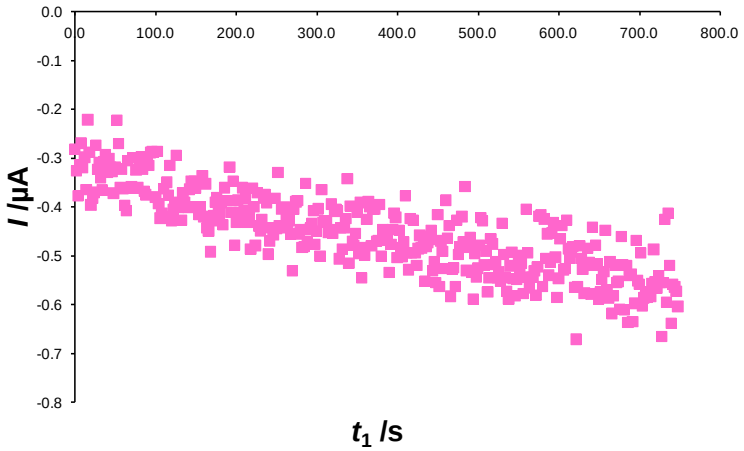

Figure 1-21 Plot of I vs t_1 during the first stage of an AGNES 1P in a solution with real wine (Raimat) where Y= 50 and t_1= 750 s.

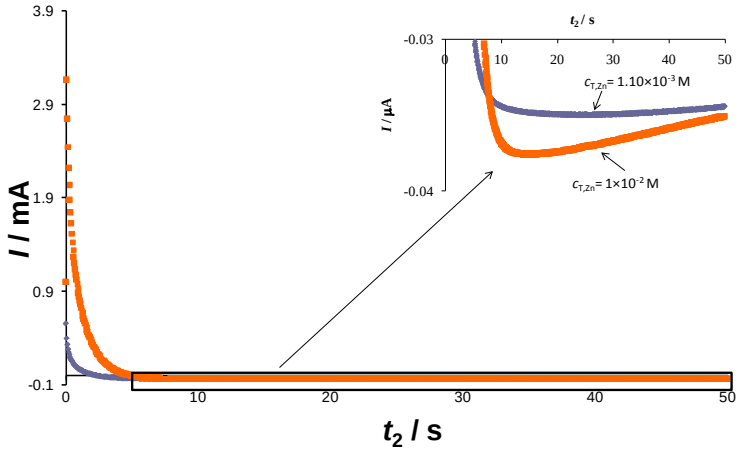

Figure 1-22 Currents recorded in the second stage of the application of AGNES to wine showing DIP effect. Plot extracted from (Chito, 2012).

e) *Humic Acids (HA) and Nanoparticles (NP)*:

Humic substances are usually classified as humic acid, fulvic acid and humines. They are present not only in soil, but also in water (being part of the Dissoved Organic Matter, DOM), taking an important role in transporting the pollutants. It is also known that metal complexation to DOM could modify the speciation of the metals and their toxicity.

AGNES has been used to study the complexation of metals such as Zn, Cd (Companys et al., 2007) and Pb to the humic substances (Puy et al., 2008). Complexation takes place in different binding sites, usually classified as carboxylic and phenolic functional groups. In a work with Pb (Pernet-Coudrier et al., 2011), different organic fractions extracted from river water were isolated according to their hydrophilic behaviour and analyzed. Apart from the complexation study, it was also tested that electrodic adsorption (even in presence of a high HA concentration) was not a problem to determine the free metal complexation. This issue will be discussed in detail in Chapter 2.

On the other hand, the concentration of free zinc coming from the dissolution of ZnO nanoparticles (NP) dispersed in aqueous salt solutions has also been determined with AGNES with the aim of obtaining thermodynamic and kinetic information about the dissolution process (David et al., 2012). In that study, adsorption led to more than often fallings of the drop, but it was solved avoiding the use of higher total ZnO NP concentrations (50 mg L^{-1}) and cleaning the capillary when necessary.

AGNES has also been applied to study other kind of NP: the adsorption of Cd onto titanium dioxide nanoparticles ($nTiO_2$) (Vale et al., 2015), to determine the free Cd concentration after the exposition of *Chlamydomonas reinhardtii* to Quantum Dots (Domingos et al., 2011) and for several latex samples (Domingos et al., 2008) and (Duval et al., 2013).

1.5 Donnan Membrane Technique (DMT)

1.5.1 Theoretical background

DMT is a useful technique to determine free metal ion concentrations which is based on the use of a donor solution (containing the analyte) and an acceptor solution (Temminghoff et al., 2000; Weng et al., 2005). The two solutions are separated by a semi-permeable cation exchange membrane. The membrane allows the passage of cations through it and at the same time does not allow the transport of the anions due to its negative charge. The acceptor solution is typically prepared so that the ionic strength of both (donor and acceptor) is the same (Chito et al., 2012).

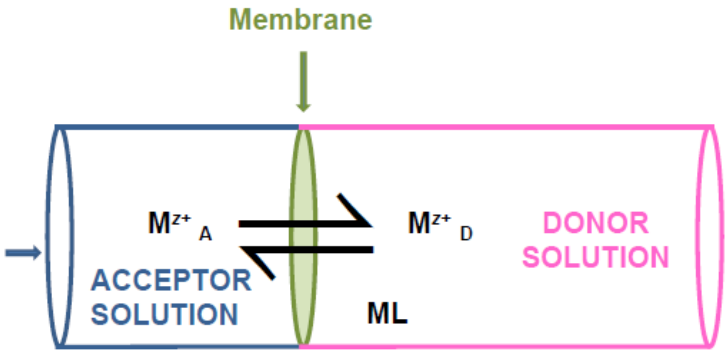

Figure 1-23. Scheme of a DMT cell

The physicochemical basis of the technique is that equilibrium between the acceptor and donor phases means that the electrochemical potential of the species able to cross the membrane should be the same in the donor as in the acceptor solution.

$$\tilde{\mu}^{A}_{M^{z+}} = \tilde{\mu}^{D}_{M^{z+}}$$

where superscripts D and A refer to the Donor and Acceptor solutions and *z* to the charge of the cation.

Previous expression can be expanded taking into account the activity (indicated by curly brackets), its standard value and the electrostatic potential (ϕ):

$$\mu^{0}_{M^{z+}} + RT\ln\left\{M^{z+}\right\}^{A} + 2F\phi^{A} = \mu^{0}_{M^{z+}} + RT\ln\left\{M^{z+}\right\}^{D} + 2F\phi^{D} \quad (1\text{-}18)$$

Then, a specific ion (whose main requirement is not to form complexes in the donor solution) is taken as the "reference" ion (R), so that when the equilibrium state is reached, the electrochemical potential of this ion is the same in both solutions (donor and acceptor).

$$\tilde{\mu}^{A}_{R^{z+}} = \tilde{\mu}^{D}_{R^{z+}}$$

$$\mu^{0}_{R^{z+}} + RT\ln\left\{R^{z+}\right\}^{A} + 2F\phi^{A} = \mu^{0}_{R^{z+}} + RT\ln\left\{R^{z+}\right\}^{D} + 2F\phi^{D} \quad (1\text{-}19)$$

By simple algebra subtracting eqns (1-18) and (1-19), one obtains

$$\left\{M^{z_M}\right\}_D = \left\{M^{z_M}\right\}_A \left(\frac{\left\{R^{z_R}\right\}_D}{\left\{R^{z_R}\right\}_A}\right)^{z_M/z_R} \quad (1\text{-}20)$$

This relationship between the reference ion and the analyte means that the activity of the metal of interest M present in the donor side can be computed from the activity of that analyte in the acceptor solution and the activities of the reference cation (Kalis et al., 2007).

Eq (1-20) indicates that equilibrium might have not been reached even if the activities of a given cation have a common value in both donor and acceptor solutions. Instead, both activities can differ at equilibrium by the presence of a Donnan factor due to the arising of an electric potential between both solutions. Indeed:

$$\Pi = \left(\frac{\left\{R^{z_R}\right\}_D}{\left\{R^{z_R}\right\}_A}\right)^{1/z_R} \quad (1\text{-}21)$$

where Π corresponds to the Donnan factor for a monovalent cation (Temminghoff et al., 2000).

If the activity coefficients are similar in the donor and in the acceptor solutions, the free concentration of M in the donor solution can be computed from concentrations as:

$$\left[M^{z_M}\right]_D = \left[M^{z_M}\right]_A \left(\frac{\left[R^{z_R}\right]_D}{\left[R^{z_R}\right]_A}\right)^{z_M/z_R} \quad (1\text{-}22)$$

The selection of the anions of the salt present in the acceptor is important as, up to a certain point, all of them could form (positive, negative or uncharged) complexes with the cations. So, in the typical configuration, the selected anion forms a very weak complex with the cation in order to have a negligible contribution of inorganic cation complex on the acceptor side when the system reaches equilibrium.

1.5.2 Experimental implementation

Initially, one key point to ensure a good development of the experiment is to prepare the membranes in a correct way. In that sense, a cleaning method has to be followed where the membranes are submerged in different media, but always with a constant stirring:

- ✓ in HNO_3 0.1 mol L^{-1} during 1h 30min to avoid a possible contamination due to metals that could remain in the membranes. (This action is repeated twice)

- ✓ in Milli-Q water during 1h 30min to clean and eliminate the acid. (This action is repeated twice)

- ✓ in a solution of the chosen supporting electrolyte at the desired pH, but 500 times more concentrated with the aim of saturating the membranes with the desired salt (this action is repeated twice). This is a very important point as the objective when saturating the membrane is to make sure that the protons which finally remain in the membrane correspond to the desired pH, and this usually implies a drastic pH change takes place in that point.

With that aim in mind, it is recommended to leave the membranes during at least one night to ensure a complete saturation of the membrane making the necessary pH adjustment. Then, when this concentrated solution is removed to repeat the process, the pH should not decrease as much as previously. As mentioned before, this is an important point as a change in pH will affect the system which is to be studied.

- ✓ Milli-Q water 1h 30min to clean the membranes.
- ✓ in a solution with the desired supporting electrolyte at the same concentration as in the DMT measurement during 1h 30 min (this action is repeated three times). So we make sure that the membrane will be in equilibrium with the supporting electrolyte.

Once the membranes are ready, they are put in the cell as seen in Figure 1-23. In the device (see Fig 1-24), the donor and the acceptor sides of the cell are connected to the donor and acceptor reservoirs, with tubes indicated by the pink and blue tubes, respectively, and the flux is fixed by a peristaltic bomb.

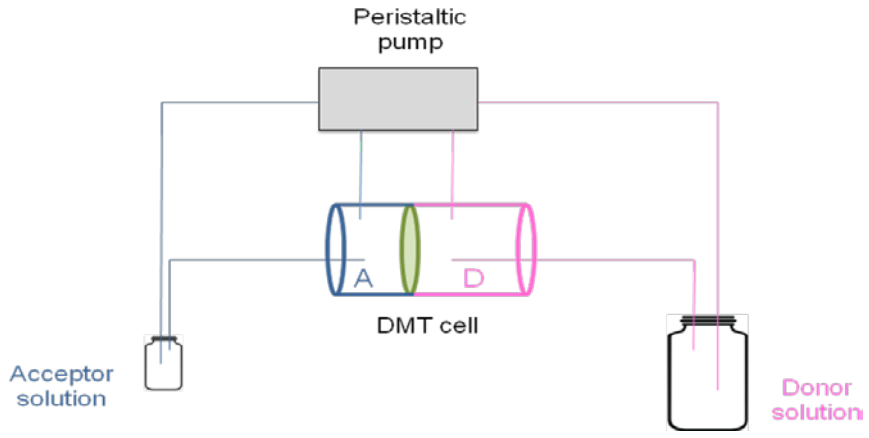

Figure 1-24. Scheme of the DMT device.

Firstly, the bomb starts with the recirculation. Here is important to eliminate the possible air bubbles formed when the solutions enter to the cell. Then, when at the both sides of the membrane the cavities are full of liquid, it is considered that the experiment has started and the sample (from the acceptor solution) at t=0 s is taken and the pH is controlled. After this first sample, every certain time the sampling procedure is repeated until the end of the experiment when both solutions have reached the equilibrium state. Finally, the total metal ion concentration in the acceptor solution, which corresponds to the free fraction (due to the negligible complexation in the acceptor solution), can be determined by ICP-MS.

1.5.3 DMT developments

With the aim of making in situ measurements, a new cell, called field-cell, was designed (Kalis et al., 2006b).

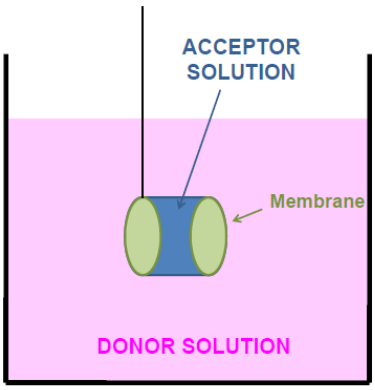

Figure 1-25. Scheme of a field DMT device.

In that case, as seen in Figure 1-25, there is just one compartment in the cell with two exchange membranes at both sides in contact with the donor solution (in that case, a natural sample) (Kalis et al., 2007). Here it is not necessary the use of a peristaltic pump as the own movement of the sample (e.g. the river flow, natural convection, or external stirring) acts like it.

1.5.4 DMT measurements in natural samples

The DMT technique has also been used to determine free metal concentrations in non-synthetic solutions such as:

a) *Natural waters*:

Several water samples from the rivers Rhine and Furtbach and lake Greifen were taken to determine free Cd, Ni, Pb, Cu and Zn concentration (Kalis et al., 2006a). In that case, 2 or 3 days were enough to reach Donnan equilibrium.

In order to validate the use of DMT technique in natural waters, the results obtained when analysing Rhine river water were compared with the corresponding ones obtained, using in that case AGNES technique (Chito et al., 2012). The results show that both techniques are useful to determine free metal ion concentrations although both have some advantages and drawbacks as for example the longer time needed in the case of DMT to obtain the results.

b) *Soils:*

DMT technique could be used to determine free metal concentrations in soil extracts. In (Kim and Owens, 2009) free Cd, Cu, Pb and Zn concentrations were determined from the extracts obtained from soil samples collected at different places which included residential areas, public parks and playgrounds among others. In this case, the final free metal concentration determined by DMT was in good agreement with the prediction. But a loss in the total Pb concentration was observed and attributed to the adsorption at the exchange membrane. This fact needed to be taken into consideration as it could be a possible source of error when using DMT.

c) Milk:

Different types of solutions (series of $CaCl_2$-KCl solutions, simulated milk ultrafiltrate, SMUF, and reconstituted skim milk) were used to determine free Ca, Mg, K and Na concentrations (Gao et al., 2009). It has been shown

that DMT technique was useful as the free concentrations were successfully determined without any matrix interference. Moreover, in this case, DMT presents a clear advantage over ISE technique when determining Ca and Mg as the determination could be done at different temperatures up to 120ºC due to the resistance of the exchange membrane. This is an important point because the calcium electrode cannot be used at the pasteurization temperature.

1.6 Outline of the thesis

The main objective of this thesis is to determine free metal concentrations in different types of natural samples using the electroanalytical technique AGNES and the non-electroanalytical technique DMT. As a prior step, the possible impact of electrodic adsorption on AGNES signal is elucidated. Then, these techniques are applied to study the system Zn-Glutathione in the root extracts of *Hordeum Vulgare* and in wine (in both cases first in synthetic samples and then in natural ones).

Below, a brief summary of each chapter is indicated:

In chapter 2, the phenomenon of the electrodic adsorption is studied in detail. AGNES is used to determine free metal concentrations in several systems which show induced adsorption by performing various titrations to check if there exist any possible alteration of the analytical signal used in AGNES (either intensity or charge) due to its presence.

In chapter 3, AGNES is applied to determine the free zinc concentration in root extracts of *Hordeum Vulgare*. First, the system Zn-Glutathione (given that this ligand is the most abundant in the natural sample) is studied in synthetic solutions. Complexation constants reported in the bibliography are used to compare theoretical and experimental results. Then the most appropriate models constant are taken to compare the theoretical predictions with AGNES determinations of the free zinc concentration in the root extracts.

In chapter 4, the determination of the free metal concentration in wine samples is performed with DMT and AGNES. As in the previous chapter, initially speciation is studied in synthetic solutions composed, in this case, by Zn, tartrate (as major wine

ligand) and 13.5% of ethanol. In the case of DMT, prior to the free metal concentration determination, a study about suitable reference ions is performed. Then, the results obtained with DMT are compared with the corresponding ones from AGNES, because (due to the non-aqueous nature of the sample), the usual speciation program used to obtain the theoretical results (VMinteq) cannot be used. Afterwards, both techniques are applied in real wine to determine the free metal concentrations of several cations.

Chapter 5 gathers the main conclusions of this work.

1.7 References

A.S.Mohammed, A.Kapri, R.Goel, 2011. Heavy Metal Pollution: Source, Impact and Remedies. Biomanagement of Metal-Contaminated Soils. Springer Science, pp. 1-28.

Aguilar,D., Parat,C., Galceran,J., Companys,E., Puy,J., Authier,L., Potin-Gautier,M., 2013. Determination of free metal ion concentrations with AGNES in low ionic strength media, *J. Electroanal. Chem.* 689, pp. 276-283.

Almestrand,L., Jagner,D., Renman,L., 1987. Automated-Determination of Cadmium and Lead in Whole-Blood by Computerized Flow Potentiometric Stripping with Carbon-Fiber Electrodes, *Anal. Chim. Acta* 193, pp. 71-79.

Alves,G.M.S., Rocha,L.S., Soares,H.M.V.M., 2017. Multi-element determination of metals and metalloids in waters and wastewaters, at trace concentration level, using electroanalytical stripping methods with environmentally friendly mercury free-electrodes: A review, *Talanta* 175, pp. 53-68.

Anderson,M.A., Morel,F.M.M., Guillard,R.R.L., 1978. Growth limitation of a coastal diatom by low zinc ion activity, *Nature* 276, pp. 70-71.

Arino,C., Serrano,N., Diaz-Cruz,J.M., Esteban,M., 2017. Voltammetric determination of metal ions beyond mercury electrodes. A review, *Anal. Chim. Acta* 990, pp. 11-53.

Bakker,E., Buhlmann,P., Pretsch,E., 1997. Carrier-based ion-selective electrodes and bulk optodes. 1. General characteristics, *Chem. Rev.* 97, pp. 3083-3132.

Bansod,B., Kumar,T., Thakur,R., Rana,S., Singh,I., 2017. A review on various electrochemical techniques for heavy metal ions detection with different sensing platforms, *Biosens. Bioelectron.* 94, pp. 443-455.

Bard,A.J., Faulkner,L.R., 1980. Electrochemical Methods, Fundamentals and Applications. Wiley, New York.

Batley,G.E., Apte,S.C., Stauber,J.L., 2004. Speciation and bioavailability of trace metals in water: Progress since 1982, *Aust. J. Chem.* 57, pp. 903-919.

Bruins,M.R., Kapil,S., Oehme,F.W., 2000. Microbial resistance to metals in the environment, *Ecotox. Environ. Safe.* 45, pp. 198-207.

Chito,D., Methodological advancements of AGNES and its implementation for the determination of free metal ion concentrations in synthetic and natural samples., PhD thesis. Universitat de Lleida., (2012).

Chito,D., Galceran,J., Companys,E., Puy,J., 2013. Determination of the Complexing Capacity of Wine for Zn Using the Absence of Gradients and Nernstian Equilibrium Stripping Technique, *J. Agric. Food Chem.* 61, pp. 1051-1059.

Chito,D., Weng,L., Galceran,J., Companys,E., Puy,J., van Riemsdijk,W.H., van Leeuwen,H.P., 2012. Determination of free Zn^{2+} concentration in synthetic and natural samples with AGNES (Absence of Gradients and Nernstian Equilibrium Stripping) and DMT (Donnan Membrane Technique), *Sci. Total Envir.* 421-422, pp. 238-244.

Cleven,R., Fokkert,L., 1994. Potentiometric Stripping Analysis of Thallium in Natural-Waters, *Anal. Chim. Acta* 289, pp. 215-221.

Companys,E., Cecília,J., Codina,G., Puy,J., Galceran,J., 2005. Determination of the concentration of free Zn^{2+} with AGNES using different strategies to reduce the deposition time., *J. Electroanal. Chem.* 576, pp. 21-32.

Companys,E., Galceran,J., Pinheiro,J.P., Puy,J., Salaün,P., 2017. A review on electrochemical methods for trace metal speciation in environmental media, *Curr. Opin. Electrochem.* 3, pp. 144-162.

Companys,E., Galceran,J., Puy,J., Sedo,M., Vera,R., Antico,E., Fontas,C., 2018. Comparison of different speciation techniques to measure Zn availability in hydroponic media, *Anal. Chim. Acta* 1035, pp. 32-43.

Companys,E., Naval-Sanchez,M., Martinez-Micaelo,N., Puy,J., Galceran,J., 2008. Measurement of free zinc concentration in wine with AGNES, *J. Agric. Food Chem.* 56, pp. 8296-8302.

Companys,E., Puy,J., Galceran,J., 2007. Humic acid complexation to Zn and Cd determined with the new electroanalytical technique AGNES, *Environ. Chem.* 4, pp. 347-354.

Cremazy,A., Leclair,S., Mueller,K., Vigneault,B., Campbell,P., Fortin,C., 2015. Development of an In Situ Ion-Exchange Technique for the Determination of Free Cd, Co, Ni, and Zn Concentrations in Freshwaters, *Aquat. Geochem.* 21, pp. 259-279.

David,C., Galceran,J., Rey-Castro,C., Puy,J., Companys,E., Salvador,J., Monné,J., Wallace,R., Vakourov,A., 2012. Dissolution kinetics and solubility of ZnO nanoparticles followed by AGNES., *J. Phys. Chem. C* 116, pp. 11758-11767.

Davison,W., Zhang,H., 2012. Progress in understanding the use of diffusive gradients in thin films (DGT) – back to basics, *Environ. Chem.* 9, pp. 1-13.

Davison,W., Zhang,H., Grime,G.W., 1994. Performance-characteristics of gel probes used for measuring the chemistry of pore waters, *Environ. Sci. Technol.* 28, pp. 1623-1632.

Domingos,R.F., Carreira,S., Galceran,J., Salaün,P., Pinheiro,J.P., 2016. AGNES at vibrated gold microwire electrode for the direct quantification of free copper concentrations, *Anal. Chim. Acta* 920, pp. 29-36.

Domingos,R.F., Huidobro,C., Companys,E., Galceran,J., Puy,J., Pinheiro,J.P., 2008. Comparison of AGNES (Absence of Gradients and Nernstian Equilibrium

Stripping) and SSCP (Scanned Stripping Chronopotenciometry) for Trace Metal Speciation Analysis, *J. Electroanal. Chem.* 617, pp. 141-148.

Domingos,R.F., Simon,D.F., Hauser,C., Wilkinson,K.J., 2011. Bioaccumulation and Effects of CdTe/CdS Quantum Dots on Chlamydomonas reinhardtii - Nanoparticles or the Free Ions?, *Environ. Sci. Technol.* 45, pp. 7664-7669.

Duffus,J.H., 2002. "Heavy metals" - A meaningless term? (IUPAC technical report), *Pure Appl. Chem.* 74, pp. 793-807.

Duval,J.F.L., Farinha,J.P.S., Pinheiro,J.P., 2013. Impact of Electrostatics on the Chemodynamics of Highly Charged Metal-Polymer Nanoparticle Complexes, *Langmuir* 29, pp. 13821-13835.

Estela,J.M., Tomas,C., Cladera,A., CERDA,V., 1995. Potentiometric Stripping Analysis - A Review, *Crit. Rev. Anal. Chem.* 25, pp. 91-141.

Fortin,C., Campbell,P.G.C., 1998. An ion-exchange technique for free-metal ion measurements (Cd^{2+}, Zn^{2+}): Applications to complex aqueous media, *Int. J. Environ. Anal. Chem.* 72, pp. 173-194.

Fortin,C., Couillard,Y., Vigneault,B., Campbell,P.G.C., 2010. Determination of free Cd, Cu and Zn concentrations in lake waters by *in situ* diffusion followed by column equilibration ion-exchange., *Aquat. Geochem.* 16, pp. 151-172.

Froning,M., Mohl,C., Ostapczuk,P., 1993. Interlaboratory Quality-Control for Lead Determination in Wine by Potentiometric Stripping Analysis, *Fresenius J. Anal. Chem.* 345, pp. 233-235.

Galceran,J., Chito,D., Martinez-Micaelo,N., Companys,E., David,C., Puy,J., 2010. The impact of high Zn^{o} concentrations on the application of AGNES to determine free Zn(II) concentration, *J. Electroanal. Chem.* 638, pp. 131-142.

Galceran,J., Companys,E., Puy,J., Cecília,J., Garcés,J.L., 2004. AGNES: a new electroanalytical technique for measuring free metal ion concentration, *J. Electroanal. Chem.* 566, pp. 95-109.

Galceran,J., Huidobro,C., Companys,E., Alberti,G., 2007. AGNES: a technique for determining the concentration of free metal ions. The case of Zn(II) in coastal Mediterranean seawater., *Talanta* 71, pp. 1795-1803.

Galceran,J., Lao,M., David,C., Companys,E., Rey-Castro,C., Salvador,J., Puy,J., 2014. The impact of electrodic adsorption on Zn, Cd or Pb speciation measurements with AGNES, *J. Electroanal. Chem.* 722-723, pp. 110-118.

Galceran,J., Puy,J., 2015. Interpretation of diffusion gradients in thin films (DGT) measurements: a systematic approach, *Environ. Chem.* 12, pp. 112-122.

Gao,R., Temminghoff,E.J.M., van Leeuwen,H.P., van Valenberg,H.J.F., Eisner,M.D., van Boekel,M.A.J.S., 2009. Simultaneous determination of free calcium, magnesium, sodium and potassium ion concentrations in simulated milk ultrafiltrate and reconstituted skim milk using the Donnan Membrane Technique, *Int. Dairy J.* 19, pp. 431-436.

Gozzo,M.L., Colacicco,L., Calla,C., Barbaresi,G., Parroni,R., Giardina,B., Lippa,S., 1999. Determination of copper, zinc, and selenium in human plasma and urine samples by potentiometric stripping analysis and constant current stripping analysis, *Clinica Chimica Acta* 285, pp. 53-68.

Gramlich,A., Tandy,S., Slaveykova,V.I., Duffner,A., Schulin,R., 2012. The use of permeation liquid membranes for free zinc measurements in aqueous solution, *Environ. Chem.* 9, pp. 429-437.

Gunkel-Grillon,P., Buffle,J., 2008. Speciation of Cu(II) with a flow-through permeation liquid membrane: discrimination between free copper, labile and inert Cu(II) complexes, under natural water conditions, *Analyst.* 133, pp. 954-961.

Gustafsson,J.P. Visual MINTEQ version 3.1. https://vminteq.lwr.kth.se/download/. 2016.

Helaluddin,A.B.M., Khalid,R.S., Alaama,M., Abbas,S.A., 2016. Main Analytical Techniques Used for Elemental Analysis in Various Matrices, *Tropical Journal of Pharmaceutical Research* 15, pp. 427-434.

Huidobro,C., Companys,E., Puy,J., Galceran,J., Pinheiro,J.P., 2007. The use of microelectrodes with AGNES, *J. Electroanal. Chem.* 606, pp. 134-140.

Jagner,D., 1982. Potentiometric stripping analysis - A review, *Analyst.* 107, pp. 593-599.

Jagner,D., Josefson,M., Westerlund,S., 1981. Simultaneous Determination of Cadmium and Lead in Urine by Means of Computerized Potentiometric Stripping Analysis, *Anal. Chim. Acta* 128, pp. 155-161.

Kalis,E.J.J., Temminghoff,E.J.M., Weng,L.P., van Riemsdijk,W.H., 2006a. Effects of humic acid and competing cations on metal uptake by Lolium perenne, *Environ. Toxicol. Chem.* 25, pp. 702-711.

Kalis,E.J.J., Weng,L.P., Dousma,F., Temminghoff,E.J.M., van Riemsdijk,W.H., 2006b. Measuring free metal ion concentrations in situ in natural waters using the Donnan Membrane Technique, *Environ. Sci. Technol.* 40, pp. 955-961.

Kalis,E.J.J., Weng,L.P., Temminghoff,E.J.M., van Riemsdijk,W.H., 2007. Measuring free metal ion concentrations in multicomponent solutions using the Donnan membrane technique, *Anal. Chem.* 79, pp. 1555-1563.

Kim,K.R., Owens,G., 2009. Chemodynamics of heavy metals in long-term contaminated soils: Metal speciation in soil solution, *Journal of Environmental Sciences* 21, pp. 1532-1540.

Lu,Y.Y., Liang,X.Q., Niyungeko,C., Zhou,J.J., Xu,J.M., Tian,G.M., 2018. A review of the identification and detection of heavy metal ions in the environment by voltammetry, *Talanta* 178, pp. 324-338.

Menegario,A.A., Yabuki,L.N.M., Luko,K.S., Williams,P.N., Blackburn,D.M., 2017. Use of diffusive gradient in thin films for in situ measurements: A review on the progress in chemical fractionation, speciation and bioavailability of metals in waters, *Anal. Chim. Acta* 983, pp. 54-66.

Mongin,S., Uribe,R., Puy,J., Cecilia,J., Galceran,J., Zhang,H., Davison,W., 2011. Key role of the resin layer thickness in the lability of complexes measured by DGT, *Environ. Sci. Technol.* 45, pp. 4869-4875.

Mongin,S., Uribe,R., Rey-Castro,C., Cecilia,J., Galceran,J., Puy,J., 2013. Limits of the Linear Accumulation Regime of DGT Sensors, *Environ. Sci. Technol.* 47, pp. 10438-10445.

Mota,A.M., Correia dos Santos,M.M., 1995. Trace Metal Speciation of Labile Chemical Species in Natural Waters: Electrochemical Methods. In: A. Tessier and D. R. Turner (Eds.). Metal Speciation and Bioavailability in Aquatic Systems. John Wiley & Sons, Chichester, pp. 205-258.

Paquin,P.R., Gorsuch,J.W., Apte,S., Batley,G.E., Bowles,K.C., Campbell,P.G.C., Delos,C.G., Di Toro,D.M., Dwyer,R.L., Galvez,F., Gensemer,R.W., Goss,G.G., Hogstrand,C., Janssen,C.R., McGeer,J.C., Naddy,R.B., Playle,R.C., Santore,R.C., Schneider,U., Stubblefield,W.A., Wood,C.M., Wu,K.B., 2002. The biotic ligand model: a historical overview, *Comp. Biochem. Physiol. C* 133, pp. 3-35.

Parat,C., Aguilar,D., Authier,L., Potin-Gautier,M., Companys,E., Puy,J., Galceran,J., 2011a. Determination of Free Metal Ion Concentrations Using Screen-Printed Electrodes and AGNES with the Charge as Response Function, *Electroanal.* 23, pp. 619-627.

Parat,C., Authier,L., Aguilar,D., Companys,E., Puy,J., Galceran,J., Potin-Gautier,M., 2011b. Direct determination of free metal concentration by implementing stripping chronopotentiometry as second stage of AGNES, *Analyst.* 136, pp. 4337-4343.

Parat,C., Authier,L., Castetbon,A., Aguilar,D., Companys,E., Puy,J., Galceran,J., Potin-Gautier,M., 2015. Free Zn^{2+} determination in natural freshwaters of the Pyrenees: towards on-site measurements with AGNES, *Environ. Chem.* 12, pp. 329-337.

Parat,C., Schneider,A., Castetbon,A., Potin-Gautier,M., 2011c. Determination of trace metal speciation parameters by using screen-printed electrodes in stripping chronopotentiometry without deaerating, *Anal. Chim. Acta* 688, pp. 156-162.

Pearson,H.B.C., Galceran,J., Companys,E., Braungardt,C., Worsfold,P., Puy,J., Comber,S., 2016. Absence of Gradients and Nernstian Equilibrium Stripping (AGNES) for the determination of [Zn2+] in estuarine waters, *Anal. Chim. Acta* 912, pp. 32-40.

Pernet-Coudrier,B., Companys,E., Galceran,J., Morey,M., Mouchel,J.M., Puy,J., Ruiz,N., Varrault,G., 2011. Pb-binding to various dissolved organic matter in urban aquatic systems: Key role of the most hydrophilic fraction, *Geochim. Cosmochim. Ac.* 75, pp. 4005-4019.

Pesavento,M., Alberti,G., Biesuz,R., 2009. Analytical methods for determination of free metal ion concentration, labile species fraction and metal complexation capacity of environmental waters: A review, *Anal. Chim. Acta* 631, pp. 129-141.

Puy,J., Galceran,J., Huidobro,C., Companys,E., Samper,N., Garcés,J.L., Mas,F., 2008. Conditional Affinity Spectra of Pb^{2+}-Humic Acid Complexation from Data Obtained with AGNES, *Environ. Sci. Technol.* 42, pp. 9289-9295.

Puy,J., Galceran,J., Rey-Castro,C., 2016. Interpreting the DGT measurement: speciation and dynamics. In: W. Davison (Eds.). Diffusive Gradients in Thin-Films for environmental measurements. Cambridge University Press, Cambridge, pp. 93-122.

Ribeiro,W.F., da Costa,D.J.E., Lourenco,A.S., de Medeiros,E.P., Salazar-Banda,G.R., do Nascimento,V.B., Araujo,M.C.U., 2017. Adsorptive Stripping Voltammetric Determination of Trace Level Ricin in Castor Seeds Using a Boron-doped Diamond Electrode, *Electroanal.* 29, pp. 1783-1793.

Rocha,L.S., Companys,E., Galceran,J., Carapuca,H.M., Pinheiro,J.P., 2010. Evaluation of thin mercury film rotating disc electrode to perform Absence of Gradients and Nernstian Equilibrium Stripping (AGNES) measurements, *Talanta* 80, pp. 1881-1887.

Rocha,L.S., Galceran,J., Puy,J., Pinheiro,J.P., 2015. Determination of the Free Metal Ion Concentration Using AGNES Implemented with Environmentally Friendly Bismuth Film Electrodes, *Anal. Chem.* 87, pp. 6071-6078.

Serrano,N., Diaz-Cruz,J.M., Arino,C., Esteban,M., 2007. Stripping chronopotentiometry in environmental analysis, *Electroanal.* 19, pp. 2039-2049.

Skoog,D.A., Holler,F.A., Nieman,T.A., 2001. Principios de análisis instrumental. McGraw Hill, Madrid.

Temminghoff,E.J.M., Plette,A.C.C., van Eck,R., van Riemsdijk,W.H., 2000. Determination of the chemical speciation of trace metals in aqueous systems by the Wageningen Donnan Membrane Technique, *Anal. Chim. Acta* 417, pp. 149-157.

Tomaszewski,L., Buffle,J., Galceran,J., 2003. Theoretical and analytical characterization of a flow-through permeation liquid membrane with controlled flux for metal speciation measurements, *Anal. Chem.* 75, pp. 893-900.

Tonello,P.S., Goveia,D., Rosa,A., Fraceto,L., Menegario,A., 2011. Determination of labile inorganic and organic species of Al and Cu in river waters using the diffusive gradients in thin films technique, *Anal. Bioanal. Chem.* 399, pp. 2563-2570.

Town,R.M., Chakraborty,P., van Leeuwen,H.P., 2009. Dynamic DGT speciation analysis and applicability to natural heterogeneous complexes, *Environ. Chem.* 6, pp. 170-177.

Town,R.M., van Leeuwen,H.P., 2001. Fundamental features of metal ion determination by stripping chronopotentiometry, *J. Electroanal. Chem.* 509, pp. 58-65.

Uribe,R., Availability of metal cations in aquatic systems from DGT measurements, PhD thesis. Universitat de Lleida, (2012).

Vale,G., Franco,C., Brunnert,A.M., dos Santos,M.M.C., 2015. Adsorption of Cadmium on Titanium Dioxide Nanoparticles in Freshwater Conditions - A Chemodynamic Study, *Electroanal.* 27, pp. 2439-2447.

van den Berg,C.M.G., 1991. Potentials and potentialities of cathodic stripping voltammetry of trace-elements in natural-waters, *Anal. Chim. Acta* 250, pp. 265-276.

van Leeuwen,H.P., Town,R.M., 2002. Stripping chronopotentiometry for metal ion speciation analysis at a microelectrode, *J. Electroanal. Chem.* 523, pp. 16-25.

van Leeuwen,H.P., Town,R.M., 2007. Adsorptive stripping chronopotentiometry (AdSCP). Part 1: Fundamental features, *J. Electroanal. Chem.* 610, pp. 9-16.

Vera,R., Fontàs,C., Galceran,J., Serra,O., Anticó,E., 2018. Polymer inclusion membrane to access Zn speciation: Comparison with root uptake, *Sci. Total Envir.* 622–623, pp. 316-324.

Vigneault,B., Campbell,P.G.C., 2005. Uptake of cadmium by freshwater green algae: Effects of pH and aquatic humic substances, *J. Phycol.* 41, pp. 55-61.

Weng,L.P., van Riemsdijk,W.H., Temminghoff,E.J.M., 2005. Kinetic aspects of donnan membrane technique for measuring free trace cation concentration, *Anal. Chem.* 77, pp. 2852-2861.

Zavarise,F., Companys,E., Galceran,J., Alberti,G., Profumo,A., 2010. Application of the new electroanalytical technique AGNES for the determination of free Zn concentration in river water, *Anal. Bioanal. Chem.* 397, pp. 389-394.

CHAPTER 2

The impact of electrodic adsorption on Zn, Cd and Pb speciation measurements with AGNES

Results obtained in this chapter have been published in:

Journal of Electroanalytical Chemistry 722-723 (2014) 110-118

2.1. Abstract

The systems studied in this chapter (Cd with iodide or polyacrilic acid, Pb or Zn with xylenol orange, etc.) together with others previously studied in our laboratory (Pb/Cd/Zn with humic acids, Pb with pyridinedicarboxylic acid and organic extracts from river waters, etc), show induced adsorption of the metallic electroactive species on the mercury electrode. But this fact does not prevent the possibility of a correct determination of the free metal concentration in the solution with AGNES (Absence of Gradients and Nernstian Equilibrium Stripping). The special AGNES equilibrium situation reached at the end of the first stage is not affected by induced adsorption and the adoption of some strategies (like the use of charge as stripping analytical signal) could avoid a possible kinetic interference on the quantification stage. It has been demonstrated that the effect of adsorption on the blanks is not significant, but in case of being relevant, its impact could be avoided by choosing a higher gain or an AGNES variant (such as AGNELSV or AGNES-SCP) that does not require the blank substraction. Some surfactants in solution, even not exhibiting metal complexation, might block the electrode surface, so that more accurated methodologies have to be used in such systems. In the case of the dispersant accompanying Nanotek ZnO nanoparticles, the complete blockage of the electrode could be reached in around 100 s, and consequently electrodes with renovating drops are key for dealing with such kind of difficulties. The free Zn concentration in equilibrium with these nanoparticles determined by AGNES (with minimization of the deposition times and suppression of any stirring) is consistent with the one expected according to their primary particle size.

2.2. Introduction

The determination of free metal concentrations is significant to understand the availability and mobility of toxic metals and micronutrients in environmental and biological systems. Interpretative frameworks such as the Free Ion Activity Model (Tessier et al., 1994) and the Biotic Ligand Model (Campbell et al., 2002; Paquin et al., 2002) present the free ion concentration as the key variable for the assessment of such availability. In addition, in the modelling of the biogeochemical cycles of metals, information is needed about the binding properties of ligands, like natural organic matter, towards these elements, whose experimental determination

sometimes requires the specific measurement of the fraction of metal remaining as free ionic species.

The electroanalytical technique AGNES (*Absence of Gradients and Nernstian Equilibrium Stripping*), which is extensively presented in Chapter 1 (see section 1.4) has been particularly designed to measure free metal ion concentrations (Galceran et al., 2004; Companys et al., 2017). AGNES is divided into two stages: i) deposition step and ii) stripping step where the accumulated metal is quantified. The analytical signal used in the stripping stage could be the current or the charge (see section 1.4.3.3) and, depending on that, the suitable AGNES variant (AGNES-I, AGNES-Q (Galceran et al., 2010; Parat et al., 2011a), AGNELSV (Galceran et al., 2010) or AGNES-SCP (Parat et al., 2011a)) is choosen. AGNES has been successfully applied to the determination of free metal concentrations in a wide range of systems, as for example synthetic ligand solutions (Alberti et al., 2007; Huidobro et al., 2007; Domingos et al., 2008; Pinheiro et al., 2010; Rocha et al., 2010; Chito et al., 2010; Parat et al., 2011a; Parat et al., 2011b; Aguilar et al., 2013a; Aguilar et al., 2013b), natural samples (sea water (Galceran et al., 2007), river water (Zavarise et al., 2010; Chito et al., 2012) and soil extracts (Chito et al., 2012)), wine (Companys et al., 2008; Chito et al., 2013), solutions containing dissolved organic matter (Companys et al., 2007; Puy et al., 2008; Pernet-Coudrier et al., 2011), clay minerals (Rotureau, 2014) and also systems containing quantum dots (Domingos et al., 2011) and ZnO nanoparticles (David et al., 2012; Adam et al., 2013; Domingos et al., 2013; Mu et al., 2014a). However, a detailed analysis of the possible effects of adsorptive processes on the electrode surface regarding the accuracy of AGNES is still lacking.

Although induced electrodic adsorption (i.e. adsorption of an electroactive species via formation of a complex) is the base of some electroanalytical techniques (e.g. Cathodic Stripping Voltammetry (van den Berg, 1984) or AdSCP (van Leeuwen and Town, 2007; Town and van Leeuwen, 2007)), minimising its possible effect has been a challenge for most voltammetric techniques (including Anodic Stripping Voltammetry) (van Leeuwen et al., 1992; Garrigosa et al., 2008; Louis et al., 2008). The adsorption interference could even question the validity of several reported stability constants (Bond and Hefter, 1976). Reverse Pulse Polarography (RPP) was shown to be not affected by induced adsorption, but RPP could yet be affected by ligand adsorption (Galceran et al., 1994; Pinheiro et al., 1996; Puy et al., 1998; Companys et al., 2003). The minimisation of induced adsorption effects in SCP and SSCP has also been described (Town and van Leeuwen, 2002; Town and van Leeuwen, 2003; Serrano et al., 2007b).

Adsorption of non-electroactive species can also impact on voltammetric techniques. Their physical deposition on the electrode surface (resulting from this kind of adsorption) can hinder a correct application of various voltammetric techniques (Tercier and Buffle, 1996; Hoyer and Jensen, 2004), being one of the most serious sources of obstruction to reliable measurements of trace metal speciation. Strategies developed for overcoming interferences of adsorption based on the introduction of some modifications of the electrode surface have the drawback of their lack of reproducibility (Town and van Leeuwen, 2002).

As a result of the relative long deposition times in AGNES (typically of the order of 200 to 400 s, but also, of the order of 1000s or longer, depending on the system and the preconcentration gain), the extent of the various kinds of adsorption might be relevant and, consequently, its possible interference on AGNES measurements should be assessed.

The aim of this chapter is to study how electrodic adsorption can affect AGNES measurements. The study that has been carried out is based on the possible impact of adsorption on the first and second stage of AGNES firstly, for later on making a distinction in the quantification step depending on the chosen analytical response (current or charge). A few experimental systems have been selected (iodide, xylenol orange, polyacrylic acid and ZnO nanoparticles) as representatives of different chemical compositions (organic, inorganic) and molecular sizes (monoatomic ions, simple molecules, polymers and particles). All of them have been demonstrated to have a predisposition to adsorb on the mercury electrode and, as a result, they constitute suitable options for the testing of hypothetical interferences on the measurement of Zn, Cd and Pb (the most typical ions probed in voltammetry and having just one oxidation state in solution) with AGNES.

2.3. Experimental

2.3.1. Equipment

The voltammetric measurements were done using a μ-AUTOLAB type III potentiostat attached to a Metrohm 663 VA Stand and to a computer by means of the GPES 4.9 (Eco Chemie) and NOVA 1.8 (Eco Chemie) package softwares. The working electrode was a Metrohm Hanging Mercury Drop Electrode (HMDE) where the smallest drop (drop 1, which according to the catalogue corresponds to a radius r_0 = 1.41×10^{-4}m) was selected to perform AGNES experiments and the largest drop (drop 3, which corresponds to a radius r_0= 2.03×10^{-4} m) to perform Differential Pulse Polarograms (DPP) (see section 1.3.1.5) and Normal Pulse Polarograms (NPP). The auxiliary electrode was a glassy carbon electrode and the reference electrode was Ag|AgCl (3 mol L^{-1}) KCl, encased in a 0.1 mol L^{-1} KNO_3 jacket. Metrohm Ion Selective Electrodes (ISE) (see section 1.3.1.1) for Cd and Pb were used to measure free metal concentration. A CRISON 5203 glass combined electrode was attached to an Orion Research 720A+ ion analyser and introduced in the cell to control the pH. A glass jacketed cell, thermostated at 25.0ºC, was used in all experiments.

2.3.2. Reagents

Zn, Cd and Pb solutions were prepared from Merck 1000 mg/L standard solutions. Potassium nitrate or potassium chloride were used as supporting electrolytes and prepared from solid KNO_3 and KCl reagents (Fluka, Trace Select), respectively. Xylenol Orange (XO) and potassium iodide solutions were prepared from solid Sigma-Aldrich and Fluka (p.a.), respectively. Tris (hydroxymethyl)aminomethane (Merck, p.a.) and 2-(N-morpholino)ethanesulfonic acid (MES hydrate), (Sigma-Aldrich, >99.5%) were used to prepare buffer solutions to adjust the pH.

Polyacrylic acid, PAA, (Adrich, 35% wt. in water) has an average molecular weight of 250000. Stock solutions of 0.1 M (on a monomer basis) were prepared by dilution.

Nanotek ZnO nanoparticles (NP), with a nominal average primary particle diameter of 36 nm (according to the provider), were purchased from AlfaAesar (40% dispersion in water). The characterization data are detailed elsewhere (Mu et al., 2014a). These ZnO NPs have a surfactant coating so as to stabilize the dispersion, so no sonication was required during sample pretreatment. The exact composition of this additive was not disclosed by the supplier, although ATR-FTIR indicates the coating to be an aliphatic polyether (Mu et al., 2014b). In spite of their stability, Dynamic Light Scattering (using a Malvern Zetasizer Nano ZS) indicates that these NPs are somewhat aggregated in solution, with an average size of 180±8 nm. The analyzed dispersions were prepared by a large dilution of the commercial stock solution to reach an approximate concentration of 2×10^{-4} M in ZnO at pH=8.25 buffered with Tris 0.01M.

In all experiments, ultrapure water (Milli-Q, Millipore) was used.

2.3.3. Procedures

2.3.3.1. AGNES

This technique, which has been presented in section 1.4 of Chaptert 1, aims at the determination of free metal concentration after a special equilibrium situation is reached at the end of the deposition step (Chito et al., 2010) (see section 1.4.1) which leads to an absence of gradients in the concentration profiles at both sides of the electrode.

$$Y = \frac{[\mathrm{M}^0]}{[\mathrm{M}^{n+}]} = \exp\left[-\frac{2F}{RT}\left(E_1 - E^{0'}\right)\right] \quad (2\text{-}1)$$

Where $[M]^0$ corresponds to the concentration of reduced metal, $[M^{n+}]$ to the bulk free metal concentration, F to the Faraday constant, R to the gas constant, T to the temperature, E_1 to the the applied deposition potential and $E^{o'}$ to the formal potential of the redox couple. Y is the gain in metal concentration across the surface resulting from its preconcentration in the amalgam (see section 1.4.1) following the application of E_1 and, experimentally, is typically computed from the peak potential

of a DPP experiment with just metal and the background electrolyte (Galceran et al., 2004).

In its first implementations, the variant AGNES 1P was used: just one deposition potential (E_1) was applied at the first stage during a long enough time (t_1). But with the purpose of reducing this deposition time, later on, AGNES 2P (Companys et al., 2005) was implemented. It consisted in the splitting of the deposition stage into two sub-stages (1.4.3.2), where, for $t_{1,a}$ seconds, the applied potential $E_{1,a}$ corresponds to diffusion limited conditions for reduction (first substage) and, then, for $t_{1,b}$ seconds, the applied potential $E_{1,b}$ corresponds to the desired gain (denoted $Y_{1,b}$, Y_1 or just Y). During the time $t_{1,b}$ (second substage), the desired gain $Y_{1,b}$ is applied to compensate any excess (overshoot) or defect (undershoot) of material accumulated along in the first substage until *agne* (Absence of Gradients and Nernstian Equilibrium situation desired at the end of the first stage) is reached with the desired gain. Then, a waiting period of duration t_w is also applied at the $Y_{1,b}$ without stirring.

The goal of the second stage is the quantification of the accumulated metal (M^0) in the amalgam (1.4.1). The current or the charge in the stripping stage can be measured for this quantification (Galceran et al., 2014; Companys et al., 2017).

2.3.3.2. Other voltammetric techniques

NPP (Galceran et al., 1995; Bard and Faulkner, 2001) has been used to show induced adsorption through the appearance of a peak in the polarogram on top of the usual wave. Used parameters: pulse time 0.05 s, interval time 1 s, step potential 0.00105 and 0.00495 V and base potential -0.4 V.

DPP (pages 286-293 in (Bard and Faulkner, 2001)) has been used to establish the desired gains in AGNES (see Section 1.4). Parameters used: pulse time 0.05 s, interval time 1 s, step potential 0.00105 V and modulation potential 0.04995 V.

2.4. Results and discussion

2.4.1. Adsorption impact on the first stage

Firstly, let us consider the situation reached at the end of the first stage of AGNES (see Section 1.4.1): the Nernstian equilibrium stablished between the two forms of the metal. In these conditions, fundamental thermodynamic considerations lead to the straightforward conclusion that the presence of an *equilibrated* intermediate phase (for instance adsorbed metal, ligand or complex) would not influence the activities of the element related by the Nernstian equation, because the interfacial species would also be in equilibrium with the bulk species. Of course, we are also assuming that the masses of this intermediate phase and the one accumulated in the amalgam are negligible in comparison with the total mass of the analyte in the solution (as the bulk composition remains unalterable) and that the transference of metal between phases is possible.

Secondly, adsorption could modify the required time for equilibration or even delay it beyond its practical reach. Notice that, for *agne*, it is implicitly required that the amount of adsorbed complex ML (or L or any other connected to M) also fulfils its equilibrium with the bulk concentration of ML (van Leeuwen and Town, 2005). For this reason, any possible impact of electrodic adsorption on the first stage could only come from kinetic limitations, which can, in principle, be overcome (by waiting until stabilization) except in very dramatic situations (such as perfect blocking of the charge transfer at the electrode surface, see section 2.4.1.2 below).

2.4.1.1. Induced adsorption

We first consider accuratelly the case of induced adsorption where the analyte (the metal M^{n+}) accumulates on the electrode surface, during the deposition stage, via the formation of a complex ML (van Leeuwen et al., 1992).

The systems Pb+XO (Wu and Batley, 1995; Town and van Leeuwen, 2007), Zn+XO (Ensafi et al., 2004), Cd+PAA (Díaz-Cruz et al., 1991) and Cd+I (Casassas and Arino, 1986; Guaus and Sanz, 1999; Zelic and Lovric, 2003) have been chosen as

previously they had been reported in the literature to show induced adsorption on the mercury electrode.

A diagnostic of induced adsorption can be obtained from the observation of a peak in an NPP. In the particular case of PbXO, the peak is also shifted with respect to the half wave potential (see Fig 2-1) as predicted for very strong induced adsorption (Puy et al., 1993). We have checked that similar phenomena take place with ZnXO (see Fig 2-2).

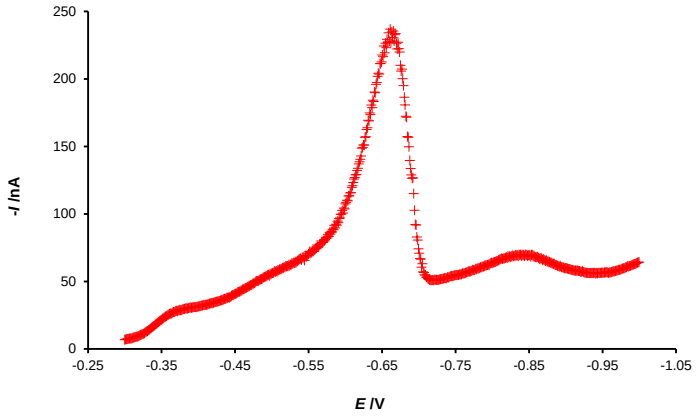

Figure 2-1. Normal Pulse Polarogram in the system Pb+xylenol orange, showing the typical peak of strong induced adsorption. $c_{T,Pb}$= 1.57×10^{-5} mol L^{-1}, $c_{T,XO}$= 8.99×10^{-6} mol L^{-1} and pH=6.802 in 0.1 mol L^{-1} KNO_3. E_{base}= -0.1 V.

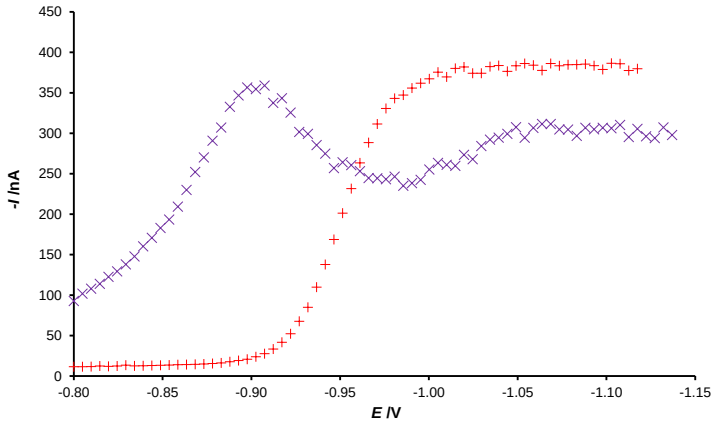

Figure 2-2. NPP in KNO_3 0.1mol L^{-1} background electrolyte. Markers (+) correspond to the solution with just metal where $c_{T,Zn}$= 5.03×10^{-5} mol L^{-1}. Markers (×), showing the typical adsorption peak, correspond to the solution with the metal and the ligand $c_{T,XO}$= 1.01×10^{-4} mol L^{-1}.

2.4.1.1.1. Impact of induced adsorption on equilibrium

In the case of the Cd+PAA system, as seen in Fig 2-3, the values recorded following the standard application of AGNES are in excellent agreement with the ones obtained by Cd-ISE at the various essayed pH. It should be noted that there are other voltammetric techniques that require elaborate procedures to retrieve the free Cd concentrations in a system (Cd + polymethacrylic acid) very similar to this one (Puy et al., 1992; Mas et al., 1993; Garrigosa et al., 2008).

Another example of the negligible impact of induced electrodic adsorption on AGNES is given by the system Cd-I (see Fig 2-4). In fact, AGNES measurements of free Cd^{2+} concentrations in the titration experiments with iodide show a good agreement with speciation calculations using literature values (NIST 46.7) of the stability constants for CdI, as shown in Fig 2-5. Here, as the ionic strength increases with the addition of relevant amounts of iodide (in the same way as in (Chito et al., 2013)), there is a change in the prescribed gain even if the applied deposition potential is kept constant. This real gain can be computed with eqn (12) of ref. (Aguilar et al., 2013b), which simplifies to:

$$Y = \frac{\gamma_{M^{n+}}}{\gamma_{M^{n+}}^{\mu=0.1}} Y^{\mu=0.1} \qquad (2\text{-}2)$$

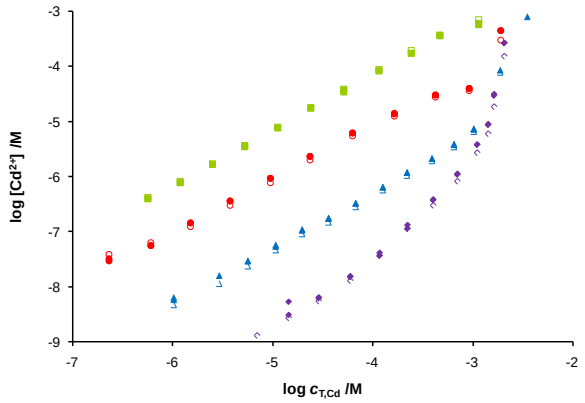

Figure 2-3. Free Cd concentration measured with AGNES-I (full markers) and with Cd-ISE (empty markers) at different pH (□ for pH = 4; ○ for pH = 5; Δ for pH = 6 and ◊ for pH = 7). PAA concentration = 5×10^{-3} mol L^{-1} and [KNO_3] = 0.1 mol L^{-1}. $Y_{1,a} = 10^{10}$, $t_{1,a}$ = 70 s, $Y_{1,b}$ = 100 s, $t_{1,b}$ = 210 s.

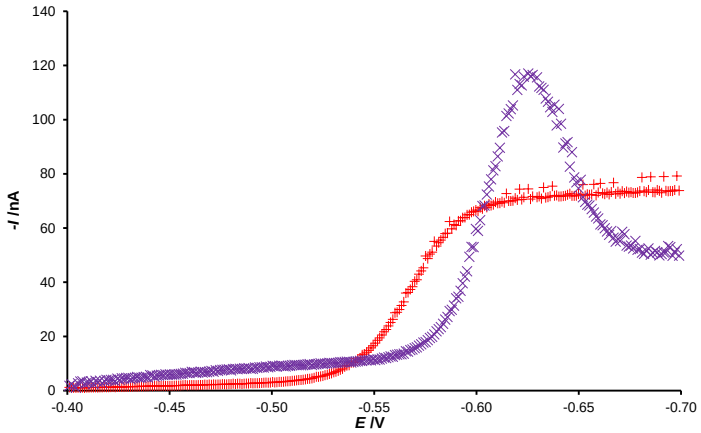

Figure 2-4. Normal Pulse Polarogram (NPP) in a solution at pH 6.04. Markers (+) correspond to the solution with just $c_{T,Cd}$= 1.12×10^{-5} mol L^{-1}, and markers (×) correspond to measurements after an addition of $c_{T,I}$= 2.70×10^{-2} mol L^{-1}.

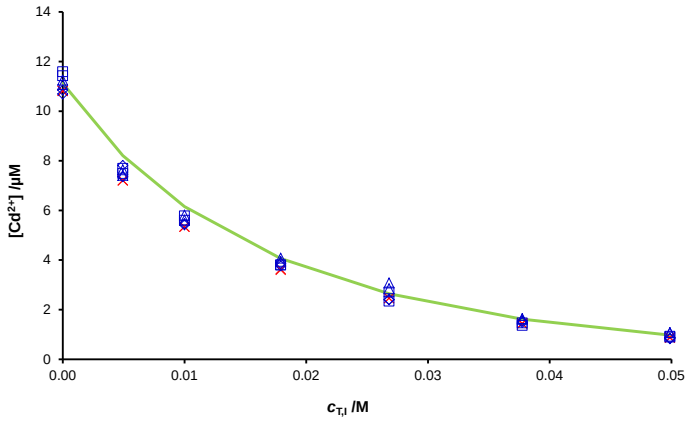

Figure 2-5. Free Cd concentration for different total iodide concentrations ($c_{T,I}$) added to a solution with initial total Cd concentration $c_{T,Cd}$= 1.24×10^{-}5 mol L^{-1} at pH= 6. Markers (×) correspond to the data obtained from AGNES-I, (Δ) to AGNES-Q, (□) to AGNELSV, (◊) to AGNES-SCP and green solid line to VMinteq prediction (NIST 46.7).

A titration of Pb with XO (see Fig 2-6) suggests a close agreement between AGNES and ISE measurements, and the theoretical expectations from literature values of the stability constants, see Table 2-1 are only a little below the experimental data (note the linear scale in the y-axis, in contrast with other logarithmic scales, e.g., in Fig 2-3). For additions of XO around 2 µmol L^{-1}, the difference between theoretical and experimental results might be due to small inaccuracies in the values of the constants or in the experimental setup.

Table 2-1. Stability constants taken from (Murakami et al., 1980)

Reaction	**Log K**
$M^{2+} + L^{6-} \rightleftharpoons ML^{4-}$	13.68 (K_{ML})
$M^{2+} + HL^{5-} \rightleftharpoons MHL^{3-}$	11.63 (K_{MHL})
$M^{2+} + H_2L^{4-} \rightleftharpoons MH_2L^{2-}$	5.39 (K_{MH_2L})
$H^{+} + ML^{4-} \rightleftharpoons MHL^{3-}$	10.08 (K^{H}_{MHL})
$H^{+} + MHL^{3-} \rightleftharpoons MH_2L^{2-}$	4.32 ($K^{H}_{MH_2L}$)
$M^{2+} + ML^{4-} \rightleftharpoons M_2L^{2-}$	12.45 (K_{M_2L})
$M^{2+} + MHL^{3-} \rightleftharpoons M_2HL^{-}$	6.47 (K_{M_2HL})
$H^{+} + M_2L^{2-} \rightleftharpoons M_2HL^{-}$	4.1 ($K^{H}_{M_2HL}$)

From these experiments and others performed in our lab with other systems exhibiting induced adsorption (humic acids (Companys et al., 2007; Puy et al., 2008; Pernet-Coudrier et al., 2011), pyridinedicarboxylic acid (Alberti et al., 2007; Huidobro et al., 2007), etc.), we conclude that induced adsorption does not distort the final equilibrium of AGNES in any of the systems studied so far, which is consistent with our current physicochemical interpretative framework of equilibrium not being affected by other equilibria processes.

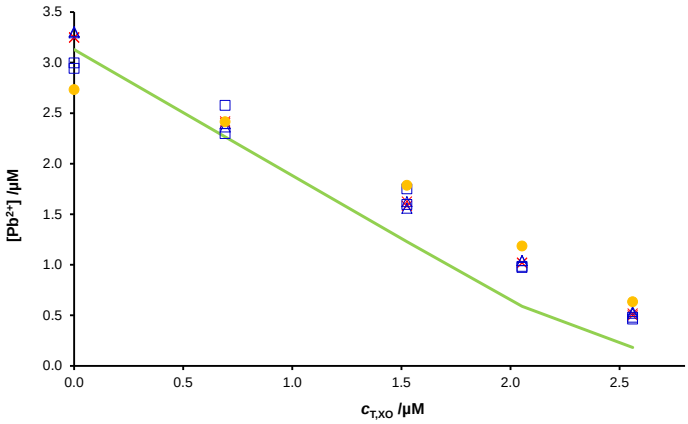

Figure 2-6. Plot of $[Pb^{2+}]$ vs $c_{T,XO}$ in a solution with initial $c_{T,Pb}$= 5.01×10^{-6} mol L^{-1} and different XO concentrations. pH= 6.090 (buffer MES 0.01 mol L^{-1}). Markers (×) correspond to the data obtained from AGNES-I, (Δ) to AGNES-Q, (□) to AGNELSV and (●) to ISE. The green line corresponds to a VMINTEQ calculation.

2.4.1.1.2. Impact of induced adsorption on the kinetics of equilibration

Even though reaching the prescribed *agne*, induced adsorption might delay the practical approach to the equilibrium by blocking the surface or by requiring the slow transport of a huge amount of ML so as to satisfy its adsorption equilibrium at the electrode surface (i.e. for some strongly adsorbing systems (van Leeuwen and Town, 2005)).

In all systems analyzed in this chapter, we do not have evidence for any case of induced adsorption increasing the deposition times. From a practical point of view, we can set an upper limit to the deposition time as the one needed when there is only metal in the solution. If the required deposition time (for a specific gain) in the system with induced adsorption is larger than the only-metal deposition time, we would know, then, that adsorption has been taken an impact on the system. In this case, the adsorption would have been large enough to overcompensate the contribution of the complexes to the flux (which shortens the deposition times unless they are totally inert complexes). The required deposition times depend on the program used for the first stage: either 1P (the simplest one, see Section 1.4.1) or 2P

(Companys et al., 2005) (1.4.3.2). In our experience (Chito et al., 2010), for HMDE the rules for a sufficiently long deposition time are:

$$\begin{aligned} t_1 - t_w &= 7\,Y \qquad 1-\text{Pulse} \\ t_{1,a} &= 0.7\,Y \qquad 2-\text{Pulses} \end{aligned} \tag{2-3}$$

Fig 2-7 indicates that t_1-t_w≈200 s is enough to reach a gain of 50 and t_1-t_w≈1000 s for Y=200, which are much shorter than the times derived from the rule (350 s and 2800 s, respectively). This also means that the contribution of the complexes (possibly very labile) shortens the deposition time more than the increase in deposition time (if any) due to adsorption.

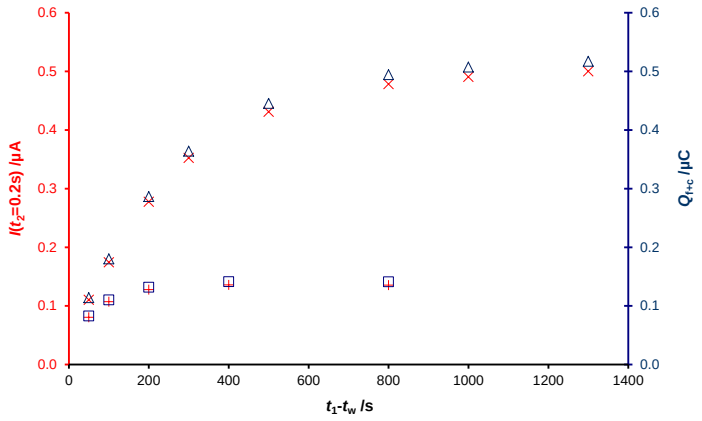

Figure 2-7. Trajectories of current (blue markers referred to the right ordinate axis) and charge (red markers referred to the left ordinate axis) *vs.* deposition time (t_1-t_w with t_w=50 s) for two gains: Y=50 (+ and □) and Y=200 (× and Δ). $c_{T,Pb}$= 4.99×10^{-6}mol L^{-1}, $c_{T,XO}$= 2.08×10^{-6} mol L^{-1} and pH=6.104 (buffer MES 0.01 mol L^{-1})

For PbXO under other conditions (of concentrations and pH), as for the other systems studied in this chapter, the comparison has always indicated that the possible delay of the adsorption on the deposition time is shorter than the reduction of time arising from the contribution of the complexes, because of this the standard rules (2-3) continue to be a useful guidelines.

2.4.1.2. Blockage of the electrode by surfactants

Otherwise, AGNES equilibrium could not be reached in a reasonable deposition time when there is some compound that quickly adsorbs onto the electrode surface to form a film, so densely packed and so strongly bound, as to kinetically hinder the reduction and oxidation processes.

We have found this blocking behaviour (or fouling, (Tercier and Buffle, 1996)) when studying the dissolution equilibrium of Nanotek ZnO nanoparticles, as a follow up of a work with other nanoparticles (David et al., 2012). The particularity of these NPs (in comparison to other NPs in a previous work) is the presence of an aliphatic polyether coating (Mu et al., 2014b), which acts as a dispersant to stabilize the ZnO suspensions, and whose exact composition is not disclosed by the manufacturer.

The undistorted shape of the NPP (see Fig 2-8) of the dispersion of NPs at pH=8.25 does not reveal induced adsorption. The DPP (Fig 2-9) in a solution containing the dispersant (e.g. a sample of Nanotek NPs at a sufficiently low pH, where all the ZnO is dissolved) is very similar to polarograms of Zn^{2+} solutions in absence of the dispersant. Furthermore, the lack of shift from pH=8.2 to pH=4.0 in the DPP peak measured in Nanotek samples (see 2-9) also indicates that the dispersant does not extensively complex Zn, so -if there is any induced adsorption-, it would have a negligible impact on AGNES. Additionally, the lack of distortions also suggest that dispersant adsorption during the short time of pulse polarography (1 s) without stirring is not significant.

Despite these findings, the performance of AGNES reveals some kind of interference occasioned by the presence of the dispersant. Fig 2-10 shows a plot of a strategy typically used in previous works to adjust the deposition times $t_{1,a}$ and $t_{1,b}$ (Companys et al., 2008; Pernet-Coudrier et al., 2011). Usually one finds that too long $t_{1,a}$-values produce overshoots (i.e. values above the equilibrium) which progressively decay ("relax") to the equilibrium value for increasing times $t_{1,b}$ while for short $t_{1,a}$-values the undershoot has to be compensated with additional (longer) $t_{1,b}$ times (see Section 1.4.3.2). But in all cases there is a convergence towards the equilibrium concentration. In Fig 2-10, however, we find that the different series (for different $t_{1,a}$) do not completely converge to any common equilibrium value for the longer $t_{1,b}$ time of 3000 s. In fact, we would expect (Companys et al., 2005) that within $t_{1,b}$=3 $t_{1,a}$, which is less than 25 s for all the series, *agne* was reached at the

longest $t_{1,b}$ values shown in this figure. For that, we conclude that there is some kind of blockage of the electrode surface or other irreversibilities affecting the redox process (notice that the blocking can also be considered an irreversibility, see p 623 in (Bard and Faulkner, 2001)). We discuss first the hypothesis of the surfactant blocking the electrode surface.

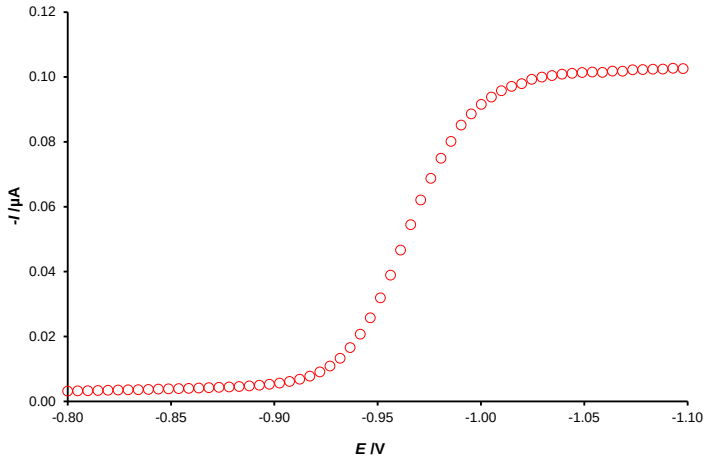

Figure 2-8. NPP of Zn released from the dissolution of NPs containing the undisclosed surfactant. pH=8.25 with Tris 0.01 mol L^{-1}; μ=0.1 mol L^{-1} (as KCl). Pulse time: 0.05s. Interval time: 1 s. Step potential: 0.005 V. Base potential: -0.400 V

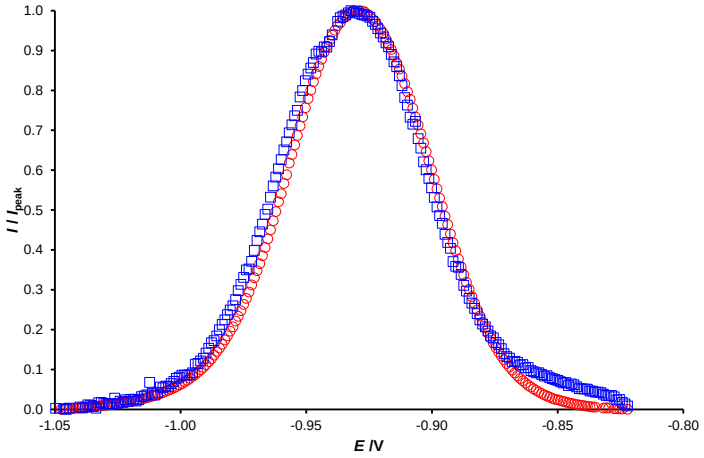

Figure 2-9. Normalized Differential Pulse Polarograms (DPP) of Zn released from the dissolution of NPs containing the undisclosed surfactant. (□): pH 8.25; (○): pH=4.0 (where all NPs have dissolved). Pulse time: 0.05s. Interval time: 1 s. Step potential: 0.00105 V. Modulation potential: 0.04995 V.

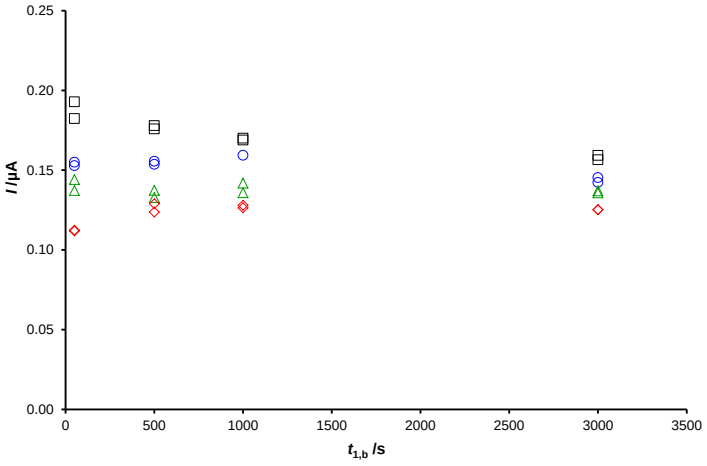

Figure 2-10. Currents leading to an unresolved free metal concentration with the standard application of AGNES (stirring along $t_{1,a}$ and $t_{1,b}$; no stirring along t_w=50 s) to a Nanotek ZnO dispersion. Parameters: $Y_{1,a}=10^{12}$; $Y=Y_{1,b}=10$; $Y_2=10^{-10}$; t_2=50 s. Markers: (◊) for $t_{1,a}$=3 s; (Δ) for $t_{1,a}$=4 s; (○) for $t_{1,a}$=5 s and (□) for $t_{1,a}$=6 s.

So as to see how the blockage proceeds with time, we repeated experiments without dislodging the drop in between them. Hence, each of the 3 series in Fig 2-11 corresponds to successive experiments performed with one drop immersed in a dispersion of Nanotek NPs. In experiments denoted with blue circle markers, Zn was accumulated at Y=10 for a time t_1=10 s (with stirring and without waiting period, t_w=0). We warn that these are not AGNES experiments (but rather ancillary ones) given that we do not check that *agne* is reached. The obtained currents decrease rapidly after the first 25 seconds to a nearly negligible value, thus supporting the hypothesis of the blocking dispersant being adsorbed in a very short time because of the facilitation of mass transport with the stirring. The repetition of the same potential program with another drop (see green square markers), but without stirring (same total deposition time, i.e.: t_1=t_w=10 s), shows that the period before total blocking without stirring is longer than that with stirring. This can be understood in consequence of a transport limitation of the dispersant needed for total blocking of the electrode surface. We conclude that, for this system where blocking is diffusion limited (while the required gains are small), it is convenient to avoid stirring in the deposition stage of AGNES. We also observe that, without stirring, there are around 100 s left before total blocking is attained (for this gain), with that purpose in the final design of the parameters we seek to have total deposition times shorter than 100s. Red triangle markers in Fig 2-11 correspond to a very negative deposition potential: we see that, even with the time elapsed (since the formation of the drop) and the amount of adsorbed dispersant, no change in the current appears within the drop lifetime, indicating that Zn^{2+}converts into Zn^o at Y=10^{12} and, also, that Zn^o converts into Zn^{2+} at Y=10^{-10}.

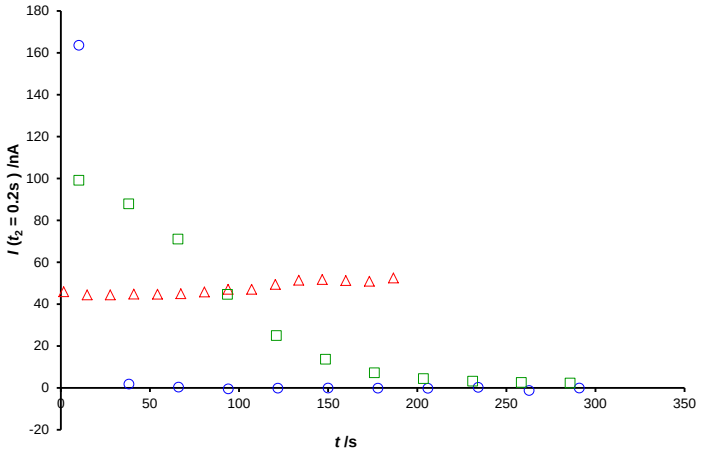

Figure 2-11. Plot showing that stirring favours the quick dispersant blockage of the electrode for the Zn^{o}/Zn^{2+} process, whilst extreme gains break it. A unique drop is used for each series along which a common procedure (where equilibrium is not reached) is repeated. Series with markers (○): Y_1=10, t_1=10 s (with stirring), t_w=0. Series with (□): Y_1=10, t_1=t_w=10 s (no stirring during deposition stage). Series with (Δ): Y_1=10^{12}, t_1=t_w=1.5 s (no stirring). Currents are measured at t_2=0.2 s of the stripping stage which lasts 5s and are represented *vs.* the time since the birth of the drop. In all experiments Y_2=10^{-10}. The medium contained a dispersion of NanotekZnO NPs approximately 2×10^{-4} mol L^{-1} at pH=8.25.

In order to have a better idea if the application of a very negative potential (Y=10^{12}) might clean the electrode surface from surfactants (Louis et al., 2008), we alternated in just one series (i.e. in just one drop) the previous two series without stirring (now, subseries). As observed in Fig 2-12, after 200 s of drop lifetime, the first subseries at Y=10 indicates full blockage. The application of the second subseries, at Y=10^{12} is not affected by this full blockage. The third subseries, again at Y=10, indicates that reduction of Zn^{2+} is hindered to the same extent as at the end of the first subseries. So, it seems that the application of a very negative potential (applied in the previous subseries from 200 to 400 s of droplife) does not seem to remove the surfactant away from the electrode surface. The progress of the blockage with time is also clearly confirmed by cyclic voltammetry (see Fig 2-13).

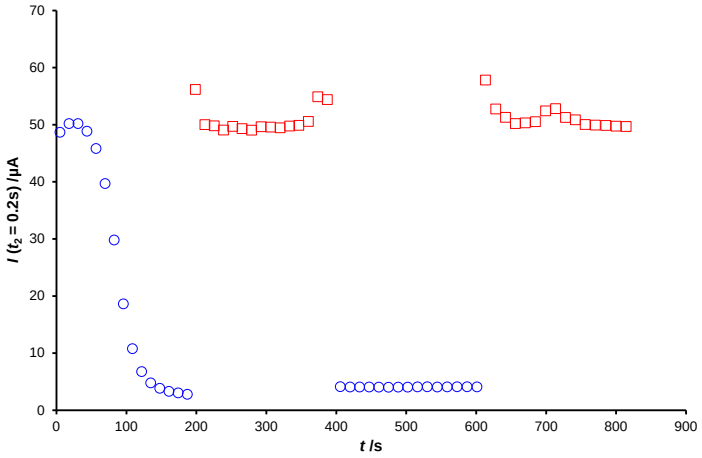

Figure 2-12. Ancillary experiments of current *vs.* drop lifetime showing that the surfactant is not removed from the electrode surface after the application of a very negative potential. Only one drop was used for all the data in this plot. Red square markers (□) represent subseries with parameters $Y_1=10^{12}$, $t_1=t_w=1.5$ s (no stirring during deposition stage) with total stripping time $t_2=8.5$ s. Blue circle markers (○) stand for subseries where $Y_1=10$, $t_1=t_w=5$ s (no stirring) and $t_2=5$ s. In all cases $Y_2=10^{-10}$.

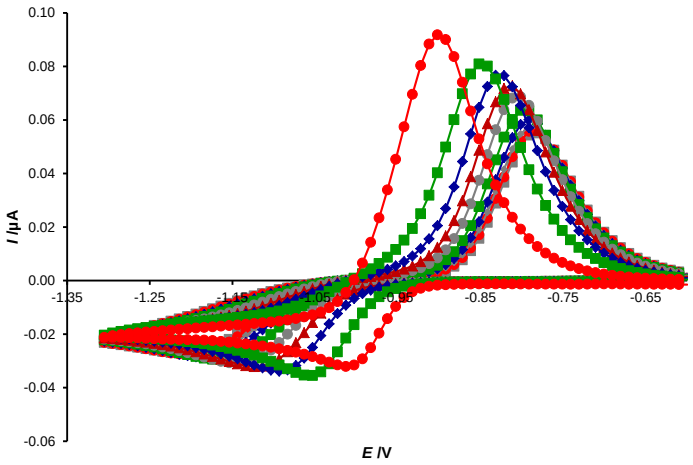

Figure 2-13. Cyclic voltammogram showing the progressive blockage of the active surface of the Hg drop by the surfactant accompanying ZnO Nanotek NPs. Each scan begins at 0 V (region not shown) and moves down to -1.4 V and then back to 0 V. The first cycle, plotted as (●), goes through a minimum around -1 V in the forward scan and through a maximum (around -0.9 V) in the reverse scan. The second cycle is represented by (■). Due to the blockage, the separation between both peaks increases with the drop life. Each cycle takes 28s (scan rate 0.05 V s^{-1})

From a practical point of view, we conclude that AGNES has to be applied without stirring along a deposition time that should be as short as possible (below 100 s for our conditions), reach *agne* and proceed to the stripping stage and, then, start with a new drop for the next experiment. Renovating mercury electrodes (such as HMDE) are, in this respect, more convenient than Rotating Disk Electrodes, Screen Printed Electrodes or microelectrodes (see Section 1.4.3.4.1), given that with a fixed mercury film one could not avoid or reverse the blocking of the surface (see page 569 in (Bard and Faulkner, 2001)). AGNES 2P (see Section 1.4.3.2) can reduce the deposition time down to a minimum with a suitable $t_{1,a,w}$ (where subscript w recalls that no stirring is applied) to accumulate in the drop almost the exact amount of Zn^o needed for *agne* at the prescribed gain in the solution of interest.

In order to find a deposition time close to the optimum $t_{1,a,w}$ value, we designed a new kind of ancillary experiments (in this case, each series corresponds to a new drop). We call Exp1 to experiments where we let for a short second substage of the deposition program (i.e. $t_{1,b}$=0; $t_w \neq 0$) to approach equilibrium at the desired gain. We

call Exp2 to experiments where the stripping stage immediately follows the diffusion limited deposition substage ($t_{1,b}$=t_w=0), so that we assess the amount of material that has entered along the first substage. For $t_{1,a,w}$ shorter than the optimum one (undershoot), the substage at the desired gain will accumulate more Zn^o in the drop, so that I(Exp1)>I(Exp2). Conversely, for $t_{1,a,w}$ longer than the optimum one (overshoot), I(Exp1)<I(Exp2) because the fine-tuning substage of Exp1 tends to remove Zn^o from the amalgam. In the particular case of Fig 2-14, we aim at a gain of Y=5 (given that the free Zn concentration in this NP dispersion is quite high). The intersection of the series of Exp1 and Exp2 should provide, in principle, an optimum $t_{1,a,w}$ around 10 s (which is sufficiently away from the total blockage time of 100 s). In practice, with just $t_{1,a,w}$=10 s, an undershoot was very clear. The application of $t_{1,a,w}$= 12.5 and 15 s with t_w=10, 50, 100 and 200 s provides concentrations listed in Table 2-2. The application of the same methodology with different gains leads to approximately a proportionally longer or shorter optimum $t_{1,a,w}$, but essentially the same free metal concentration.

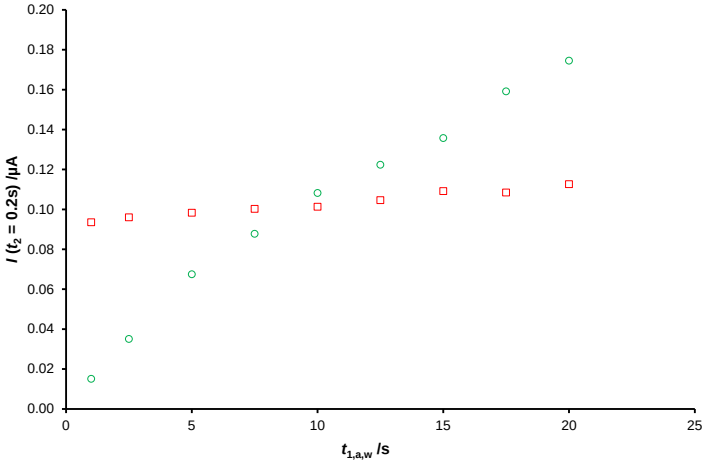

Figure 2-14. Finding of an optimized $t_{1,a,w}$ for Y=5 at the intersection of both series of ancillary experiments. No stirring in any substage. Green circles (○) stand for experiments of type Exp1 with Y_1=10^{12}. Red squares (□) stand for experiments of type Exp2 with $Y_{1,a}$=10^{12}, $Y_{1,b}$=5 and $t_{1,b}$=0; t_w=100 s. A different drop per marker and experiment. In all cases Y_2=10^{-10}. The medium contained a dispersion of Nanotek ZnO NPs approximately 2×10^{-4} mol L^{-1} at pH=8.29.

Table 2-2. Free Zn concentration obtained from the application of AGNES with the optimized deposition time under diffusion limited conditions without stirring to a dispersion of Nanotek ZnO NPs around 2×10^{-4} mol L^{-1}, pH=8.29, [KCl]=0.1 mol L^{-1}

$[Zn^{2+}]$ /mol L^{-1}	***Y*=2; $t_{1,a,w}$ = 3 s**	***Y*=5; $t_{1,a,w}$ =12.5 s**	***Y*=5; $t_{1,a,w}$ =15 s**
t_w = 10 s	$(8.69\pm 0.21)\times10^{-6}$	$(9.65\pm 0.08)\times10^{-6}$	$(1.08\pm 0.02)\times10^{-5}$
t_w = 50 s	$(1.02\pm 0.01)\times10^{-5}$	$(1.02\pm 0.02)\times10^{-5}$	$(1.03\pm 0.01)\times10^{-5}$
t_w = 100 s	$(1.05\pm 0.01)\times10^{-5}$	$(1.02\pm 0.01)\times10^{-5}$	$(1.05\pm 0.01)\times10^{-5}$
t_w = 200 s	$(1.04\pm 0.01)\times10^{-5}$	$(1.02\pm 0.01)\times10^{-5}$	$(1.05\pm 0.01)\times10^{-5}$

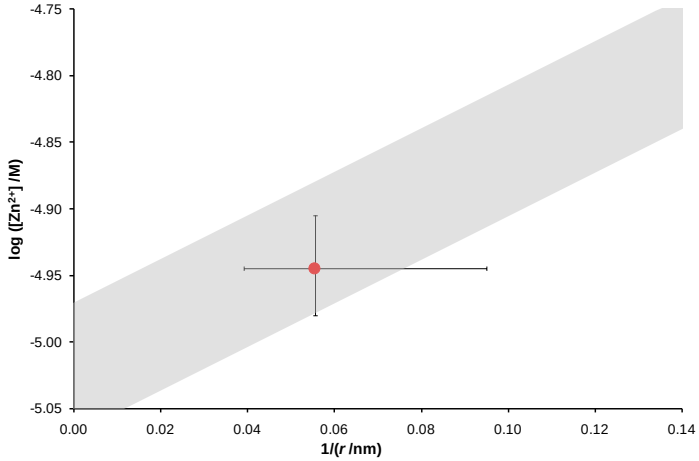

Figure 2-15. Diagram of the logarithm of equilibrium free Zn concentration *vs* the inverse of the radius of the ZnO nanoparticles. The red bullet indicates the average experimental concentration retrieved by AGNES (average of Table 2-2 and other experiments) in a dispersion of Nanotek ZnO NPs. The vertical error bar corresponds to the error in AGNES determinations. The horizontal error bar indicates the estimated range of the nanoparticle diameters 36±15 nm.The shaded region stands for the theoretical values according to eqns. 3 and 5 in ref (David et al., 2012) taking into account the pH uncertainty 8.2 ± 0.1

Fig 2-15 shows that the average [Zn^{2+}] experimental value of 1.04×10^{-5} mol L^{-1} falls within the range of theoretically expected concentrations for diameters in between 36±15nm at this pH-value, when applying eqn. 5 from ref. (David et al., 2012):

$$\left[Zn^{2+}\right]_{NP} = \left[Zn^{2+}\right]_{bulk} \exp\left\{\frac{3.76}{r_{NP}/\mathrm{nm}}\right\} \qquad (2\text{-}4)$$

where $\left[Zn^{2+}\right]_{NP}$ and $\left[Zn^{2+}\right]_{bulk}$ indicate the concentrations of free Zn in equilibrium with the studied NP and with the bulk material, respectively. Non-blocking irreversibilities (Mota and Correia dos Santos, 1995; Berbel et al., 1999), associated to a sluggish kinetics of the electron transfer, could delay the reaching of *agne*. If this case appeared, checking the attainment of a constant response function in the second stage with increasing deposition times would overcome the difficulty (see section 2.4.1.1.2). Besides, simple calculations (not shown), parallel to those in ref. (van Leeuwen and Town, 2003), suggest that, using parameters typical of Zn electrodic processes without specific adsorption (Lopez-Perez et al., 2003; Omanovic and Branica, 2004), the electron transfer is not the limiting stage by the end of the relatively long deposition stage. Experimentally, we have not found yet any impact of (a possible) irreversibility in none of the Zn systems explored here, nor with oxalate (Companys et al., 2005; Parat et al., 2011a), seawater (Galceran et al., 2007), humic acids (Companys et al., 2007), or river water (Zavarise et al., 2010; Chito et al., 2012). In the case of Zn in wine (Companys et al., 2008), we speculated that irreversibility might be responsible for the anomalously long $t_{1,b}$ required, and this irreversibility could perhaps be also because of a partial blockage. In the present case of Nanotek nanoparticles, we cannot rule out some irreversibility not related to the blockage, but the good results for a sufficiently short (optimized) $t_{1,a,w}$-value clearly suggest that the existing difficulties have been overcome.

2.4.2 Adsorption impact on the AGNES stripping diffusion limited current

Usually the analytical function used as AGNES signal to quantify the accumulated metal in the second stage is the intensity current under diffusion limited conditions (read at a fixed stripping time t_2) called AGNES-I (see Section 1.4.1).

Due to the linear nature of the diffusion equation inside the drop, it can be shown that, independently of the geometry of the electrode, in the AGNES-I variant, the faradaic current is proportional to the free metal ion concentration (Galceran et al., 2004) see Section 1.4.1:

$$I_f = Y\eta\left[\mathrm{M}^{2+}\right] \tag{2-5}$$

The normalized proportionality factor η can be found from a calibration.

The faradaic current under diffusion limited conditions cannot be affected by any phenomenon in the solution (Galceran et al., 1994; Galceran et al., 2004), so in principle, I_f is independent of electrodic adsorption. These conditions do not apply when intermetallic compounds are formed (Chito et al., 2010), when the solubility of Zn^o, Pb^o or Cd^o in Hg is approached (Galceran et al., 2010) or when the metal in solution has more than one oxidation state (which is not the case for the 3 metals studied in this chapter).

But, adsorption might impact AGNES determination via the blank, given that adsorption can modify the capacitive current (i.e. by changing the double layer structure) (Lovric, 1984). For example, the synthetic blank (where only the background electrolyte is present in the medium) might be not fully representative of the capacitive current when L or ML are adsorbed onto the electrode surface at a very different extent between the deposition and stripping potentials. Similar considerations to those justifying the use of the synthetic blank when charge is the analytical signal (see next section) also apply here to the current.

2.4.3 Adsorption impact on the stripped faradaic charge

Alternatively to the current, there is another analytical function which can be chosen as AGNES response: the total stripped faradaic charge (Q_f) (see Section 1.4.3.3). The combination of Nernst and Faraday laws allows writing (Galceran et al., 2010; Parat et al., 2011b):

$$Q_f = nFV_{Hg}[M^o] = \eta_Q Y[M^{n+}] \tag{2-6}$$

η_Q is the normalized proportionality factor (usually obtained by calibration) and should only depend on the volume of mercury.

3 variants of AGNES use the faradaic charg (Q_f) to quantify the amalgamated metal: AGNES-Q, AGNELSV and AGNES-SCP.

Induced adsorption could impact on the evolution of the transient stripping current in AGNES-Q or AGNELSV or the recorded potential in AGNES-SCP, but not on the eventual value of the total faradaic charge associated to the amount of M^o accumulated at equilibrium. In the second stage, we re-oxidate M^o, consequently the presence of adsorbed ML is irrelevant for the stripped charge Q_f (because ML – either adsorbed or in solution- cannot be neither oxidized nor reduced at the stripping potential E_2).

Just when working with the variant AGNES-Q, it is necessary the substraction of the blank. The synthetic blank yields the charge of the same potential program with just background electrolyte. The change in the double layer structure because of the adsorption might impact on the blank, as in AGNES-I (but to a lesser extent if the potential jump is smaller because E_2 does not correspond to diffusion limited conditions). The treatment detailed in the Supporting Information of (Galceran et al., 2014) indicates that, for the assayed systems, the charge of the blank is a reasonable surrogate for the capacitive charge. Moreover, as with AGNES-I, the selection of a sufficiently high gain Y usually renders the specific value of the blank negligible. In this manner, the total charge (summation of faradaic and capacitive charge) is practically constant for all stripping potentials (E_2) because the changes in $Q_{cap}(\infty)$ (due to the variation in E_2-E_1) are negligible in front of Q_f (see, Fig 2-16).

Free concentrations determined with AGNES-Q are comparable with those of AGNES-I, see, for example, Figs 2-5 and 2-6, confirming also the low impact of induced adsorption on the computed Q_f.

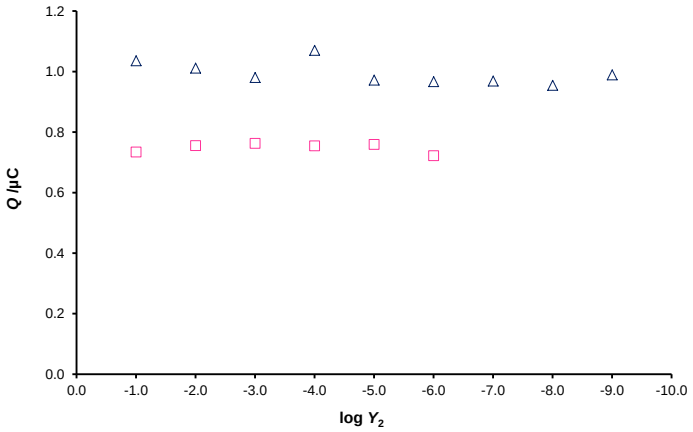

Figure 2-16. Plot of stripped charge vs log Y_2 in two different solutions showing the negligible impact of the changing capacitive charge. Solution 1 (Δ): Y_1=50, pH 6.1 (MES 0.01 mol L^{-1} buffer) and $c_{T,Zn}$= 1×10^{-5} mol L^{-1}. The values retrieved with AGNES-Q, in this experiment, yield $[Zn^{2+}]$ = 1.15×10^{-5} mol L^{-1}, which agrees with VMinteq expectation (9.73×10^{-6} mol L^{-1}). Solution 2 (□): $c_{T,Cd}$= 5.18×10^{-5} mol L^{-1}, $c_{T,I}$= 6.26×10^{-2} mol L^{-1} and pH= 6.010

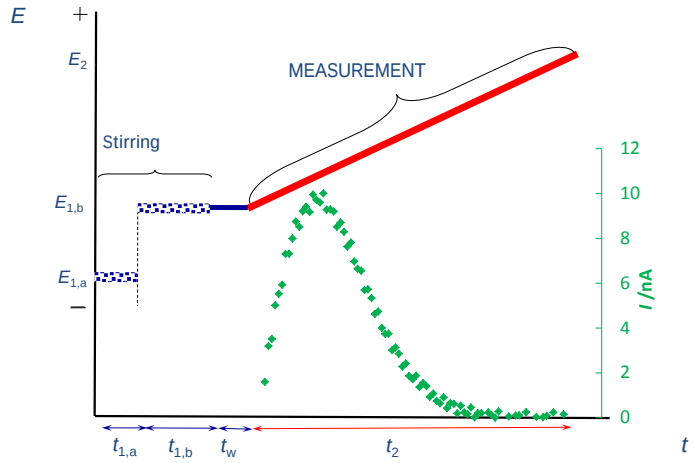

Figure 2-17. Schematic representation of the potential program for the AGNELSV variant together with an example (inset, in green) of the output current.

In AGNELSV the stripping current is recorded while the potential is scanned at a sufficiently slow constant rate from the deposition potential E_1 up to a sufficiently less negative potential (see Section 1.4.3.3), doing that on this way all M^o has been reoxidated (Galceran et al., 2010) (see Fig 2-17 for a schematic representation of the potential program). In principle, with AGNELSV it is not necessary to subtract a blank, given that Q_f can be computed from the area above the baseline (which is assumed to contain the capacitive current), (Galceran et al., 2014).

We see in Fig 2-18, that for the system Cd+I, the AGNELSV curve is a practically straight line, so we took the baseline of the various experiments with Cd+I as the prolongation of the straight region at the right of the plot (when the peak associated to the faradaic current is clearly vanished). Examples of retrieved AGNESLV voltammograms are shown in Fig 2-19.

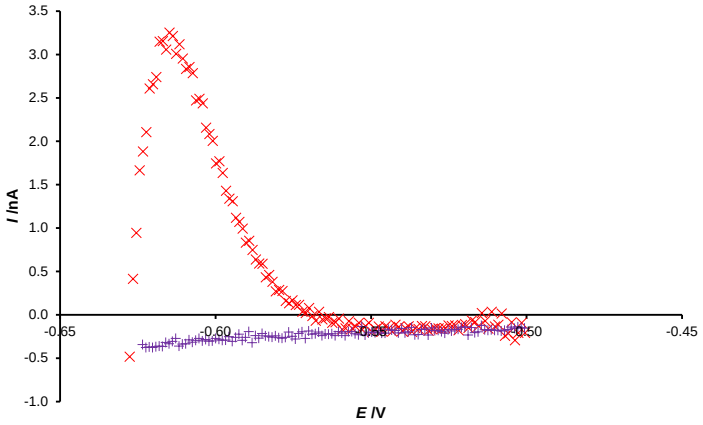

Figure 2-18. Evolution of the stripping current along the potential scan of an AGNELSV experiment where scan rate = 0.008 V s^{-1}. $c_{T,Cd}$= 1.15×10^{-5}mol L^{-1}, $c_{T,I}$= 9.53×10^{-2}mol L^{-1} (×) and pH= 6.020. The (+) signs correspond to the synthetic blank (just the background electrolyte 0.1 mol L^{-1} KNO_3).

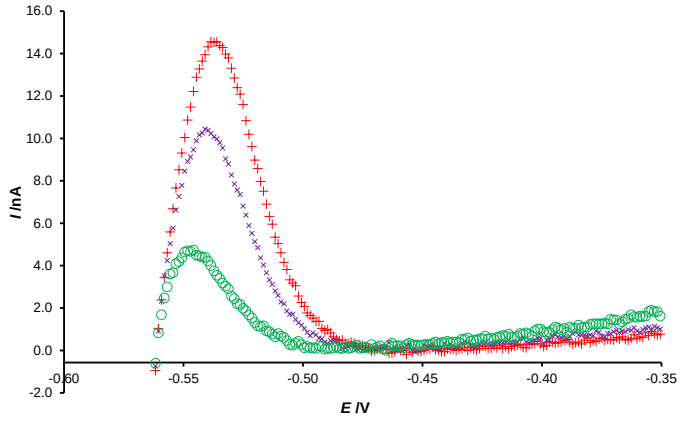

Figure 2-19. Plot of AGNELSV stripping (*I* vs *E*) in KNO_3 0.1 mol L^{-1}, $c_{T,Cd}$=1.24×10^{-5} mol L^{-1}, Y=5. The scan rate has been 0.008 V s^{-1} and $c_{T,I}$=4.93×10^{-3} mol L^{-1} (+), 1.00×10^{-2} mol L^{-1} (×) or 2.68×10^{-2} mol L^{-1} (○)

The normalized proportionality factor η_Q (see Section 1.4.3.3) found from the variant AGNELSV in various calibrations compare very well with other variants (see Table 3) and with literature values (Parat et al., 2011b). Small variations around

0.002 C/M between the different metals may be due to inaccuracies in the determination of the gains (as for example inaccurate diffusion coefficients or in the determination of the DPP E_{peak}), but such offsets cancel out between the corresponding calibration and measurement, so that the retrieved free concentrations are reliable.

The third AGNES variant using the charge as response function is AGNES-SCP (see Section 1.4.3.3). As in AGNELSV, in principle, no blank is required (see SI of reference (Parat et al., 2011b)), and one just reads the transition time, τ, from the area above the baseline. The η_Q-values found in calibrations are similar to those of other variants (see Table 3). The retrieved free concentration values obtained with this AGNES variant agree with the results of other variants and with theoretical speciation calculations (see Fig 2-5). The lack of impact of complex adsorption on the peak area using a SCP program with full depletion has already been shown theoretically and experimentally (Town and van Leeuwen, 2002).

Table 3: Normalized proportionality factor η_Q found by application of different variants of AGNES along calibrations.

Metal	**η_Q in C/mol L^{-1} (AGNES-Q)**	**η_Q in C/mol L^{-1} (AGNELSV)**
Cd	1.63×10^{-3}	1.63×10^{-3}
Cd	1.53×10^{-3}	1.49×10^{-3}
Cd	1.84×10^{-3}	1.59×10^{-3}
Zn	1.75×10^{-3}	1.72×10^{-3}
Pb	2.56×10^{-3}	2.16×10^{-3}
Pb	1.96×10^{-3}	2.03×10^{-3}
Pb	1.85×10^{-3}	1.95×10^{-3}

2.5 Conclusions

According to AGNES principles (i.e. when the aims of each stage are fulfilled), electrodic adsorption is not expected to affect the determination of the free metal concentration.

When the special AGNES equilibrium situation (*agne*) desired at the first stage is reached, the existence of other equilibria processes (like adsorption) should not impact on the amount of accumulated M^o (see section 2.4.1). The metal quantification in the second stage can be done by the diffusion-limited faradaic current (variant AGNES-I, see Section 1.4.1) or by the total faradaic charge (variants AGNES-Q, AGNELSV and AGNES-SCP, see Section 1.4.3.3). The diffusion-limited faradaic current cannot be affected by any process in solution (as adsorption). Electrodic adsorption cannot affect the faradaic charge, either, because this charge is just proportional to the accumulated M^o (see eqn. (2-6)). Adsorption can influence on the total current or the total charge via changes in the double layer, because of that suitable blanks (or a suitable baseline, in the case of AGNES-SCP) have to be subtracted. Luckily, in practice, by sufficiently increasing the gain *Y*, one can render this capacitive current or charge negligible in front of the faradaic one, consequently accurate concentrations can be finally obtained even if the capacitive estimation (via the blank measurement) is not excellent.

Experimental results obtained in the different systems with induced adsorption studied show that AGNES yields accurate values of the free metal ion concentrations. Apart from systems in previous papers, this has also been demonstrated in this chapter in the cases of Cd+Poly(acrylic)acid (Fig 2-3), Cd+Iodide (Fig 2-5) and Pb+Xylenol Orange (Fig 2-6).

The blockage or total fouling of the electrode can be a much more severe problem than induced electrodic adsorption. By way of illustration, see Figs 2-11 and 2-12, the dispersant accompanying Nanotek ZnO NPs seems to block the electrode in a relatively short time. In this case, it is necessary to optimize the deposition time and turn the stirring off (see Fig 2-14) to reach the equilibrium conditions (*agne*) before the total blockage.

2.6. References

Adam,N., Schmitt,C., Galceran,J., Companys,E., Vakourov,A., Wallace,R., Knapen,D., Blust,R., 2013. The chronic toxicity of ZnO nanoparticles and ZnCl2 to Daphnia magna and the use of different methods to assess nanoparticle aggregation and dissolution, *Nanotoxicology* 8, pp. 709-717.

Aguilar,D., Galceran,J., Companys,E., Puy,J., Parat,C., Authier,L., Potin-Gautier,M., 2013a. Non-purged voltammetry explored with AGNES, *Phys. Chem. Chem. Phys.* 15, pp. 17510-17521.

Aguilar,D., Parat,C., Galceran,J., Companys,E., Puy,J., Authier,L., Potin-Gautier,M., 2013b. Determination of free metal ion concentrations with AGNES in low ionic strength media, *J. Electroanal. Chem.* 689, pp. 276-283.

Alberti,G., Biesuz,R., Huidobro,C., Companys,E., Puy,J., Galceran,J., 2007. A comparison between the determination of free Pb(II) by two techniques: Absence of Gradients and Nernstian Equilibrium Stripping and Resin Titration, *Anal. Chim. Acta* 599, pp. 41-50.

Bard,A.J., Faulkner,L.R., 2001. Electrochemical Methods. Fundamentals and Applications. John Wiley & Sons, Inc., New York.

Berbel,F., Díaz-Cruz,J.M., Ariño,C., Esteban,M., 1999. Voltammetry of sparingly soluble metal complexes: a differential pulse polarographic study of the Zn(II) plus oxalate system, *J. Electroanal. Chem.* 475, pp. 99-106.

Bond,A.M., Hefter,G., 1976. Inequivalence of apparent polarographic and potentiometric stability-constants for cadmium(II) bromide and iodide systems, *J. Electroanal. Chem.* 68, pp. 203-216.

Campbell,P.G.C., Errecalde,O., Fortin,C., Hiriart-Baer,W.R., Vigneault,B., 2002. Metal bioavailability to phytoplankton - applicability of the Biotic Ligand Model, *Comp. Biochem. Physiol. C* 133, pp. 189-206.

Casassas,E., Arino,C., 1986. Determination of Stability-Constants of Some Cadmium Complexes by Polarographic Techniques in the Presence of Electrode Adsorption, *J. Electroanal. Chem.* 213, pp. 235-244.

Chito,D., Galceran,J., Companys,E., 2010. The Impact of Intermetallic Compounds Cu_xZn in the Determination of Free Zn^{2+} Concentration with AGNES, *Electroanal.* 22, pp. 2024-2033.

Chito,D., Galceran,J., Companys,E., Puy,J., 2013. Determination of the Complexing Capacity of Wine for Zn Using the Absence of Gradients and Nernstian Equilibrium Stripping Technique, *J. Agric. Food Chem.* 61, pp. 1051-1059.

Chito,D., Weng,L., Galceran,J., Companys,E., Puy,J., van Riemsdijk,W.H., van Leeuwen,H.P., 2012. Determination of free Zn^{2+} concentration in synthetic and natural samples with AGNES (Absence of Gradients and Nernstian Equilibrium Stripping) and DMT (Donnan Membrane Technique), *Sci. Total Envir.* 421-422, pp. 238-244.

Companys,E., Cecília,J., Codina,G., Puy,J., Galceran,J., 2005. Determination of the concentration of free Zn^{2+} with AGNES using different strategies to reduce the deposition time., *J. Electroanal. Chem.* 576, pp. 21-32.

Companys,E., Galceran,J., Pinheiro,J.P., Puy,J., Salaün,P., 2017. A review on electrochemical methods for trace metal speciation in environmental media, *Curr. Opin. Electrochem.* 3, pp. 144-162.

Companys,E., Naval-Sanchez,M., Martinez-Micaelo,N., Puy,J., Galceran,J., 2008. Measurement of free zinc concentration in wine with AGNES, *J. Agric. Food Chem.* 56, pp. 8296-8302.

Companys,E., Puy,J., Galceran,J., 2007. Humic acid complexation to Zn and Cd determined with the new electroanalytical technique AGNES, *Environ. Chem.* 4, pp. 347-354.

Companys,E., Puy,J., Torrent,M., Galceran,J., Salvador,J., Garcés,J.L., Mas,F., 2003. Binding curve from normalised limiting currents of labile heterogeneous metal-macromolecular systems. The case of Cd/humic acid., *Electroanal.* 15, pp. 452-459.

David,C., Galceran,J., Rey-Castro,C., Puy,J., Companys,E., Salvador,J., Monné,J., Wallace,R., Vakourov,A., 2012. Dissolution kinetics and solubility of ZnO nanoparticles followed by AGNES., *J. Phys. Chem. C* 116, pp. 11758-11767.

Díaz-Cruz,J.M., Ariño,C., Esteban,M., Casassas,E., 1991. Polarography and stripping voltammetry of metal polycarboxylate complexes - complexes of cadmium and zinc with polyacrylic and polymethacrylic acids, *Electroanal.* 3, pp. 299-307.

Domingos,R.F., Huidobro,C., Companys,E., Galceran,J., Puy,J., Pinheiro,J.P., 2008. Comparison of AGNES (Absence of Gradients and Nernstian Equilibrium Stripping) and SSCP (Scanned Stripping Chronopotenciometry) for Trace Metal Speciation Analysis, *J. Electroanal. Chem.* 617, pp. 141-148.

Domingos,R.F., Rafiei,Z., Monteiro,C.E., Khan,M.A.K., Wilkinson,K.J., 2013. Agglomeration and dissolution of zinc oxide nanoparticles: role of pH, ionic strength and fulvic acid, *Environ. Chem.* 10, pp. 306-312.

Domingos,R.F., Simon,D.F., Hauser,C., Wilkinson,K.J., 2011. Bioaccumulation and Effects of CdTe/CdS Quantum Dots on Chlamydomonas reinhardtii - Nanoparticles or the Free Ions?, *Environ. Sci. Technol.* 45, pp. 7664-7669.

Ensafi,A.A., Benvidi,A., Khayamian,T., 2004. Determination of cadmium and zinc in water and alloys by adsorption stripping voltammetry, *Analytical letters* 37, pp. 449-462.

Galceran,J., Chito,D., Martinez-Micaelo,N., Companys,E., David,C., Puy,J., 2010. The impact of high Zn^o concentrations on the application of AGNES to determine free Zn(II) concentration, *J. Electroanal. Chem.* 638, pp. 131-142.

Galceran,J., Companys,E., Puy,J., Cecília,J., Garcés,J.L., 2004. AGNES: a new electroanalytical technique for measuring free metal ion concentration, *J. Electroanal. Chem.* 566, pp. 95-109.

Galceran,J., Huidobro,C., Companys,E., Alberti,G., 2007. AGNES: a technique for determining the concentration of free metal ions. The case of Zn(II) in coastal Mediterranean seawater., *Talanta* 71, pp. 1795-1803.

Galceran,J., Lao,M., David,C., Companys,E., Rey-Castro,C., Salvador,J., Puy,J., 2014. The impact of electrodic adsorption on Zn, Cd or Pb speciation measurements with AGNES, *J. Electroanal. Chem.* 722-723, pp. 110-118.

Galceran,J., Rene,D., Salvador,J., Puy,J., Esteban,M., Mas,F., 1994. Reverse Pulse Polarography of labile metal + macromolecule systems with induced reactant adsorption - Theoretical analysis and determination of domplexation and adsorption parameters, *J. Electroanal. Chem.* 375, pp. 307-318.

Galceran,J., Salvador,J., Puy,J., Cecília,J., Esteban,M., Mas,F., 1995. Influence of adsorption on calibration curves in Normal Pulse Polarography, *Anal. Chim. Acta* 305, pp. 273-284.

Garrigosa,A.M., Diaz-Cruz,J.M., Arino,C., Esteban,M., 2008. Multivariate curve resolution as a tool to minimize the effects of electrodic adsorption in normal pulse voltammetry, *Electrochim. Acta.* 53, pp. 5579-5586.

Guaus,E., Sanz,F., 1999. Metal-halide-complex and ligand simultaneous adsorption. Chronocoulometry study in the Cd(II), KI Hg system at several ionic strengths, *Electroanal.* 11, pp. 424-431.

Hoyer,B., Jensen,N., 2004. Use of sodium dodecyl sulfate as an antifouling and homogenizing agent in the direct determination of heavy metals by anodic stripping voltammetry, *Analyst.* 129, pp. 751-754.

Huidobro,C., Companys,E., Puy,J., Galceran,J., Pinheiro,J.P., 2007. The use of microelectrodes with AGNES, *J. Electroanal. Chem.* 606, pp. 134-140.

Lopez-Perez,G., Andreu,R., Gonzalez-Arjona,D., Calvente,J.J., Molero,M., 2003. Influence of temperature on the reduction kinetics of Zn2+ at a mercury electrode, *J. Electroanal. Chem.* 552, pp. 247-259.

Louis,Y., Cmuk,P., Omanovic,D., Garnier,C., Lenoble,V., Mounier,S., Pizeta,I., 2008. Speciation of trace metals in natural waters: The influence of an adsorbed layer of natural organic matter (NOM) on voltammetric behaviour of copper, *Anal. Chim. Acta* 606, pp. 37-44.

Lovric,M., 1984. Reactant Adsorption in Pulse Polarography, *J. Electroanal. Chem.* 170, pp. 143-173.

Mas,F., Puy,J., Díaz-Cruz,J.M., Esteban,M., Casassas,E., 1993. Semiempirical Full-Wave Expression for Induced Reactant Adsorption in Normal Pulse Polarography of Labile Metal Polyelectrolyte Systems, *Anal. Chim. Acta* 273, pp. 297-304.

Mota,A.M., Correia dos Santos,M.M., 1995. Trace Metal Speciation of Labile Chemical Species in Natural Waters: Electrochemical Methods. In: A. Tessier and D. R. Turner (Eds.). Metal Speciation and Bioavailability in Aquatic Systems. John Wiley & Sons, Chichester, pp. 205-258.

Mu,Q., David,C.A., Galceran,J., Rey-Castro,C., Krzemiñski,L., Wallace,R., Bamiduro,F., Milne,S.J., Hondow,N.S., Brydson,R., Vizcay-Barrena,G., Routledge,M.N., Jeuken,L.J.C., Brown,A.P. A systematic investigation of the physico-chemical factors that contribute to the toxicity of ZnO nanoparticles. *Chemical Research in Toxicology* . 2014a.
Ref Type: In Press

Mu,Q.S., David,C.A., Galceran,J., Rey-Castro,C., Krzeminski,L., Wallace,R., Bamiduro,F., Milne,S.J., Hondow,N.S., Brydson,R., Vizcay-Barrena,G., Routledge,M.N., Jeuken,L.J.C., Brown,A.P., 2014b. Systematic Investigation of the Physicochemical Factors That Contribute to the Toxicity of ZnO Nanoparticles, *Chem. Res. Toxicol.* 27, pp. 558-567.

Murakami,S., Ogura,K., Yoshino,T., 1980. Equilibria of Complex-Formation Between Bivalent-Metal Ions and 3,3'-Bis[N,N'-Bis(Carboxymethyl)Aminomethyl]-Ortho-Cresolsulfonphthalein, *Bull. Chem. Soc. Jpn.* 53, pp. 2228-2235.

Omanovic,D., Branica,M., 2004. Pseudopolarography of trace metals. Part II. The comparison of the reversible, quasireversible and irreversible electrode reactions, *J. Electroanal. Chem.* 565, pp. 37-48.

Paquin,P.R., Gorsuch,J.W., Apte,S., Batley,G.E., Bowles,K.C., Campbell,P.G.C., Delos,C.G., Di Toro,D.M., Dwyer,R.L., Galvez,F., Gensemer,R.W., Goss,G.G., Hogstrand,C., Janssen,C.R., McGeer,J.C., Naddy,R.B., Playle,R.C., Santore,R.C., Schneider,U., Stubblefield,W.A., Wood,C.M., Wu,K.B., 2002. The biotic ligand model: a historical overview, *Comp. Biochem. Physiol. C* 133, pp. 3-35.

Parat,C., Aguilar,D., Authier,L., Potin-Gautier,M., Companys,E., Puy,J., Galceran,J., 2011a. Determination of Free Metal Ion Concentrations Using Screen-Printed Electrodes and AGNES with the Charge as Response Function, *Electroanal.* 23, pp. 619-627.

Parat,C., Authier,L., Aguilar,D., Companys,E., Puy,J., Galceran,J., Potin-Gautier,M., 2011b. Direct determination of free metal concentration by implementing stripping chronopotentiometry as second stage of AGNES, *Analyst.* 136, pp. 4337-4343.

Pernet-Coudrier,B., Companys,E., Galceran,J., Morey,M., Mouchel,J.M., Puy,J., Ruiz,N., Varrault,G., 2011. Pb-binding to various dissolved organic matter in urban aquatic systems: Key role of the most hydrophilic fraction, *Geochim. Cosmochim. Ac.* 75, pp. 4005-4019.

Pinheiro,J.P., Mota,A.M., Gonçalves,M.L.S.S., Vanderweijde,M., van Leeuwen,H.P., 1996. Comparison between polarographic and potentiometric speciation for cadmium/humic acid systems, *J. Electroanal. Chem.* 410, pp. 61-68.

Pinheiro,J.P., Salvador,J., Companys,E., Galceran,J., Puy,J., 2010. Experimental verification of the metal flux enhancement in a mixture of two metal complexes: the Cd/NTA/glycine and Cd/NTA/citric acid systems, *Phys. Chem. Chem. Phys.* 12, pp. 1131-1138.

Puy,J., Galceran,J., Huidobro,C., Companys,E., Samper,N., Garcés,J.L., Mas,F., 2008. Conditional Affinity Spectra of Pb^{2+}-Humic Acid Complexation from Data Obtained with AGNES, *Environ. Sci. Technol.* 42, pp. 9289-9295.

Puy,J., Mas,F., Díaz-Cruz,J.M., Esteban,M., Casassas,E., 1992. Induced reactant adsorption in metal-polyelectrolyte systems - Pulse polarographic study, *Anal. Chim. Acta* 268, pp. 261-274.

Puy,J., Salvador,J., Galceran,J., Esteban,M., Díaz-Cruz,J.M., Mas,F., 1993. Voltammetry of labile metal-complex systems with induced reactant adsorption -

Theoretical analysis for any Ligand-to- Metal Ratio, *J. Electroanal. Chem.* 360, pp. 1-25.

Puy,J., Torrent,M., Monné,J., Cecília,J., Galceran,J., Salvador,J., Garcés,J.L., Mas,F., Berbel,F., 1998. Influence of the adsorption phenomena on the NPP and RPP limiting currents for labile metal-macromolecular systems, *J. Electroanal. Chem.* 457, pp. 229-246.

Rocha,L.S., Companys,E., Galceran,J., Carapuca,H.M., Pinheiro,J.P., 2010. Evaluation of thin mercury film rotating disc electrode to perform Absence of Gradients and Nernstian Equilibrium Stripping (AGNES) measurements, *Talanta* 80, pp. 1881-1887.

Rotureau,E., 2014. Analysis of metal speciation dynamics in clay minerals dispersion by stripping chronopotentiometry techniques, *Colloids Surf. A* 441, pp. 291-297.

Serrano,N., Díaz-Cruz,J.M., Ariño,C., Esteban,M., Puy,J., Companys,E., Galceran,J., Cecilia,J., 2007. Full-wave analysis of stripping chronopotentiograms at scanned deposition potential (SSCP) as a tool for heavy metal speciation: Theoretical development and application to Cd(II)-phthalate and Cd(II)-iodide systems, *J. Electroanal. Chem.* 600, pp. 275-284.

Tercier,M.L., Buffle,J., 1996. Antifouling membrane-covered voltammetric microsensor for in- situ measurements in natural-waters, *Anal. Chem.* 68, pp. 3670-3678.

Tessier,A., Buffle,J., Campbell,P.G.C., 1994. Uptake of Trace Metals by Aquatic Organisms. In: J. Buffle and R. R. DeVitre (Eds.). Chemical and Biological Regulation of Aquatic Systems. Lewis Publishers, Boca Raton, FL, pp. 197-230.

Town,R.M., van Leeuwen,H.P., 2002. Effects of adsorption in stripping chronopotentiometric metal speciation analysis, *J. Electroanal. Chem.* 523, pp. 1-15.

Town,R.M., van Leeuwen,H.P., 2003. Stripping chronopotentiometry at scanned deposition potential (SSCP) - Part 2. Determination of metal ion speciation parameters, *J. Electroanal. Chem.* 541, pp. 51-65.

Town,R.M., van Leeuwen,H.P., 2007. Adsorptive stripping chronopotentiometry (AdSCP). Part 2: Basic experimental features, *J. Electroanal. Chem.* 610, pp. 17-27.

van den Berg,C.M.G., 1984. Direct determination of sub-nanomolar levels of zinc in sea-water by cathodic stripping voltammetry, *Talanta* 31, pp. 1069-1073.

van Leeuwen,H.P., Buffle,J., Lovric,M., 1992. Reactant Adsorption in Analytical Pulse Voltammetry - Methodology and Recommendations - (Technical Report), *Pure Appl. Chem.* 64, pp. 1015-1028.

van Leeuwen,H.P., Town,R.M., 2003. Stripping chronopotentiometry at scanned deposition potential (SSCP) Part 3. Irreversible electrode reactions, *J. Electroanal. Chem.* 556, pp. 93-102.

van Leeuwen,H.P., Town,R.M., 2005. Kinetic limitations in measuring stabilities of metal complexes by Competitive Ligand Exchange-Adsorptive Stripping Voltammetry (CLE-AdSV), *Environ. Sci. Technol.* 39, pp. 7217-7225.

van Leeuwen,H.P., Town,R.M., 2007. Adsorptive stripping chronopotentiometry (AdSCP). Part 1: Fundamental features, *J. Electroanal. Chem.* 610, pp. 9-16.

Wu,Q.G., Batley,G.E., 1995. Determination of Sub-Nanomolar Concentrations of Lead in Sea-Water by Adsorptive Stripping Voltammetry with Xylenol Orange, *Anal. Chim. Acta* 309, pp. 95-101.

Zavarise,F., Companys,E., Galceran,J., Alberti,G., Profumo,A., 2010. Application of the new electroanalytical technique AGNES for the determination of free Zn concentration in river water, *Anal. Bioanal. Chem.* 397, pp. 389-394.

Zelic,M., Lovric,M., 2003. The influence of electrolyte concentration on the parameters of the Frumkin isotherm in the Cd2+-I- system, *J. Electroanal. Chem.* 541, pp. 67-76.

CHAPTER 3

Free Zn^{2+} determination in systems with Zn-glutathione

Results obtained in this chapter have been published in:

Journal of Electroanalytical Chemistry 756 (2015) 207-211

3.1 Abstract

Zn-Glutathione speciation has been studied applying the electrochemical technique AGNES (Absence of Gradients and Nernstian Equilibrium Stripping) to determine the free zinc concentration. Several titrations varying the pH, the total concentration of gluthatione ($c_{T,GSH}$) or Zn ($c_{T,Zn}$) have been performed determining in each case the free Zn concentrations with AGNES. Then, these results have been compared with the values predicted using previously reported complexation constants. The speciation of Zn has been studied in a real sample of root extracts of *Hordeum vulgare* where the $c_{T,Zn}$ had been determined (in collaboration with the University of Barcelona) by Inductively Coupled Plasma Mass Spectrometry (ICP-MS) and $c_{T,GSH}$ by High-Performance Liquid Chromatography (HPLC). To determine the free zinc concentration with AGNES, it has been necessary the use of a special device where a mixture of N_2/CO_2 saturated through milliQ water controls the pH and avoids the evaporation of the sample. The lower free zinc concentration determined with AGNES in root extracts, in comparison with the predicted one assuming the literature complexation constants and considering only the presence of Zn and GSH, indicates that it is necessary to include more ligands apart from GSH (as other phytochelatins) in the speciation model.

3.2 Introduction

The tripeptide Glutathione (GSH) with the sequence γ-Glu-Cys-Gly is extensively present in living systems and it is one of the most abundant intracellular non-protein thiol. GSH has two peptide bonds, two carboxylic acid groups, one amino group and one thiol group. Owing to the affinity of the thiol group for heavy metals, the role of GSH is essential in the complexation and elimination of the toxic metals from the organisms (Dolphin et al., 1989). Moreover, the structure of GSH is directly related to that of phytochelatins, which are thiol-rich peptides synthesized enzymatically by plants in response to an excessive uptake of certain heavy metal ions, such as Cd(II), Pb(II), Zn(II), Ag(I), Hg(II), Cu(I) (Grill et al., 1985; Grill et al., 1987; Rauser, 1990; Ahner et al., 1994; Rauser, 1995; Zenk, 1996; Soudek et al., 2014). As a result, the interest in the study of the complexation of heavy metal ions by GSH has been increasing as it is seen as a model system for the binding of metal ions by larger thiol-containing peptides and proteins (Dago et al., 2011; Dago et al., 2014).

Heavy metals can be introduced into natural waters by different sources, such as industrial wastes, mining activities, fertilizers, paints, and atmospheric depositions. Since heavy metals cannot be degraded, humans can incorporate them into their organism by food, water, air or by absorption through the skin. Once in the body, they compete with and displace essential elements such as Zn, Cu, Mg and Ca, and interfere with organ system functions. For example, Zn deficiency is considered as a wide-spread malnutrition problem that affects the growth of children (Penland, 2000), but at elevated levels Zn becomes toxic to terrestrial and aquatic organisms. One of the main dangers of heavy metals is attributed to its tendency of being bioaccumulated, e.g. they accumulate in the soft tissues (Lawrence et al., 1998). However, the bioavailability of heavy metals to organisms depends above all on the free metal ion concentration (which is directly related to activity) (Campbell, 1995; Parker and Pedler, 1997; Sun et al., 2005). This is why it is so important to chose a suitable analytical technique for measuring free metal ion concentrations at trace levels in natural samples (Pesavento et al., 2009). In that sense, the electroanalytical technique AGNES (Absence of Gradients and Nernstian Equilibrium Stripping) has been tested as a suitable technique for the direct measurement of free Zn(II) concentration (see Section 1.4) due to its low cost and its easy interpretation in comparison with other techniques (Galceran et al., 2004; Galceran et al., 2014). Furthermore, AGNES has obtained great results when applied to synthetic and natural samples such as sea (Galceran et al., 2007) and river water (Chito et al., 2012), soil extracts (Chito et al., 2012) and nanoparticle dispersions (David et al., 2012).

The complexation of Zn(II) by GSH has been widely studied by electroanalytical techniques like differential pulse polarography (DPP) (see Section 1.3.1.5) or by constant current chronopotentiometric stripping analysis using adsorptive accumulation (AdSCP) on a mercury electrode assisted by a multivariate curve resolution method by alternating least-squares (MCR-ALS) (Serrano et al., 2006). Nevertheless, the determination of free Zn(II) concentration in plant extracts has not been reported in the literature.

The aim of this chapter is to study the Zn-GSH system in a natural sample with AGNES. Firstly, the complexation of Zn with GSH is analyzed using this voltammetric technique in synthetic systems at various pH values and different total ligand and metal concentrations to compare with existing complexation models (Diaz-Cruz et al., 2000; Krezel et al., 2003; Ferretti et al., 2007). Then, free Zn concentration is measured with AGNES in root extracts of *Hordeum vulgare*.

3.3 Materials and methods

3.3.1 Equipment and reagents

The voltammetric measurements have been performed using a μ-AUTOLAB type III potentiostat attached to a Metrohm 663 VA Stand and to a computer by means of NOVA 1.10 (Eco Chemie) package software. The Metrohm Hanging Mercury Drop Electrode (HMDE) was the working electrode. The smallest drop (drop 1, which according to the catalogue corresponds to a radius $r_0=1.41\times10^{-4}$ m) has been chosen to perform AGNES measurements and the largest drop (drop 3 which corresponds to an $r_0=2.03\times10^{-4}$ m) to perform Differential Pulse Polarograms (DPP), see Section 1.3.1.5. The auxiliary electrode was a glassy carbon electrode and the reference electrode was Ag|AgCl (3 mol L^{-1}) KCl, encased in a 0.1 mol L^{-1} KNO_3 jacket.

The total metal concentration of the natural samples has been measured with an ICP-MS, 7700x from Agilent (Santa Clara, USA).

Zn solutions have been prepared from Merck (Darmstadt, Germany) 1000 mg L^{-1} standard solutions and potassium nitrate has been used as supporting electrolyte and prepared from solid KNO_3 TraceSelect (Sigma Aldrich, St. Louis, MO, USA). The preparation of GSH solutions has been done from EMPROVE* blo Glutathione (reduced) from Merck. The buffer 4-(2-Hydroxyethyl)-1-piperazinepropanesulfonic acid (EPPS) from Sigma Aldrich (≥ 99.5 %) has been selected to keep the pH fixed at 7.5 and 8.0. In all experiments, ultrapure water (Synnergy UV Millipore) is used.

To prepare the Hoagland solution (nutrient solution) for culturing plants, $Ca(NO_3)_2$, $Fe(NO_3)_3\cdot9\,H_2O$ and $CuSO_4\cdot5\,H_2O$ from Probus (Badalona, Spain), KNO_3, $MnSO_4\cdot H_2O$ and $ZnCl_2$ from Merck (Darmstadt, Germany) and $Mg(NO_3)_2\cdot6\,H_2O$, KH_2PO_4, H_3BO_3 and $Mo_7O_{24}(NH_4)_6$ from Panreac (Barcelona, Spain), were used. Plants were stressed adding $Zn(NO_3)_2\cdot4\,H_2O$ from Merck to the nutrient solution.

An Agilent (Santa Clara, CA, USA) 1100 chromatographic system has been used for GSH determination in plant root extracts. The system is equipped with a quaternary pump, a Rheodyne 7725i 20 μL loop manual injector (Rohnert Park, CA, USA), a vacuum degasser and a handheld control module. An Ascentis C18 5 μm particle size analytical column measuring 25 cm x 4.6 mm was provided by Supelco (Bellefonte, PA, USA). The electrochemical detector (ED) consisted of a CC-5C flow cell BASi (West Lafayette, IN, USA), with a three electrode system: a glassy

carbon working electrode (BASi), a stainless steel auxiliary electrode and an Ag/AgCl (NaCl 3 mol L^{-1}) reference electrode. The separation between the working and the auxiliary electrodes was performed by a gasket whose thickness was 0.005 inches that creates the cell volume. The system was connected to an Autolab PGSTAT 12 potentiostat (Eco Chemie, Utrecht, the Netherlands). GPES software version 4.9.007 (Eco Chemie) was used for potentiostatic control and data acquisition.

To prepare the mobile phase for GSH determination by HPLC, trifluoroacetic acid (TFA) provided by Sigma-Aldrich (St. Louis, MO, USA) and acetonitrile from Merck has been used.

3.3.2 Sample preparation

Barley (*Hordeum vulgare* cv. Graphic) seedlings were cultivated hydroponically using Hoagland solution adjusted to pH 6 (in the middle of the recommended range 5.5-6.5). The nutrient solution (Hoagland solution) contained 268 mg L^{-1} of N, 235 mg L^{-1} of K, 200 mg L^{-1} of Ca, 31 mg L^{-1} of P, 0.30 mg L^{-1} of S and 48.6 mg L^{-1} of Mg as macronutrients, and 0.5 mg L^{-1} of B, 2.50 mg L^{-1} of Fe, 0.5 mg L^{-1} of Mn, 0.05 mg L^{-1} of Zn, 0.02 mg L^{-1} of Cu and 0.01 mg L^{-1} of Mo as micronutrients. Seeds were placed on top of a mesh situated over a plastic container filled with nutrient solution, so that the seeds were to a small extent in contact with the nutrient solution. Five days after seeds were sowed, the nutrient solutions were changed for Hoagland solutions where Zn^{2+} had been added at a concentration of 500 µmol L^{-1}.

Three pots with 20 seeds per pot were considered. Barley roots were collected after 9 days of metal treatment. Plants were cleaned first with 0.1 mol L^{-1} EDTA solution and then with milliQ water, frozen at once with liquid nitrogen to disrupt cell walls and stored at -80ºC. Later, samples were ground separately in liquid nitrogen.

For the extraction of GSH (Fig 3-1), 120 mg of sample fresh weight (thawed at room temperature) were mixed with 12 mL of ultrapure filtered water for 1 hour in a rotatory horizontal stirrer from SBS (Barcelona, Spain). Prior to analysis, samples were filtrated through 0.45 µm nylon filter discs by Osmonics (Minnetonka, MN, USA). The filtered solution was stored at -25ºC.

Figure 3-1. Picture of the GSH extraction process

3.3.3 Free zinc determination

3.3.3.1 AGNES technique

As mentioned in Section 1.4.1 of Chapter 1, AGNES is divided in two stages: accumulation and quantification (Galceran et al., 2004). At the end of the first step the metal in solution (Zn^{2+} here) is reduced by the application of a negative potential (E_1) for a long enough time (t_1), reaching Nernstian equilibrium and flat concentration profiles of Zn^{2+} and Zn^0. The established concentration ratio at both sides of the electrode surface is named the gain (Y) which is described in 1.4.1.

Experimentally, the required potential (E_1) to reach the desired gain (Y) can be computed from the peak potential of a differential pulse polarogram (DPP):

$$Y = \sqrt{\frac{D_{Zn^{n+}}}{D_{Zn^0}}} \exp\left[-\frac{nF}{RT}\left(E_1 - E_{peak} - \frac{\Delta E}{2}\right)\right] \qquad (3\text{-}1)$$

where E_{peak} is the potential of the maximum obtained in a I vs E DPP-plot.

In the second step, the quantification of the reduced metal by the application of a re-oxidation potential (E_2) can be done by choosing either current or charge under diffusion limited conditions (see Section 1.4.3.3). The free metal ion concentration can be computed with the corresponding proportionality factor η or η_Q (Galceran et al., 2010; Galceran et al., 2014).

$$I = Y\eta\left[\mathrm{Zn}^{2+}\right] \tag{3-2}$$

$$Q = Y\eta_{\mathrm{Q}}\left[\mathrm{Zn}^{2+}\right] \tag{3-3}$$

3.3.3.2 Special device to control the evaporation and fixing the pH

The usual way of working with voltammetric techniques is under nitrogen atmosphere since the presence of oxygen could produce an impact in the response due to the oxygen current or to a local pH change near the electrode surface (Aguilar et al., 2013a). But, as the usual nitrogen flux used can change the nature of the sample (removing gases such as CO_2 and even breaking the equilibrium state between the dissolved gas, dissolved CO_3^{2-} and the precipitated carbonates), a particular purging system (with a mixture of N_2/O_2 (Pei et al., 2000; Zavarise et al., 2010; Chito et al., 2013)) has been used for the measurements in the root extracts of *Hordeum vulgare*.

As seen in figure 3-2, when the measurement is running, the tube a (which in the standard stand is used to provide the nitrogen to the cell), goes through a T-shaped teflon key labelled as B to a glass bottle filled with water (c1 tube in pink). Simultaneously, the tube d transports the CO_2 to the same bottle. Both gases bubble into the milliQ water (glass bottle E) to get them saturated and the resulting gas mixture goes out via tube f (in blue) and goes through the other T-shaped Teflon key labelled as G to the cell I (via tube h). But, at the moment of the drop formation, the keys' position is switched to have the necessary pressure, see inset in figure 3-2).

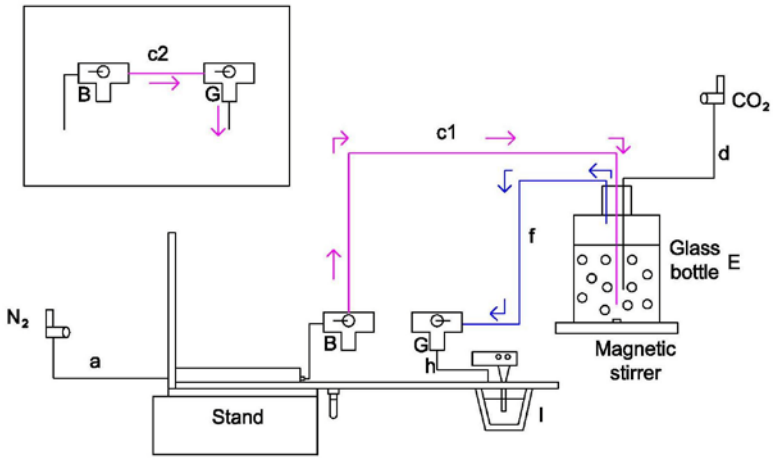

Figure 3-2: Device used to control the evaporation and to fix the pH. The position of the keys B and G and the arrows in this scheme correspond to the situation during the measurement. For drop formation, the keys position has to be changed as shown in the inset.

3.3.4 GSH determination

HPLC with amperometric detection has been used for GSH determination in plant root extracts. The mobile phase consisted of 0.1% trifluoroacetic acid (TFA) in ultrapure filtered water, pH=2.00, and 0.1% TFA in acetonitrile. Gradient separation was achieved at ambient temperature with a gradient profile as described in (Dago et al., 2011). The flow rate was 1.2 mL min^{-1}.

For preparing the surface of the working electrode, mechanical polishing was daily done using a suspension of 0.3 μm alumina particles from Metrohm (Herisau, Switzerland), followed by ethanol rinsing and sonication for 5 min in ethanol and 5 min in ultrapure filtered water. The optimised potential for the working electrode was 1.2 V.

3.4 Results and discussion

3.4.1 Free zinc determination in synthetic solutions of Zn-GSH

Literature values reported in (Diaz-Cruz et al., 2000; Krezel et al., 2003; Ferretti et al., 2007) for the thermodynamic constants of the different species of GSH, extrapolated to zero ionic strength by using Davies correction, are shown in Table 3-1. Four VMINTEQ database have been introduced to the programme to obtain the theoretical free metal concentration when needed for the different models named as follows: DiazCruz I (considering two complexes with just one metal ion), DiazCruz II (contemplating one complex with one metal ion and another with two metal ions), Ferretti (8 complexes) and Krezel (6 complexes).

3.4.1.1 Zn-GSH speciation varying the pH

A titration with fixed amounts of $c_{T,Zn}$ and $c_{T,GSH}$ while varying the pH (by the addition of potassium hydroxide) has been performed. The free zinc concentration obtained by AGNES is compared with the predicted values from VMinteq for the 4 considered speciation models (see Figure 3-3). As seen, below pH 4.5, almost all Zn is in its free form. As the pH increases, the competition of proton for GSH sites is less important and the free zinc concentration decreases. The theoretical results corresponding to both models from DiazCruz do not agree with the experimental results. It is not an unexpected fact as in both models the formation of just two complexes is considered: ZnG^- and ZnG_2^{4-} (model I) or ZnG_2^{4-} and $Zn_2G_2^{4-}$ (model II). Furthermore the use of borate buffer, whose complexation has not been considered, might also be behind the mismatch.

Table 3-1. Thermodynamic cumulative constants, log β^{th}, that have been used for DiazCruzI, DiazCruzII (2000), Ferretti (2007) and Krezel (2003) models, where G^{3-} denotes the completely deprotonated glutathione form (i.e. H_3G is GSH).

Reaction	**Model**			
	DiazCruzI	**DiazCruzII**	**Ferretti**	**Krezel**
$H^+ + G^{3-} \rightleftharpoons HG^{2-}$	10.25	10.25	10.11	10.30
$2H^+ + G^{3-} \rightleftharpoons H_2G^-$	19.37	19.37	19.25	19.46
$3H^+ + G^{3-} \rightleftharpoons H_3G$	23.09	23.09	22.94	23.19
$4H^+ + G^{3-} \rightleftharpoons H_4G^+$	25.17	25.17	25.03	25.32
$Zn^{2+} + G^{3-} \rightleftharpoons ZnG^-$	8.24	-	9.20	9.60
$Zn^{2+} + 2G^{3-} \rightleftharpoons ZnG_2^{4-}$	12.62	12.72	13.03	14.26
$2Zn^{2+} + 2G^{3-} \rightleftharpoons Zn_2G_2^{2-}$	-	21.38	-	-
$Zn^{2+} + G^{3-} + H^+ \rightleftharpoons ZnGH$	-	-	15.71	16.24
$Zn^{2+} + 2G^{3-} + 2H^+ \rightleftharpoons ZnG_2H_2^{2-}$	-	-	31.18	31.65
$Zn^{2+} + 2G^{3-} + H^+ \rightleftharpoons ZnG_2H^{3-}$	-	-	23.22	24.04
$Zn^{2+} + 2G^{3-} \rightleftharpoons ZnG_2H_{-2}^{6-} + 2H^+$	-	-	-10.30	-8.20
$2Zn^{2+} + 2G^{3-} \rightleftharpoons Zn_2G_2H_{-1}^{3-} + H^+$	-	-	11.28	-
$2Zn^{2+} + 2G^{3-} \rightleftharpoons Zn_2G_2H_{-2}^{4-} + 2H^+$	-	-	1.01	-

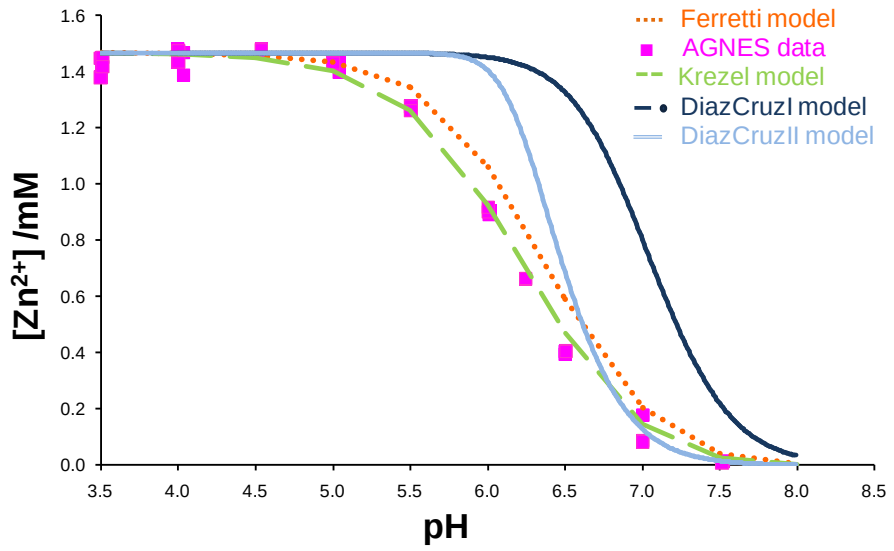

Figure 3-3: Change of $[Zn^{2+}]$ with pH in a solution where $c_{T,Zn}$= 1.6×10^{-3} mol L^{-1}, $c_{T,GSH}$= 2.9×10^{-3} mol L^{-1} and KNO_3 0.1 mol L^{-1}. Pink square marker corresponds to two replicates of AGNES measurements. Theoretical computations: green dashed line stands for Krezel model, orange dotted line for Ferretti model, dark blue dashed dotted line for DiazCruzI model and double blue line for DiazCruzII model.

According to the obtained data, the most suitable models for studying Zn-GSH speciation seems to be Ferretti and Krezel as their results are closer to the experimental ones, particularly in the case of Krezel model, which almost agrees with AGNES (Figure 3-3). When examining accurately the Zn-GSH complexes described in each model, it is seen that both are quite similar in terms of the considered complexes and the reported values of the stability constants. Actually there are just two more species in the model of Ferretti ($Zn_2G_2H_{-1}^{-3}$ and $Zn_2G_2H_{-2}^{-4}$, whose concentrations are nearly negligible in the used conditions as those species appear from pH 8 on) than in Krezel model.

For the particular concentration conditions (total Zn concentration, $c_{T,Zn}$=1.6×10^{-3} mol L^{-1} and total GSH concentration, $c_{T,GSH}$=2.9×10^{-3} mol L^{-1}) used in the figure 3-3, the differences between the free Zn concentrations predicted by Krezel's and

Ferretti's models are maximum in the pH region 7-8. Those can be seen (Figure 3-4) as the percentage of difference between the fractions of Zn, x_j (concentration of the species over the total concentration of Zn), predicted by both models for a given species. The main differences are due to the species ZnG_2^{4-} and $ZnG_2H_2^{2-}$. The first one (ZnG_2^{4-}) is more abundant in Krezel's model (where it reaches 0.2% of the total Zn at pH 7 and 4.9% at pH 8) than in Ferretti's. The second one ($ZnG_2H_2^{2-}$) is more abundant in Ferreti's model (28.5% of the total Zn at pH 7 and 11.6% at pH 8) than in Krezel's. An accurate distribution of the species can be seen comparing figures 3-5 and 3-6.

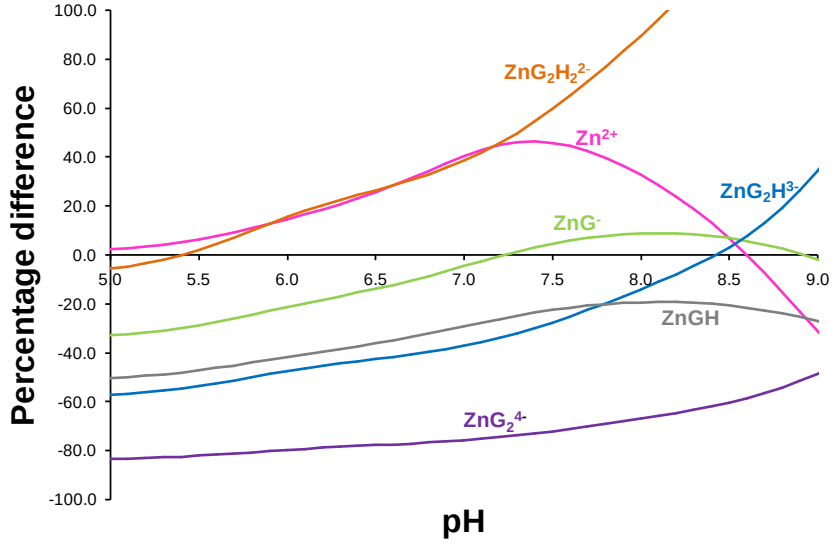

Figure 3-4: Percentage of difference between Ferretti and Krezel models (expressed as $(\chi_{j;Ferretti} - \chi_{j,Krezel})/\ \chi_{j,Krezel})\times 100$, where χ_j is the fraction of Zn as species *j*) for main species of Zn in front of pH. Total concentrations: $c_{T,Zn}= 1.6\times10^{-3}$ mol L^{-1}, $c_{T,GSH}= 2.9\times10^{-3}$ mol L^{-1} and KNO_3 0.1 mol L^{-1}.

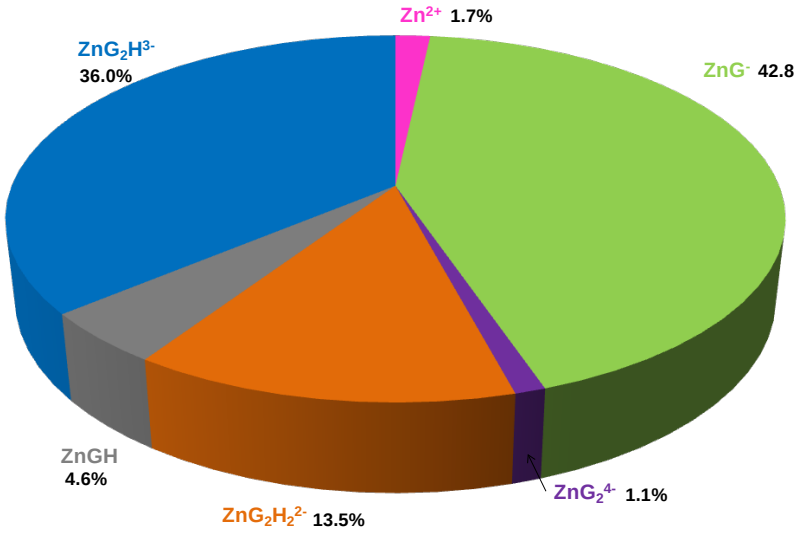

Figure 3-5. Distribution of species according to Krezel's model for the system Zn-GSH with $c_{T,Zn}$= 1.6×10^{-3} mol L^{-1}, $c_{T,GSH}$= 2.9×10^{-3} mol L^{-1}, pH 7.5 and KNO_3 0.1 mol L^{-1} (same concentration conditions as in Figure 3-4) .

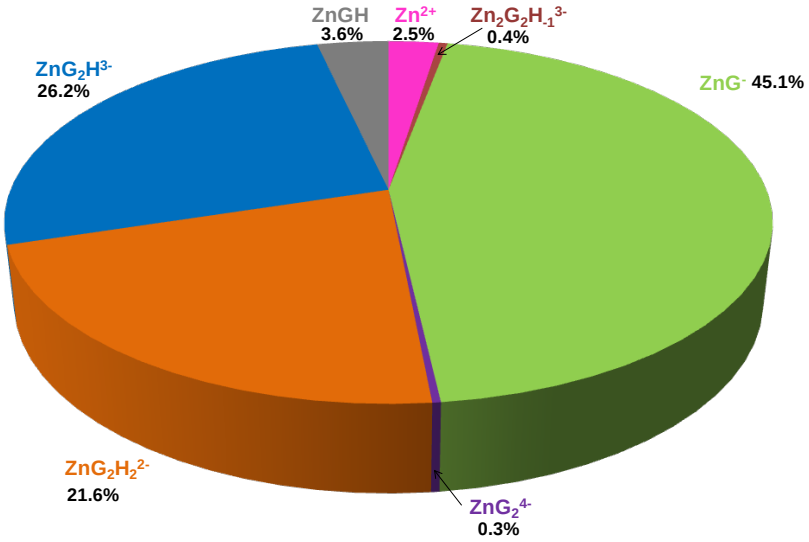

Figure 3-6. Distribution of species according to Ferretti's model for the system Zn-GSH with $c_{T,Zn}$= 1.6×10^{-3} mol L^{-1}, $c_{T,GSH}$= 2.9×10^{-3} mol L^{-1}, pH 7.5 and KNO_3 0.1 mol L^{-1} (same concentration conditions as in Figure 3-4)

3.4.1.2 Zn-GSH titrations fixing $c_{T,Zn}$ and pH while varying $c_{T,GSH}$

The appropriateness of the models has also been examined by performing two titrations where the pH has been fixed at two different values: 7.5 and 8. The $c_{T,Zn}$ range has also been chosen taking into account the concentration region in the μmol L^{-1} range, where the difference between models is larger (for resulting free concentrations above nanomolar). To work with pH fixed, several buffer solutions such as borate, tris(hydroxymethyl)aminomethane (TRIS) and 3-[4-(2-hidroxietil)piperazin-1-il]propane-1-sulfonic Acid (EPPS) have been tested. Finally, EPPS has been selected because previous DPP experiments indicated complexation of Zn by borate and TRIS, but not by EPPS.

As seen in Figure 3-7, at lower total Zn concentration, it is again revealed that the predictions of $[Zn^{2+}]$ in DiazCruz models are distant from the experimental results with AGNES, if we compare them with Ferretti and Krezel models. At those concrete conditions, the most accurate model appears to be Ferretti's. An analogous behaviour is showed in figure 3-8, now at a total Zn concentration of 0.1 mmol L^{-1}. We considered whether the differences in the predictions of free Zn between Ferretti and Krezel models could be explained because of the slightly different protonation constants. To prove that hyphotesis, we forced the protonation GSH constants of Krezel into the model of Ferretti, though there is no agreement neither with the experimental data nor with the predictions of Krezel's model. The same takes place when introducing the protonation GSH constants of Ferretti into Krezel's model.

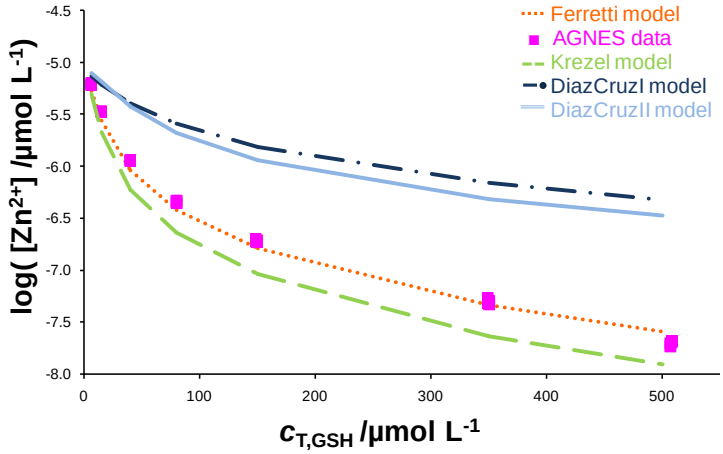

Figure 3-7: Evolution of $[Zn^{2+}]$ when adding glutathione to a solution where $c_{T,Zn}$= 1×10^{-5} mol L^{-1}, pH 8.00 (10^{-2} mol L^{-1} EPPS) and KNO_3 0.1 mol L^{-1}. Markers and lines as in Fig 3-3.

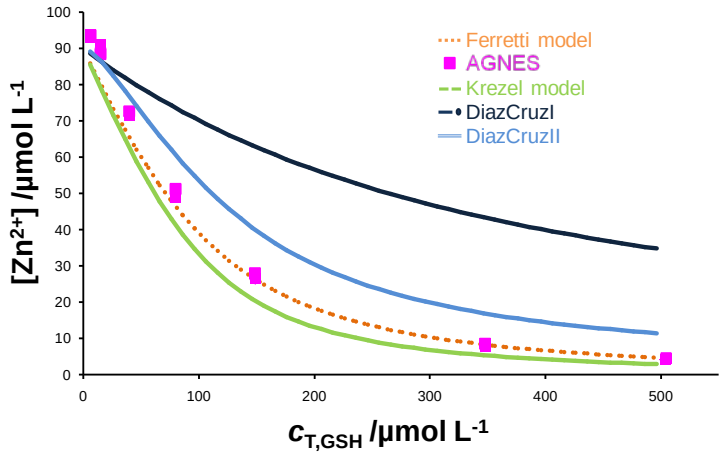

Figure 3-8. $[Zn^{2+}]$ vs $c_{T,GSH}$ added to a solution where $c_{T,Zn}$= 1×10^{-4} mol L^{-1}, pH 7.5 (10^{-2} mol L^{-1} EPPS) and KNO_3 0.1 mol L^{-1}. Pink square marker corresponds to two replicates of AGNES measurements. Markers and lines as in Fig 3-3.

3.4.2 Zn speciation in root extracts of *Hordeum Vulgare*

The analysis of GSH in root extracts of *Hordeum vulgare* plants has been done by HPLC with amperometric detection. The quantification has been made by external calibration curve with high linearity (determination coefficient r^2=0.9998) with standards ranging from 1 to 10 µmol L^{-1}. The obtained limits of detection and quantification were 1.57×10^{-7} and 5.23×10^{-7} mol L^{-1}, respectively. Three independent replicates (labelled 1, 2 and 3) have been analysed obtaining an average concentration of GSH of 1.327 ± 0.003 µmol L^{-1}.

The total Zinc concentration in these three samples has been determined by ICP-MS. As observed in Table 3-2, the total concentration is about 10 µmol L^{-1}, leading to a sufficiently high free zinc concentration as to be determined with AGNES-1P (see Section 1.4.1) and "modest" gains.

Table 3-2. Compilation of $[Zn^{2+}]$ determined by AGNES in root extracts of *Hordeum vulgare* for two different gains (*Y*=20 and *Y*=50). In all cases the experimental results are compared with theoretical predictions by VMinteq using the databases of Ferretti and Krezel.

Sample	**pH**	$c_{T,GSH}$ **/mol L^{-1}**	$c_{T,Zn}$ **/mol L^{-1} (ICP)**	$[Zn^{2+}]_{AGNES\_I}$ **/mol L^{-1}**	$[Zn^{2+}]_{AGNES\_Q}$ **/mol L^{-1}**	$[Zn^{2+}]_{VMinteq}$ **/mol L^{-1}**
1	7.30	1.33×10^{-6}	8.58×10^{-5}	1.72×10^{-6} (Y=50) 1.70×10^{-6} (Y=20)	1.70×10^{-6} (Y=50) 1.66×10^{-6} (Y=20)	8.28×10^{-5} (Ferretti) 8.27×10^{-5} (Krezel)
2	7.33	1.33×10^{-6}	8.53×10^{-5}	1.70×10^{-6} (Y=50) 1.70×10^{-6} (Y=20)	1.66×10^{-6} (Y=50) 1.63×10^{-6} (Y=20)	8.21×10^{-5} (Ferretti) 8.208×10^{-5} (Krezel)
3	7.25	1.32×10^{-6}	9.12×10^{-5}	1.63×10^{-6} (Y=50) 1.62×10^{-6} (Y=20)	1.64×10^{-6} (Y=50) 1.62×10^{-6} (Y=20)	8.84×10^{-5} (Ferretti) 8.82×10^{-5} (Krezel)

To increase the reliability of the results, all measurements have been done twice and with two different gains (*Y*=20 and *Y*=50), taking as AGNES response both the

intensity (AGNES-I) and the charge (AGNES-Q), see Section 1.4.3.3. The applied deposition times have been 350 and 500 s for *Y*=50 and 175 and 250 s for *Y*=20, respectively, which unquestionably satisfy or overpass the usual rule (Chito et al., 2010):

$$t_1 - t_w = 7\mathrm{Y} \tag{3-4}$$

We work with two different deposition times (for each gain) to ensure that AGNES equilibrium is reached.

All replicates within each sample presented a good agreement between them. The reproducibility between samples is also good (see Table 3-2).

The experimental free zinc concentration determined (just around 2% of the total zinc) is lower than the theoretically expected just considering GSH complexation following the models of Ferretti and Krezel by a factor around 50. This means that in the samples there exist other ligands apart from GSH which are complexing most of the metal. This could be explained from the complexation of Zn with phytochelatins (synthesized by its precursor GSH), as seen with other metals and metalloids as for example Hg, Cd or As (Dago et al., 2011; Dago et al., 2014), triggered by the large level of the stressor Zn in the hydroponic medium.

3.5 Conclusions

The electroanalytical technique AGNES can be successfully applied to evaluate the accuracy in the predictions of free Zn concentrations between competing complexation models, by comparing the determined free zinc concentration in various titrations with the theoretical ones achieved with a speciation program (like VMinteq). In the particular studied case, four different models of the system Zn-GSH, whose complexation constants are reported in the literature, are compared.

When pH is changed with $c_{T,GSH}$ in the mmol L^{-1} range, Krezel model seems to be the most appropriate one, closely followed by Ferretti's, showing the biggest difference between them in the pH region 7-8. The principal difference is the diverse relevance for particular species that each model proposes (ZnG_2^{4-} in the case of

Krezel and $ZnG_2H_2^{2-}$ for Ferretti). But, when that concrete pH region has been studied in the μmol L^{-1} range, the contrary has happened (the most appropriate model has been Ferretti). Considering the possible experimental uncertainty, a clear prioritisation of these two models cannot be done. That is why, when the root extracts of *Hordeum vulgare* have been analyzed, the experimental results are compared with both models (even if the difference between the predictions is smaller than the experimental error). In the extracts nearly all Zn is complexed (98%). On the other hand, the experimental free zinc concentration is 50 times lower than the theoretical one. Thus, the free Zn concentration is not mostly determined just by GSH, being necessary to consider a more complex scheme including other ligands (like other types of phytochelatins), as seen in the case of other metals, as for example Cd or Hg.

3.6 References

A.S.Mohammed, A.Kapri, R.Goel, 2011. Heavy Metal Pollution: Source, Impact and Remedies. Biomanagement of Metal-Contaminated Soils. Springer Science, pp. 1-28.

Adam,N., Schmitt,C., Galceran,J., Companys,E., Vakourov,A., Wallace,R., Knapen,D., Blust,R., 2013. The chronic toxicity of ZnO nanoparticles and ZnCl2 to Daphnia magna and the use of different methods to assess nanoparticle aggregation and dissolution, *Nanotoxicology* 8, pp. 709-717.

Aguilar,D., Galceran,J., Companys,E., Puy,J., Parat,C., Authier,L., Potin-Gautier,M., 2013a. Non-purged voltammetry explored with AGNES, *Phys. Chem. Chem. Phys.* 15, pp. 17510-17521.

Aguilar,D., Parat,C., Galceran,J., Companys,E., Puy,J., Authier,L., Potin-Gautier,M., 2013b. Determination of free metal ion concentrations with AGNES in low ionic strength media, *J. Electroanal. Chem.* 689, pp. 276-283.

Ahner,B.A., Price,N.M., Morel,F.M.M., 1994. Phytochelatin production by marine-phytoplankton at low free metal-ion concentrations - Laboratory studies and field data from massachusetts bay, *Proceedings of the National Academy of Sciences of the United States of America* 91, pp. 8433-8436.

Alberti,G., Biesuz,R., Huidobro,C., Companys,E., Puy,J., Galceran,J., 2007. A comparison between the determination of free Pb(II) by two techniques: Absence of Gradients and Nernstian Equilibrium Stripping and Resin Titration, *Anal. Chim. Acta* 599, pp. 41-50.

Almestrand,L., Jagner,D., Renman,L., 1987. Automated-Determination of Cadmium and Lead in Whole-Blood by Computerized Flow Potentiometric Stripping with Carbon-Fiber Electrodes, *Anal. Chim. Acta* 193, pp. 71-79.

Alves,G.M.S., Rocha,L.S., Soares,H.M.V.M., 2017. Multi-element determination of metals and metalloids in waters and wastewaters, at trace concentration level, using electroanalytical stripping methods with environmentally friendly mercury free-electrodes: A review, *Talanta* 175, pp. 53-68.

Anderson,M.A., Morel,F.M.M., Guillard,R.R.L., 1978. Growth limitation of a coastal diatom by low zinc ion activity, *Nature* 276, pp. 70-71.

Arino,C., Serrano,N., Diaz-Cruz,J.M., Esteban,M., 2017. Voltammetric determination of metal ions beyond mercury electrodes. A review, *Anal. Chim. Acta* 990, pp. 11-53.

Bakker,E., Buhlmann,P., Pretsch,E., 1997. Carrier-based ion-selective electrodes and bulk optodes. 1. General characteristics, *Chem. Rev.* 97, pp. 3083-3132.

Bansod,B., Kumar,T., Thakur,R., Rana,S., Singh,I., 2017. A review on various electrochemical techniques for heavy metal ions detection with different sensing platforms, *Biosens. Bioelectron.* 94, pp. 443-455.

Bard,A.J., Faulkner,L.R., 1980. Electrochemical Methods, Fundamentals and Applications. Wiley, New York.

Bard,A.J., Faulkner,L.R., 2001. Electrochemical Methods. Fundamentals and Applications. John Wiley & Sons, Inc., New York.

Batley,G.E., Apte,S.C., Stauber,J.L., 2004. Speciation and bioavailability of trace metals in water: Progress since 1982, *Aust. J. Chem.* 57, pp. 903-919.

Berbel,F., Díaz-Cruz,J.M., Ariño,C., Esteban,M., 1999. Voltammetry of sparingly soluble metal complexes: a differential pulse polarographic study of the Zn(II) plus oxalate system, *J. Electroanal. Chem.* 475, pp. 99-106.

Bond,A.M., Hefter,G., 1976. Inequivalence of apparent polarographic and potentiometric stability-constants for cadmium(II) bromide and iodide systems, *J. Electroanal. Chem.* 68, pp. 203-216.

Bruins,M.R., Kapil,S., Oehme,F.W., 2000. Microbial resistance to metals in the environment, *Ecotox. Environ. Safe.* 45, pp. 198-207.

Campbell,P.G.C., 1995. Interactions between Trace Metal and Aquatic Organisms: A Critique of the Free-ion Activity Model. In: A. Tessier and D. R. Turner (Eds.). Metal Speciation and Bioavailability in Aquatic Systems. John Wiley & Sons, Chichester (UK), pp. 45-102.

Campbell,P.G.C., Errecalde,O., Fortin,C., Hiriart-Baer,W.R., Vigneault,B., 2002. Metal bioavailability to phytoplankton - applicability of the Biotic Ligand Model, *Comp. Biochem. Physiol. C* 133, pp. 189-206.

Casassas,E., Arino,C., 1986. Determination of Stability-Constants of Some Cadmium Complexes by Polarographic Techniques in the Presence of Electrode Adsorption, *J. Electroanal. Chem.* 213, pp. 235-244.

Chito,D., Methodological advancements of AGNES and its implementation for the determination of free metal ion concentrations in synthetic and natural samples., PhD thesis. Universitat de Lleida., (2012).

Chito,D., Galceran,J., Companys,E., 2010. The Impact of Intermetallic Compounds Cu_xZn in the Determination of Free Zn^{2+} Concentration with AGNES, *Electroanal.* 22, pp. 2024-2033.

Chito,D., Galceran,J., Companys,E., Puy,J., 2013. Determination of the Complexing Capacity of Wine for Zn Using the Absence of Gradients and Nernstian Equilibrium Stripping Technique, *J. Agric. Food Chem.* 61, pp. 1051-1059.

Chito,D., Weng,L., Galceran,J., Companys,E., Puy,J., van Riemsdijk,W.H., van Leeuwen,H.P., 2012. Determination of free Zn^{2+} concentration in synthetic and natural samples with AGNES (Absence of Gradients and Nernstian Equilibrium

Stripping) and DMT (Donnan Membrane Technique), *Sci. Total Envir.* 421-422, pp. 238-244.

Cleven,R., Fokkert,L., 1994. Potentiometric Stripping Analysis of Thallium in Natural-Waters, *Anal. Chim. Acta* 289, pp. 215-221.

Companys,E., Cecília,J., Codina,G., Puy,J., Galceran,J., 2005. Determination of the concentration of free Zn^{2+} with AGNES using different strategies to reduce the deposition time., *J. Electroanal. Chem.* 576, pp. 21-32.

Companys,E., Galceran,J., Pinheiro,J.P., Puy,J., Salaün,P., 2017. A review on electrochemical methods for trace metal speciation in environmental media, *Curr. Opin. Electrochem.* 3, pp. 144-162.

Companys,E., Galceran,J., Puy,J., Sedo,M., Vera,R., Antico,E., Fontas,C., 2018. Comparison of different speciation techniques to measure Zn availability in hydroponic media, *Anal. Chim. Acta* 1035, pp. 32-43.

Companys,E., Naval-Sanchez,M., Martinez-Micaelo,N., Puy,J., Galceran,J., 2008. Measurement of free zinc concentration in wine with AGNES, *J. Agric. Food Chem.* 56, pp. 8296-8302.

Companys,E., Puy,J., Galceran,J., 2007. Humic acid complexation to Zn and Cd determined with the new electroanalytical technique AGNES, *Environ. Chem.* 4, pp. 347-354.

Companys,E., Puy,J., Torrent,M., Galceran,J., Salvador,J., Garcés,J.L., Mas,F., 2003. Binding curve from normalised limiting currents of labile heterogeneous metal-macromolecular systems. The case of Cd/humic acid., *Electroanal.* 15, pp. 452-459.

Cremazy,A., Leclair,S., Mueller,K., Vigneault,B., Campbell,P., Fortin,C., 2015. Development of an In Situ Ion-Exchange Technique for the Determination of Free Cd, Co, Ni, and Zn Concentrations in Freshwaters, *Aquat. Geochem.* 21, pp. 259-279.

Dago,A., Gonzalez,I., Arino,C., Diaz-Cruz,J.M., Esteban,M., 2014. Chemometrics applied to the analysis of induced phytochelatins in Hordeum vulgare plants stressed with various toxic non-essential metals and metalloids, *Talanta* 118, pp. 201-209.

Dago,A., Gonzalez-Garcia,O., Arino,C., Diaz-Cruz,J.M., Esteban,M., 2011. Characterization of Hg(II) binding with different length phytochelatins using liquid chromatography and amperometric detection, *Anal. Chim. Acta* 695, pp. 51-57.

David,C., Galceran,J., Rey-Castro,C., Puy,J., Companys,E., Salvador,J., Monné,J., Wallace,R., Vakourov,A., 2012. Dissolution kinetics and solubility of ZnO nanoparticles followed by AGNES., *J. Phys. Chem. C* 116, pp. 11758-11767.

Davison,W., Zhang,H., 2012. Progress in understanding the use of diffusive gradients in thin films (DGT) – back to basics, *Environ. Chem.* 9, pp. 1-13.

Davison,W., Zhang,H., Grime,G.W., 1994. Performance-characteristics of gel probes used for measuring the chemistry of pore waters, *Environ. Sci. Technol.* 28, pp. 1623-1632.

Díaz-Cruz,J.M., Ariño,C., Esteban,M., Casassas,E., 1991. Polarography and stripping voltammetry of metal polycarboxylate complexes - complexes of cadmium and zinc with polyacrylic and polymethacrylic acids, *Electroanal.* 3, pp. 299-307.

Diaz-Cruz,M.S., Díaz-Cruz,J.M., Mendieta,J., Tauler,R., Esteban,M., 2000. Soft- and hard-modeling approaches for the determination of stability constants of metal-peptide systems by voltammetry, *Anal. Biochem.* 279, pp. 189-201.

Dolphin,D., Avramovic,O., Poulson,R., 1989. Glutathione. Chemical, Biochemical and Medical Aspects. Wiley-Interscience, New York.

Domingos,R.F., Carreira,S., Galceran,J., Salaün,P., Pinheiro,J.P., 2016. AGNES at vibrated gold microwire electrode for the direct quantification of free copper concentrations, *Anal. Chim. Acta* 920, pp. 29-36.

Domingos,R.F., Huidobro,C., Companys,E., Galceran,J., Puy,J., Pinheiro,J.P., 2008. Comparison of AGNES (Absence of Gradients and Nernstian Equilibrium Stripping) and SSCP (Scanned Stripping Chronopotenciometry) for Trace Metal Speciation Analysis, *J. Electroanal. Chem.* 617, pp. 141-148.

Domingos,R.F., Rafiei,Z., Monteiro,C.E., Khan,M.A.K., Wilkinson,K.J., 2013. Agglomeration and dissolution of zinc oxide nanoparticles: role of pH, ionic strength and fulvic acid, *Environ. Chem.* 10, pp. 306-312.

Domingos,R.F., Simon,D.F., Hauser,C., Wilkinson,K.J., 2011. Bioaccumulation and Effects of CdTe/CdS Quantum Dots on Chlamydomonas reinhardtii - Nanoparticles or the Free Ions?, *Environ. Sci. Technol.* 45, pp. 7664-7669.

Duffus,J.H., 2002. "Heavy metals" - A meaningless term? (IUPAC technical report), *Pure Appl. Chem.* 74, pp. 793-807.

Duval,J.F.L., Farinha,J.P.S., Pinheiro,J.P., 2013. Impact of Electrostatics on the Chemodynamics of Highly Charged Metal-Polymer Nanoparticle Complexes, *Langmuir* 29, pp. 13821-13835.

Ensafi,A.A., Benvidi,A., Khayamian,T., 2004. Determination of cadmium and zinc in water and alloys by adsorption stripping voltammetry, *Analytical letters* 37, pp. 449-462.

Estela,J.M., Tomas,C., Cladera,A., CERDA,V., 1995. Potentiometric Stripping Analysis - A Review, *Crit. Rev. Anal. Chem.* 25, pp. 91-141.

Ferretti,L., Elviri,L., Pellinghelli,M.A., Predieri,G., Tegoni,M., 2007. Glutathione and N-acetylcysteinylglycine: Protonation and Zn2+ complexation, *J. Inorg. Biochem.* 101, pp. 1442-1456.

Fortin,C., Campbell,P.G.C., 1998. An ion-exchange technique for free-metal ion measurements (Cd^{2+}, Zn^{2+}): Applications to complex aqueous media, *Int. J. Environ. Anal. Chem.* 72, pp. 173-194.

Fortin,C., Couillard,Y., Vigneault,B., Campbell,P.G.C., 2010. Determination of free Cd, Cu and Zn concentrations in lake waters by *in situ* diffusion followed by column equilibration ion-exchange., *Aquat. Geochem.* 16, pp. 151-172.

Froning,M., Mohl,C., Ostapczuk,P., 1993. Interlaboratory Quality-Control for Lead Determination in Wine by Potentiometric Stripping Analysis, *Fresenius J. Anal. Chem.* 345, pp. 233-235.

Galceran,J., Chito,D., Martinez-Micaelo,N., Companys,E., David,C., Puy,J., 2010. The impact of high Zn^{o} concentrations on the application of AGNES to determine free Zn(II) concentration, *J. Electroanal. Chem.* 638, pp. 131-142.

Galceran,J., Companys,E., Puy,J., Cecília,J., Garcés,J.L., 2004. AGNES: a new electroanalytical technique for measuring free metal ion concentration, *J. Electroanal. Chem.* 566, pp. 95-109.

Galceran,J., Huidobro,C., Companys,E., Alberti,G., 2007. AGNES: a technique for determining the concentration of free metal ions. The case of Zn(II) in coastal Mediterranean seawater., *Talanta* 71, pp. 1795-1803.

Galceran,J., Lao,M., David,C., Companys,E., Rey-Castro,C., Salvador,J., Puy,J., 2014. The impact of electrodic adsorption on Zn, Cd or Pb speciation measurements with AGNES, *J. Electroanal. Chem.* 722-723, pp. 110-118.

Galceran,J., Rene,D., Salvador,J., Puy,J., Esteban,M., Mas,F., 1994. Reverse Pulse Polarography of labile metal + macromolecule systems with induced reactant adsorption - Theoretical analysis and determination of domplexation and adsorption parameters, *J. Electroanal. Chem.* 375, pp. 307-318.

Galceran,J., Salvador,J., Puy,J., Cecília,J., Esteban,M., Mas,F., 1995. Influence of adsorption on calibration curves in Normal Pulse Polarography, *Anal. Chim. Acta* 305, pp. 273-284.

Galceran,J., Puy,J., 2015. Interpretation of diffusion gradients in thin films (DGT) measurements: a systematic approach, *Environ. Chem.* 12, pp. 112-122.

Gao,R., Temminghoff,E.J.M., van Leeuwen,H.P., van Valenberg,H.J.F., Eisner,M.D., van Boekel,M.A.J.S., 2009. Simultaneous determination of free calcium, magnesium, sodium and potassium ion concentrations in simulated milk ultrafiltrate and reconstituted skim milk using the Donnan Membrane Technique, *Int. Dairy J.* 19, pp. 431-436.

Garrigosa,A.M., Diaz-Cruz,J.M., Arino,C., Esteban,M., 2008. Multivariate curve resolution as a tool to minimize the effects of electrodic adsorption in normal pulse voltammetry, *Electrochim. Acta.* 53, pp. 5579-5586.

Gozzo,M.L., Colacicco,L., Calla,C., Barbaresi,G., Parroni,R., Giardina,B., Lippa,S., 1999. Determination of copper, zinc, and selenium in human plasma and urine samples by potentiometric stripping analysis and constant current stripping analysis, *Clinica Chimica Acta* 285, pp. 53-68.

Gramlich,A., Tandy,S., Slaveykova,V.I., Duffner,A., Schulin,R., 2012. The use of permeation liquid membranes for free zinc measurements in aqueous solution, *Environ. Chem.* 9, pp. 429-437.

Grill,E., Winnacker,E.L., Zenk,M.H., 1985. Phytochelatins - the Principal Heavy-Metal Complexing Peptides of Higher-Plants, *Science* 230, pp. 674-676.

Grill,E., Winnacker,E.L., Zenk,M.H., 1987. Phytochelatins, A Class of Heavy-Metal-Binding Peptides from Plants, Are Functionally Analogous to Metallothioneins, *Proceedings of the National Academy of Sciences of the United States of America* 84, pp. 439-443.

Guaus,E., Sanz,F., 1999. Metal-halide-complex and ligand simultaneous adsorption. Chronocoulometry study in the Cd(II), KI Hg system at several ionic strengths, *Electroanal.* 11, pp. 424-431.

Gunkel-Grillon,P., Buffle,J., 2008. Speciation of Cu(II) with a flow-through permeation liquid membrane: discrimination between free copper, labile and inert Cu(II) complexes, under natural water conditions, *Analyst.* 133, pp. 954-961.

Gustafsson,J.P. Visual MINTEQ version 3.1. https://vminteq.lwr.kth.se/download/. 2016.

Ref Type: Computer Program

Helaluddin,A.B.M., Khalid,R.S., Alaama,M., Abbas,S.A., 2016. Main Analytical Techniques Used for Elemental Analysis in Various Matrices, *Tropical Journal of Pharmaceutical Research* 15, pp. 427-434.

Hoyer,B., Jensen,N., 2004. Use of sodium dodecyl sulfate as an antifouling and homogenizing agent in the direct determination of heavy metals by anodic stripping voltammetry, *Analyst.* 129, pp. 751-754.

Huidobro,C., Companys,E., Puy,J., Galceran,J., Pinheiro,J.P., 2007. The use of microelectrodes with AGNES, *J. Electroanal. Chem.* 606, pp. 134-140.

Jagner,D., 1982. Potentiometric stripping analysis - A review, *Analyst.* 107, pp. 593-599.

Jagner,D., Josefson,M., Westerlund,S., 1981. Simultaneous Determination of Cadmium and Lead in Urine by Means of Computerized Potentiometric Stripping Analysis, *Anal. Chim. Acta* 128, pp. 155-161.

Kalis,E.J.J., Temminghoff,E.J.M., Weng,L.P., van Riemsdijk,W.H., 2006a. Effects of humic acid and competing cations on metal uptake by Lolium perenne, *Environ. Toxicol. Chem.* 25, pp. 702-711.

Kalis,E.J.J., Weng,L.P., Dousma,F., Temminghoff,E.J.M., van Riemsdijk,W.H., 2006b. Measuring free metal ion concentrations in situ in natural waters using the Donnan Membrane Technique, *Environ. Sci. Technol.* 40, pp. 955-961.

Kalis,E.J.J., Weng,L.P., Temminghoff,E.J.M., van Riemsdijk,W.H., 2007. Measuring free metal ion concentrations in multicomponent solutions using the Donnan membrane technique, *Anal. Chem.* 79, pp. 1555-1563.

Kim,K.R., Owens,G., 2009. Chemodynamics of heavy metals in long-term contaminated soils: Metal speciation in soil solution, *Journal of Environmental Sciences* 21, pp. 1532-1540.

Krezel,A., Wojcik,J., Maciejczyk,M., Bal,W., 2003. May GSH and L-His contribute to intracellular binding of zinc? Thermodynamic and solution structural study of a ternary complex, *Chemical Communications* pp. 704-705.

Lawrence,E., Jackson,A.R.W., Jackson,J.M., 1998. Longman Dictionary of Enviromental Science. Addison Wesley Longman Ltd., London (UK).

Lopez-Perez,G., Andreu,R., Gonzalez-Arjona,D., Calvente,J.J., Molero,M., 2003. Influence of temperature on the reduction kinetics of Zn2+ at a mercury electrode, *J. Electroanal. Chem.* 552, pp. 247-259.

Louis,Y., Cmuk,P., Omanovic,D., Garnier,C., Lenoble,V., Mounier,S., Pizeta,I., 2008. Speciation of trace metals in natural waters: The influence of an adsorbed layer of natural organic matter (NOM) on voltammetric behaviour of copper, *Anal. Chim. Acta* 606, pp. 37-44.

Lovric,M., 1984. Reactant Adsorption in Pulse Polarography, *J. Electroanal. Chem.* 170, pp. 143-173.

Lu,Y.Y., Liang,X.Q., Niyungeko,C., Zhou,J.J., Xu,J.M., Tian,G.M., 2018. A review of the identification and detection of heavy metal ions in the environment by voltammetry, *Talanta* 178, pp. 324-338.

Mas,F., Puy,J., Díaz-Cruz,J.M., Esteban,M., Casassas,E., 1993. Semiempirical Full-Wave Expression for Induced Reactant Adsorption in Normal Pulse Polarography of Labile Metal Polyelectrolyte Systems, *Anal. Chim. Acta* 273, pp. 297-304.

Menegario,A.A., Yabuki,L.N.M., Luko,K.S., Williams,P.N., Blackburn,D.M., 2017. Use of diffusive gradient in thin films for in situ measurements: A review on the progress in chemical fractionation, speciation and bioavailability of metals in waters, *Anal. Chim. Acta* 983, pp. 54-66.

Mongin,S., Uribe,R., Puy,J., Cecilia,J., Galceran,J., Zhang,H., Davison,W., 2011. Key role of the resin layer thickness in the lability of complexes measured by DGT, *Environ. Sci. Technol.* 45, pp. 4869-4875.

Mongin,S., Uribe,R., Rey-Castro,C., Cecilia,J., Galceran,J., Puy,J., 2013. Limits of the Linear Accumulation Regime of DGT Sensors, *Environ. Sci. Technol.* 47, pp. 10438-10445.

Mota,A.M., Correia dos Santos,M.M., 1995. Trace Metal Speciation of Labile Chemical Species in Natural Waters: Electrochemical Methods. In: A. Tessier and D. R. Turner (Eds.). Metal Speciation and Bioavailability in Aquatic Systems. John Wiley & Sons, Chichester, pp. 205-258.

Mu,Q., David,C.A., Galceran,J., Rey-Castro,C., Krzemiñski,L., Wallace,R., Bamiduro,F., Milne,S.J., Hondow,N.S., Brydson,R., Vizcay-Barrena,G., Routledge,M.N., Jeuken,L.J.C., Brown,A.P. A systematic investigation of the physico-chemical factors that contribute to the toxicity of ZnO nanoparticles. Chemical Research in Toxicology . 2014a.

Ref Type: In Press

Mu,Q.S., David,C.A., Galceran,J., Rey-Castro,C., Krzeminski,L., Wallace,R., Bamiduro,F., Milne,S.J., Hondow,N.S., Brydson,R., Vizcay-Barrena,G., Routledge,M.N., Jeuken,L.J.C., Brown,A.P., 2014b. Systematic Investigation of the Physicochemical Factors That Contribute to the Toxicity of ZnO Nanoparticles, *Chem. Res. Toxicol.* 27, pp. 558-567.

Murakami,S., Ogura,K., Yoshino,T., 1980. Equilibria of Complex-Formation Between Bivalent-Metal Ions and 3,3'-Bis[N,N'-Bis(Carboxymethyl)Aminomethyl]-Ortho-Cresolsulfonphthalein, *Bull. Chem. Soc. Jpn.* 53, pp. 2228-2235.

Omanovic,D., Branica,M., 2004. Pseudopolarography of trace metals. Part II. The comparison of the reversible, quasireversible and irreversible electrode reactions, *J. Electroanal. Chem.* 565, pp. 37-48.

Paquin,P.R., Gorsuch,J.W., Apte,S., Batley,G.E., Bowles,K.C., Campbell,P.G.C., Delos,C.G., Di Toro,D.M., Dwyer,R.L., Galvez,F., Gensemer,R.W., Goss,G.G., Hogstrand,C., Janssen,C.R., McGeer,J.C., Naddy,R.B., Playle,R.C., Santore,R.C., Schneider,U., Stubblefield,W.A., Wood,C.M., Wu,K.B., 2002. The biotic ligand model: a historical overview, *Comp. Biochem. Physiol. C* 133, pp. 3-35.

Parat,C., Aguilar,D., Authier,L., Potin-Gautier,M., Companys,E., Puy,J., Galceran,J., 2011a. Determination of Free Metal Ion Concentrations Using Screen-Printed Electrodes and AGNES with the Charge as Response Function, *Electroanal.* 23, pp. 619-627.

Parat,C., Authier,L., Aguilar,D., Companys,E., Puy,J., Galceran,J., Potin-Gautier,M., 2011b. Direct determination of free metal concentration by implementing stripping chronopotentiometry as second stage of AGNES, *Analyst.* 136, pp. 4337-4343.

Parat,C., Authier,L., Castetbon,A., Aguilar,D., Companys,E., Puy,J., Galceran,J., Potin-Gautier,M., 2015. Free Zn^{2+} determination in natural freshwaters of the Pyrenees: towards on-site measurements with AGNES, *Environ. Chem.* 12, pp. 329-337.

Parat,C., Schneider,A., Castetbon,A., Potin-Gautier,M., 2011c. Determination of trace metal speciation parameters by using screen-printed electrodes in stripping chronopotentiometry without deaerating, *Anal. Chim. Acta* 688, pp. 156-162.

Parker,D.R., Pedler,J.F., 1997. Reevaluating the free-ion activity model of trace metal availability to higher plants, *Plant Soil* 196, pp. 223-228.

Pearson,H.B.C., Galceran,J., Companys,E., Braungardt,C., Worsfold,P., Puy,J., Comber,S., 2016. Absence of Gradients and Nernstian Equilibrium Stripping (AGNES) for the determination of [Zn2+] in estuarine waters, *Anal. Chim. Acta* 912, pp. 32-40.

Pei,J.H., Tercier-Waeber,M.L., Buffle,J., 2000. Simultaneous determination and speciation of zinc, cadmium, lead, and copper in natural water with minimum handling and artifacts, by voltammetry on a gel-integrated microelectrode array, *Anal. Chem.* 72, pp. 161-171.

Penland,J.G., 2000. Behavioral data and methodology issues in studies of zinc nutrition in humans, *Journal of Nutrition* 130, pp. 361S-364S.

Pernet-Coudrier,B., Companys,E., Galceran,J., Morey,M., Mouchel,J.M., Puy,J., Ruiz,N., Varrault,G., 2011. Pb-binding to various dissolved organic matter in urban aquatic systems: Key role of the most hydrophilic fraction, *Geochim. Cosmochim. Ac.* 75, pp. 4005-4019.

Pesavento,M., Alberti,G., Biesuz,R., 2009. Analytical methods for determination of free metal ion concentration, labile species fraction and metal complexation capacity of environmental waters: A review, *Anal. Chim. Acta* 631, pp. 129-141.

Pinheiro,J.P., Mota,A.M., Gonçalves,M.L.S.S., Vanderweijde,M., van Leeuwen,H.P., 1996. Comparison between polarographic and potentiometric speciation for cadmium/humic acid systems, *J. Electroanal. Chem.* 410, pp. 61-68.

Pinheiro,J.P., Salvador,J., Companys,E., Galceran,J., Puy,J., 2010. Experimental verification of the metal flux enhancement in a mixture of two metal complexes: the Cd/NTA/glycine and Cd/NTA/citric acid systems, *Phys. Chem. Chem. Phys.* 12, pp. 1131-1138.

Puy,J., Galceran,J., Huidobro,C., Companys,E., Samper,N., Garcés,J.L., Mas,F., 2008. Conditional Affinity Spectra of Pb^{2+}-Humic Acid Complexation from Data Obtained with AGNES, *Environ. Sci. Technol.* 42, pp. 9289-9295.

Puy,J., Galceran,J., Rey-Castro,C., 2016. Interpreting the DGT measurement: speciation and dynamics. In: W. Davison (Eds.). Diffusive Gradients in Thin-Films for environmental measurements. Cambridge University Press, Cambridge, pp. 93-122.

Puy,J., Mas,F., Díaz-Cruz,J.M., Esteban,M., Casassas,E., 1992. Induced reactant adsorption in metal-polyelectrolyte systems - Pulse polarographic study, *Anal. Chim. Acta* 268, pp. 261-274.

Puy,J., Salvador,J., Galceran,J., Esteban,M., Díaz-Cruz,J.M., Mas,F., 1993. Voltammetry of labile metal-complex systems with induced reactant adsorption - Theoretical analysis for any Ligand-to- Metal Ratio, *J. Electroanal. Chem.* 360, pp. 1-25.

Puy,J., Torrent,M., Monné,J., Cecília,J., Galceran,J., Salvador,J., Garcés,J.L., Mas,F., Berbel,F., 1998. Influence of the adsorption phenomena on the NPP and RPP limiting currents for labile metal-macromolecular systems, *J. Electroanal. Chem.* 457, pp. 229-246.

Rauser,W.E., 1990. Phytochelatins, *Annual Review of Biochemistry* 59, pp. 61-86.

Rauser,W.E., 1995. Phytochelatins and Related Peptides - Structure, Biosynthesis, and Function, *Plan. Physiol.* 109, pp. 1141-1149.

Ribeiro,W.F., da Costa,D.J.E., Lourenco,A.S., de Medeiros,E.P., Salazar-Banda,G.R., do Nascimento,V.B., Araujo,M.C.U., 2017. Adsorptive Stripping Voltammetric Determination of Trace Level Ricin in Castor Seeds Using a Boron-doped Diamond Electrode, *Electroanal.* 29, pp. 1783-1793.

Rocha,L.S., Companys,E., Galceran,J., Carapuca,H.M., Pinheiro,J.P., 2010. Evaluation of thin mercury film rotating disc electrode to perform Absence of Gradients and Nernstian Equilibrium Stripping (AGNES) measurements, *Talanta* 80, pp. 1881-1887.

Rocha,L.S., Galceran,J., Puy,J., Pinheiro,J.P., 2015. Determination of the Free Metal Ion Concentration Using AGNES Implemented with Environmentally Friendly Bismuth Film Electrodes, *Anal. Chem.* 87, pp. 6071-6078.

Rotureau,E., 2014. Analysis of metal speciation dynamics in clay minerals dispersion by stripping chronopotentiometry techniques, *Colloids Surf. A* 441, pp. 291-297.

Serrano,N., Diaz-Cruz,J.M., Arino,C., Esteban,M., 2007a. Stripping chronopotentiometry in environmental analysis, *Electroanal.* 19, pp. 2039-2049.

Serrano,N., Díaz-Cruz,J.M., Ariño,C., Esteban,M., Puy,J., Companys,E., Galceran,J., Cecilia,J., 2007b. Full-wave analysis of stripping chronopotentiograms at scanned deposition potential (SSCP) as a tool for heavy metal speciation:

Theoretical development and application to Cd(II)-phthalate and Cd(II)-iodide systems, *J. Electroanal. Chem.* 600, pp. 275-284.

Serrano,N., Sestakova,I., Diaz-Cruz,J.M., Arino,C., 2006. Adsorptive accumulation in constant current stripping chronopotentiometry as an alternative for the electrochemical study of metal complexation by thiol-containing peptides, *J. Electroanal. Chem.* 591, pp. 105-117.

Skoog,D.A., Holler,F.A., Nieman,T.A., 2001. Principios de análisis instrumental. McGraw Hill, Madrid.

Soudek,P., Petrova,S., Vankova,R., Song,J., Vanek,T., 2014. Accumulation of heavy metals using Sorghum sp, *Chemosphere* 104, pp. 15-24.

Sun,Q., Wang,X.R., Ding,S.M., Yuan,X.F., 2005. Effects of exogenous organic chelators on phytochelatins production and its relationship with cadmium toxicity in wheat (Triticum aestivum L.) under cadmium stress, *Chemosphere* 60, pp. 22-31.

Temminghoff,E.J.M., Plette,A.C.C., van Eck,R., van Riemsdijk,W.H., 2000. Determination of the chemical speciation of trace metals in aqueous systems by the Wageningen Donnan Membrane Technique, *Anal. Chim. Acta* 417, pp. 149-157.

Tercier,M.L., Buffle,J., 1996. Antifouling membrane-covered voltammetric microsensor for in- situ measurements in natural-waters, *Anal. Chem.* 68, pp. 3670-3678.

Tessier,A., Buffle,J., Campbell,P.G.C., 1994. Uptake of Trace Metals by Aquatic Organisms. In: J. Buffle and R. R. DeVitre (Eds.). Chemical and Biological Regulation of Aquatic Systems. Lewis Publishers, Boca Raton, FL, pp. 197-230.

Tomaszewski,L., Buffle,J., Galceran,J., 2003. Theoretical and analytical characterization of a flow-through permeation liquid membrane with controlled flux for metal speciation measurements, *Anal. Chem.* 75, pp. 893-900.

Tonello,P.S., Goveia,D., Rosa,A., Fraceto,L., Menegario,A., 2011. Determination of labile inorganic and organic species of Al and Cu in river waters using the diffusive gradients in thin films technique, *Anal. Bioanal. Chem.* 399, pp. 2563-2570.

Town,R.M., Chakraborty,P., van Leeuwen,H.P., 2009. Dynamic DGT speciation analysis and applicability to natural heterogeneous complexes, *Environ. Chem.* 6, pp. 170-177.

Town,R.M., van Leeuwen,H.P., 2001. Fundamental features of metal ion determination by stripping chronopotentiometry, *J. Electroanal. Chem.* 509, pp. 58-65.

Town,R.M., van Leeuwen,H.P., 2002. Effects of adsorption in stripping chronopotentiometric metal speciation analysis, *J. Electroanal. Chem.* 523, pp. 1-15.

Town,R.M., van Leeuwen,H.P., 2003. Stripping chronopotentiometry at scanned deposition potential (SSCP) - Part 2. Determination of metal ion speciation parameters, *J. Electroanal. Chem.* 541, pp. 51-65.

Town,R.M., van Leeuwen,H.P., 2007. Adsorptive stripping chronopotentiometry (AdSCP). Part 2: Basic experimental features, *J. Electroanal. Chem.* 610, pp. 17-27.

Uribe,R., Availability of metal cations in aquatic systems from DGT measurements, PhD thesis. Universitat de Lleida, (2012).

Vale,G., Franco,C., Brunnert,A.M., dos Santos,M.M.C., 2015. Adsorption of Cadmium on Titanium Dioxide Nanoparticles in Freshwater Conditions - A Chemodynamic Study, *Electroanal.* 27, pp. 2439-2447.

van den Berg,C.M.G., 1984. Direct determination of sub-nanomolar levels of zinc in sea-water by cathodic stripping voltammetry, *Talanta* 31, pp. 1069-1073.

van den Berg,C.M.G., 1991. Potentials and potentialities of cathodic stripping voltammetry of trace-elements in natural-waters, *Anal. Chim. Acta* 250, pp. 265-276.

van Leeuwen,H.P., Buffle,J., Lovric,M., 1992. Reactant Adsorption in Analytical Pulse Voltammetry - Methodology and Recommendations - (Technical Report), *Pure Appl. Chem.* 64, pp. 1015-1028.

van Leeuwen,H.P., Town,R.M., 2002. Stripping chronopotentiometry for metal ion speciation analysis at a microelectrode, *J. Electroanal. Chem.* 523, pp. 16-25.

van Leeuwen,H.P., Town,R.M., 2003. Stripping chronopotentiometry at scanned deposition potential (SSCP) Part 3. Irreversible electrode reactions, *J. Electroanal. Chem.* 556, pp. 93-102.

van Leeuwen,H.P., Town,R.M., 2005. Kinetic limitations in measuring stabilities of metal complexes by Competitive Ligand Exchange-Adsorptive Stripping Voltammetry (CLE-AdSV), *Environ. Sci. Technol.* 39, pp. 7217-7225.

van Leeuwen,H.P., Town,R.M., 2007. Adsorptive stripping chronopotentiometry (AdSCP). Part 1: Fundamental features, *J. Electroanal. Chem.* 610, pp. 9-16.

Vera,R., Fontàs,C., Galceran,J., Serra,O., Anticó,E., 2018. Polymer inclusion membrane to access Zn speciation: Comparison with root uptake, *Sci. Total Envir.* 622–623, pp. 316-324.

Vigneault,B., Campbell,P.G.C., 2005. Uptake of cadmium by freshwater green algae: Effects of pH and aquatic humic substances, *J. Phycol.* 41, pp. 55-61.

Weng,L.P., van Riemsdijk,W.H., Temminghoff,E.J.M., 2005. Kinetic aspects of donnan membrane technique for measuring free trace cation concentration, *Anal. Chem.* 77, pp. 2852-2861.

Wu,Q.G., Batley,G.E., 1995. Determination of Sub-Nanomolar Concentrations of Lead in Sea-Water by Adsorptive Stripping Voltammetry with Xylenol Orange, *Anal. Chim. Acta* 309, pp. 95-101.

Zavarise,F., Companys,E., Galceran,J., Alberti,G., Profumo,A., 2010. Application of the new electroanalytical technique AGNES for the determination of free Zn concentration in river water, *Anal. Bioanal. Chem.* 397, pp. 389-394.

Zelic,M., Lovric,M., 2003. The influence of electrolyte concentration on the parameters of the Frumkin isotherm in the Cd2+-I- system, *J. Electroanal. Chem.* 541, pp. 67-76.

Zenk,M.H., 1996. Heavy metal detoxification in higher plants - A review, *Gene* 179, pp. 21-30.

CHAPTER 4

Speciation of Zn, Fe, Ca and Mg
in wine with the
Donnan Membrane Technique

Results obtained in this chapter have been published in:

Food Chemistry 239 (2018) 1143-1150

4.1 Abstract

Free concentrations of Zn^{2+}, Fe^{3+}, Ca^{2+} and Mg^{2+} in a red wine (Raimat, Catalonia, Spain) have been determined, with the Donnan Membrane Technique (DMT), for the first time. The required equilibration time benefits from the acceptor solution including major cations. K^+ and Na^+, mainly unbound to any ligand in the sample, have been identified as suitable reference ions. A free Zn concentration of 1.76 μmol L^{-1} determined with DMT is in excellent agreement with the free Zn concentration independently provided by the electroanalytical technique Absence of Gradients and Nernstian Equilibrium Stripping (AGNES), 1.7 μmol L^{-1}, amounting to 14.4% of the total Zn. The free concentrations found in this wine were 1.79 μmol L^{-1} Fe^{3+}, 1.11 mmol L^{-1} Ca^{2+} and 3.4 mmol L^{-1} Mg^{2+} (8.82%, 40% and 57% of their total concentrations). Prior to the application of the techniques to the red wine, they had been cross-validated in Zn-tartrate solutions.

4.2 Introduction

Speciation is normally related to the distribution of a given element (as for example a metal) over a set of different chemical species (like the hydrated cation, different complexes with different ligands, different redox states, etc.). The interest on speciation studies has been increasing with time due to the knowledge that many biological effects (be toxic or nutritional) not only depend on the total concentration of the element in the medium, but also on its free form. The bioavailability depends on speciation, because different species of a given element diffuse and react with different rates, and only certain species can be taken up directly.

Metal speciation is also of interest in the case of wine (Pyrzynska, 2007; Ibanez et al., 2008). For example, Cu (and Fe) speciation is reported to be linked to oxidative spoilage and stalling. In this context several techniques have been employed to distinguish different forms of these elements in wine (see (Pohl and Sergiel, 2009; Rousseva et al., 2016) and references therein).

Moreover, mineral content of wine has been utilized to authenticate its region of origin (Coetzee et al., 2014). Free metal concentrations are assumed to be more specific properties than the total concentration measurements, considering that they will depend not only on the total mineral content, but also on the concentration of ligands present. Hence, free concentrations are well suited as fingerprint markers, not only of a production region but also as ageing (because of the time evolution of compounds present in wine that act as metal ligands) and quality identifiers, another matter of great commercial significance.

There is an interest for developing and consolidating techniques for determining the free ion concentrations in all types of matrices (Feldmann et al., 2009; Pesavento et al., 2009). The Ion Selective Electrode (ISE) see Section 1.3.1.1 of this thesis is usually employed for some metals (Bakker and Pretsch, 2007), but there exist others, such as Zn, (Fu et al., 2012), Mg (Lamaka et al., 2009) and Fe,(Ali et al., 2015) for which there is not a commercial ISE available. Apart from that, another drawback is that the limit of detection is too high, preventing the application to certain samples (as for example in the case of Cd and Pb in many food matrices). Other techniques that can determine the free metal concentration are the Permeation Liquid Membrane (PLM) (Gramlich et al., 2012), see Section 1.3.2.3, and the Ion-Exchange Technique (Cremazy et al., 2015), see Section 1.3.2.1.

The Donnan Membrane Technique (DMT) (Temminghoff et al., 2000), which has been extensively presented in section 1.5, is a technique designed for simultaneously determining several free ion concentrations relying on the selective permeation of cations through an ion exchange membrane. The sample (named donor solution) reaches equilibrium with a synthetic acceptor solution; both (donor and acceptor) are separated by the exchange membrane. DMT has been widely applied in soils and waters (Jones et al., 2016) and a few works have tackled food matrices, as Gao *et al.* which studied synthetic and reconstituted milk (Gao et al., 2009). But, to the best of our knowledge, the use of DMT in wine (or any hydroalcoholic medium) has not yet been reported.

As explained in section 1.4, the electroanalytical technique AGNES (Galceran et al., 2004) has been implemented in the determination of free ion concentration in different kind of matrices: sea water (Galceran et al., 2007; Diaz-de-Alba et al., 2014), river water (Parat and Pinheiro, 2015), dispersions of nanoparticles (Galceran et al., 2014), quantum dots (Domingos et al., 2011), clays (Rotureau, 2014), etc. Related to wine, AGNES has been used to find the free Zn concentration (Companys

et al., 2008) and its complexation capacity (Chito et al., 2013). There has been a cross-validating and comparison of advantages and drawbacks of DMT and AGNES (Chito et al., 2012), in the context of analysis applied to soil extracts and river water.

The aim of this chapter is to show that DMT can be used to determine the free metal concentrations of Zn, Fe, Ca and Mg in wine. This can be a first step for future applications of DMT to other alcoholic beverages or to more accurate studies with other types of wines or musts. Firstly, free Zn is determined in synthetic (model) wine samples (basically, with tartaric acid to simulate the principal metal-complexing ligand in wine) to validate the use of DMT with AGNES. Then, the main point of the chapter consists in the discussion about the need of reaching equilibrated concentrations and the selection of suitable reference cations, to finally compute the free concentrations of the target analytes.

4.3 Materials and Methods

4.3.1 Reagents and wine samples

Synthetic wines, either in aqueous medium or in hydroalcoholic one (13.5% of ethanol), are composed by $c_{T,Zn}$= 1.16×10^{-5} mol L^{-1} (the total concentration determined by elemental analysis in the commercial wine) and potassium hydrogentartrate (KHTar) $c_{T,KHTar}$= 0.011 mol L^{-1} (Bradshaw et al., 2002) at pH= 3.422. DMT analysis of the synthetic wines have been done with 0.1 mol L^{-1} $NaNO_3$ as background electrolyte in both donor and acceptor solutions. To compensate for $c_{T,KHTar}$= 0.011 mol L^{-1} in the donor and have the same initial K concentration in both chambers, 0.011 mol $L^{-1}KNO_3$ has been added in the acceptor. K^+ has been used as the reference cation.

For DMT analysis of the red wine Raimat Clamor Tinto Roble 2012 (to act as donor solution), two homogenizations have been prepared from 8 bottles of 0.75 L by putting half of each bottle of wine in homogenization 1 and the other half in homogenization 2, so that at the end, one obtains 3 L of each homogenization.

The results obtained for the total concentrations in the elemental analysis of the red wine have been: $c_{T,Zn}$=12±1 μmol L^{-1}, $c_{T,Fe}$=20±2 μmol L^{-1}, $c_{T,Cu}$=14±1 μmol L^{-1},

$c_{T,Na}$=0.93±0.04 mmol L^{-1}, $c_{T,K}$=33±2 mmol L^{-1}, $c_{T,Ca}$=2.8±0.2 mmol L^{-1} and $c_{T,Mg}$=6.0±0.3 mmol L^{-1} (mean ± standard deviation, with n=8). All these values are in the usual ranges of wines (Pyrzynska, 2007; Tariba, 2011). Two acceptor solutions have been evaluated: Acceptor 1 with only K in the acceptor that will be referred to as "just K" and Acceptor 2, with the four principal cations at total concentrations given at the beginning of this paragraph, which is named "multimetal".

Potassium hydrogen L-tartrate (Fluka, analytical grade), ethanol absolute 99.9% (Merck, p.a.), 1000 mg L^{-1}Zn, Fe, Cu, K, Na, Ca, and Mg standards solutions (High Purity Standards), potassium nitrate (Fluka, Trace Select), sodium nitrate (Sigma-Aldrich, p.a.), calcium nitrate tetrahydrate (Fluka, p.a.), magnesium nitrate hexahydrate (Merck, p.a.), 0.1 mol L^{-1} KOH and HNO_3 (Riedel de Haen) have been used to prepare the solutions. A multielement isotopically-enriched standard (IES-WAK, ISC Science) with 2000 ng g^{-1} of Fe (2.91% ^{56}Fe and 95.15% ^{57}Fe), 2000 ng g^{-1} of Cu (0.90% ^{63}Cu and 99.10% ^{65}Cu) and 2000 ng g^{-1} of Zn (3.88% ^{66}Zn and 89.60% ^{67}Zn) was used for the quantification of Fe, Cu and Zn.

In all experiments ultrapure water (Milli-Q, Millipore) has been employed.

4.3.2 Equipments

Total Zn, Fe, Cu, K, Na and Mg concentrations have been quantified using a 7700x ICP-MS (Agilent Technologies, Inc, Tokyo, Japan) with Ni sampler and skimmer cons, a MicroMist glass concentric nebulizer and a He collision cell.

DMT experiments have been performed using lab DMT cells (see (Temminghoff et al., 2000; Chito et al., 2012)) and two peristaltic pumps (Gilson Minipuls3) (one for each homogenization). A membrane (BDH Laboratory Supplies, Poole, UK) of polystyrene and divinylbenzene with sulfonic acid groups has been used as cation exchange membrane in DMT experiments. The ion-exchange capacity of the membrane is 0.8 mmol g^{-1} and its thickness is 0.15–0.17 mm (Weng et al., 2005). Prior to the measurement of the sample, the membranes were allowed to equilibrate with the same electrolyte solution of the acceptor. Each pump was connected to 4 DMT cells to have 4 measurements for each homogenization. Two (of the four) cells

were connected to acceptor solutions containing just K and two with the acceptor containing K, Na, Mg and Ca ("multimetal")

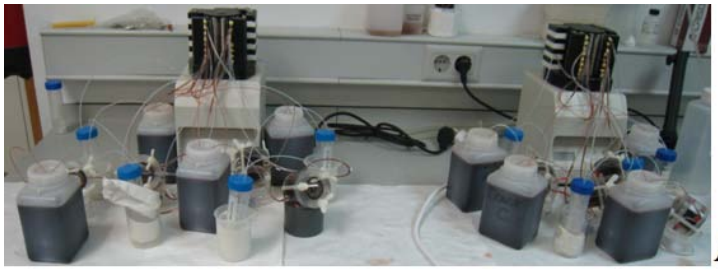

A

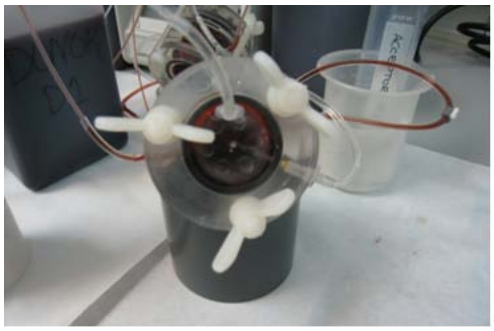

B

Figure 4-1. Panels A and B show the DMT device used in the lab for DMT measurements

Figure 4-2. Detail of the DMT cell used in the lab for DMT measurements

500 mL of wine have been used as donor solution, while 26 mL of "just K" or "multimetal" solution as initial acceptor solution. Aliquots of 1 mL from the acceptor and donor solutions have been taken at selected interval times and diluted 10 times (Gonzalvez et al., 2008) with a mixture of 1% HNO_3 and 0.5% HCl for further total elemental analysis by ICP-MS.

Voltammetric measurements have been carried out with an Eco Chemie Autolab PGSTAT12 or a μ-Autolab type III potentiostat attached to a Metrohm 663VA Stand and to a computer by means of the NOVA 1.7 (Eco Chemie) software package. The working electrode has been a Metrohm multimode mercury drop electrode. The smallest drop in our stand was chosen for AGNES experiments (r_0=1.41×10^{-4} m). The auxiliary electrode has been a glassy carbon electrode and the reference electrode was Ag/AgCl/3 mol L^{-1} KCl, encased in a 0.1 mol L^{-1} KNO_3 jacket. A glass jacketed cell thermostated at 25.0 ºC has been used in all measurements. N_2 (99.999 %) saturated in a hydroalcoholic medium (13% ethanol) has been used for deaeration and blanketing the wine.

A glass combined electrode (Crison 5103) has been attached to a Dual Star Orion ion analyser to control the pH.

4.3.3 Procedures

4.3.3.1 Determination of free metal ion concentration using DMT

As mentioned in Section 1.5, DMT consists in the equilibration between a sample (or donor solution) and an acceptor solution, separated by a cationic exchange membrane which allows the passage of cations but blocks the practical permeation of negative species. When this equilibration is reached, the electrochemical potential in both solutions (donor and acceptor) is eventually the same leading to the expression:

$$\left\{M^{z_M}\right\}_D = \left\{M^{z_M}\right\}_A \left(\frac{\left\{R^{z_R}\right\}_D}{\left\{R^{z_R}\right\}_A} \right)^{z_M / z_R} \qquad (4\text{-}1)$$

where subscripts D and A refers to the Donor and Acceptor solutions and z_j stands for the charge of the cation *j* (Temminghoff et al., 2000).

If the activity coefficients are similar in the donor and acceptor solutions, the free concentration of M in the donor solution, can be computed from concentrations as:

$$\left[M^{z_M}\right]_D = \left[M^{z_M}\right]_A \left(\frac{\left[R^{z_R}\right]_D}{\left[R^{z_R}\right]_A}\right)^{z_M/z_R} \quad (4\text{-}2)$$

4.3.3.2 Elemental analysis by ICP-MS

The operating conditions have been as follows: RF power 1550 W, carrier gas flow rate 1.01 L min^{-1}, helium collision gas flow rate 4.3 mL min^{-1}, spray chamber temperature 2.0 ºC, sample depth 10.0 mm, nebulizer pump 0.1 rps, extract lens 1 voltage 0.0 V and extract lens 2 voltage -195.0 V. For Fe and Zn, the measurement has been conducted through isotope dilution analysis, using the multielemental isotopically-enriched spike solution. The monitored isotopes have been ^{56}Fe and ^{57}Fe for Fe, ^{63}Cu and ^{65}Cu for Cu and ^{66}Zn and ^{67}Zn for Zn. The isotopic ratio is determined from a metal solution with a known concentration which is prepared from a standard. Then, when this ratio is established it is possible to know the concentration of any sample by comparing the isotopic ratios. For Na, Mg, K and Ca, ^{23}Na, ^{24}Mg, ^{39}K and ^{44}Ca have been monitored, respectively, and external calibration have been done for the quantification. Compared to the direct mass measurement, the isotope dilution analysis is less vulnerable to matrix effect in the ICP-MS analysis and more accurate (Quetel et al., 2001; Centineo et al., 2001).

The limit of detection of DMT strongly depends on the quantifying technique used for the total element in the acceptor compartment (Pesavento et al., 2009).

4.3.3.3 Determination of free Zn concentration using AGNES

AGNES technique (see Section 1.4) could be divided into two steps: a) deposition step where the metal is reduced and b) stripping step where the metal is reoxidated and quantified. When at the end of the first stage, a special situation of equilibrium is reached, one can establish a relationship (called gain *Y*) between concentrations at both sides of the electrode surface:

$$Y = \frac{\left[\mathrm{M}^{\mathrm{o}}\right]}{\left[\mathrm{M}^{\mathrm{n+}}\right]} = \exp\left[-\frac{zF}{RT}\left(E_1 - E^{\mathrm{o}\,\prime}\right)\right] \tag{4-3}$$

where *F* is the Faraday constant, *R* is the gas constant, *T* is the absolute temperature and $E^{0\prime}$ is the standard formal potential. For wine, the deposition potential E_1, can be computed for the peak potential of a DPP (see Section 1.3.1.5) obtained in the same hydroalcoholic medium via:

$$E_j = {}_{\mathrm{EtOH}}E_{\mathrm{peak}} + \frac{\Delta E}{2} + \frac{RT}{nF}\ln\left({}_{\mathrm{EtOH}}Y_j\sqrt{\frac{D_{\mathrm{M}^0}}{{}_{\mathrm{EtOH}}D_{\mathrm{M}}}}\right) \tag{4-4}$$

where pre-subscript EtOH indicates the 13.5% ethanolic medium and *j* any stage or sub-stage in AGNES. This equation is the correct form of eqn. 4 in (Chito et al., 2013) and of eqn. 10 in (Companys et al., 2008), where an error of transcription led to an undue replacement of D_{M^0} by ${}_{\mathrm{w}}D_{\mathrm{M}}$.

In the second stage, a derivation (Galceran et al., 2014) leads to a direct proportionality between the faradaic current and the free Zn concentration in the sample

$$I_{\mathrm{faradaic}} = \eta Y_1\left[\mathrm{Zn}^{2+}\right] \tag{4-5}$$

The proportionality factor η can be found from a calibration and Y_1 stands to the achieved gain (corresponding to ${}_{\mathrm{EtOH}}Y_{\mathrm{j}}$, in this case with ethanol)

4.4 Results and Discussion

4.4.1 Synthetic solutions

In the aqueous synthetic wine (see Section 4.3.1), the majoritary species containing Zn are: free Zn^{2+} and $HZnTar^{+}$, so that both species could have reached equilibrium across the DMT membrane. However, the determined free Zn^{2+} concentration from DMT analysis $[Zn^{2+}]_{DMT}$= 5.2 ± 0.5 µmol L^{-1} is consistent with the prediction of the speciation code VMinteq (Gustafsson, 2010) $[Zn^{2+}]_{VMinteq}$= 5.35 µmol L^{-1} (see Fig 4-3), assuming that only free Zn^{2+} species reached equilibrium.

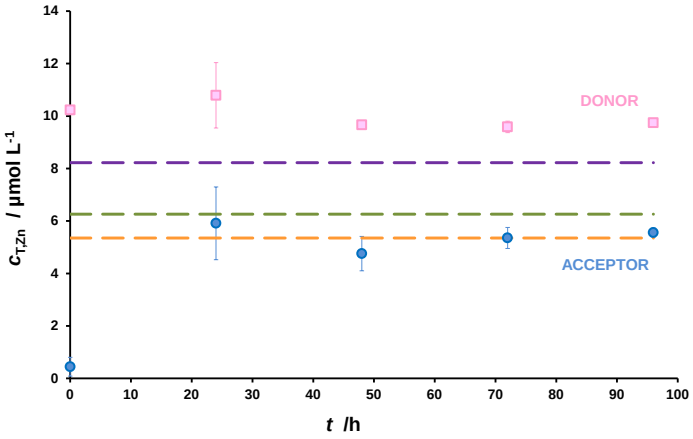

Figure 4-3. Evolution of total Zn concentrations with time in the donor (pink squares) and the acceptor solutions (blue circles) for the synthetic solution in aqueous medium. The orange dashed line stands for the free zinc concentration in the donor solution predicted by VMinteq considering the measured total Zn concentration at equilibrium ($c_{T,Zn}$= 9.64 µmol L^{-1}). The green dashed line stands for the summation of free zinc and the positive complexes and the purple dashed line for the summation of free zinc and the neutral complexes. Other conditions for donor: $c_{T,KHTar}$= 0.011mol L^{-1}, pH=3.422. Initial conditions for acceptor: $c_{T,NaNO3}$ = 0.1 mol L^{-1}, $c_{T,KNO3}$= 0.011 mol L^{-1}, pH=3.422.The error bars represent the standard deviation (n=3).

In fact, if other positive or neutral Zn species (e.g. $HZnTar^{+}$ or ZnTar) had also reached equilibrium, the total Zn concentration measured in the acceptor would have increased by more than 30% (see table 4-1).

Table 4-1. Concentration and % Zn of selected species (free Zn and main neutral and positive species) predicted by VMinteq for the aqueous synthetic wine

Specie	**Concentration /mol L^{-1}**	**% Zn**
Zn^{2+}	5.35×10^{-6}	55.5
Zn-Tartrate (aq)	2.86×10^{-6}	29.7
Zn-$(Tartrate)_2^{2-}$	5.13×10^{-7}	5.3
$ZnNO_3^+$	4.77×10^{-7}	4.9
ZnH-$Tartrate^+$	4.33×10^{-7}	4.5

The preferential "filtering" of just the free divalent cations can be justified considering the membrane as an extra phase domain (which we will label with the subscript "membrane") so that 3 phases are present in the system: donor, membrane and acceptor. Applying the Donnan equilibrium conditions at the donor/membrane interphase, a Boltzmann (or partitioning) factor $\Pi\approx35$ appears for a monovalent cation, following from the application of (Temminghoff et al., 2000; Puy et al., 2014)

$$\Pi = \exp\left(-\operatorname{arcsinh}\left(-\frac{\rho}{2I}\right)\right) \tag{4-6}$$

considering an estimated ρ=-3.5 mol L^{-1} charge density of the membrane phase and an ionic strength of the background electrolyte I=0.1 mol L^{-1} $NaNO_3$. This factor indicates that the equilibrium concentration of a monovalent cation at the membrane/donor interface in the membrane side is 35 times its concentration at the donor side. A rough model for the (initial) ratio of fluxes of Zn-containing species can consider the initial concentrations in donor and acceptor solutions with a steady-

state profile established inside the membrane for each Zn species (see schematic diagram in Fig 4-4).

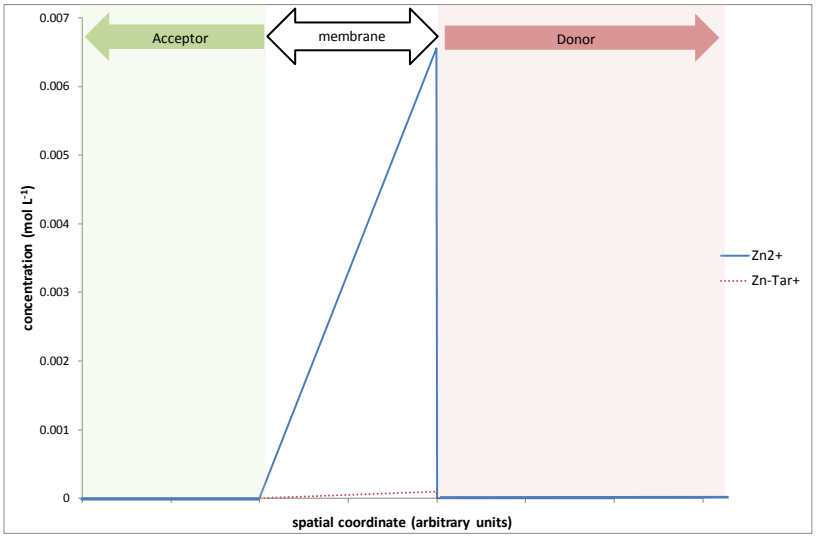

Figure 4-4. Schematic representation of the concentration profiles of Zn^{2+} and Zn-Tar^{+}(aq) for a very rough model to justify the initial large difference between fluxes across the membrane according to the charge of the transported species.

In this way, for a concentration ratio of 12.3 (in solution, as predicted by VMINTEQ, see Table 4-1) between Zn^{2+} and $ZnHTar^{+}$, the same ratio of concentrations in the cation exchange membrane (at the interface with the donor solution) becomes:

$$\frac{\left[Zn^{2+}\right]_{membrane}}{\left[ZnHTar^{+}\right]_{membrane}} = \frac{\left[Zn^{2+}\right]_{solution} \times 35^{2}}{\left[ZnHTar^{+}\right]_{solution} \times 35} = 12.3 \times 35 = 432 \qquad (4\text{-}7)$$

For the concentrations in this synthetic solution, still assuming a common diffusion coefficient for these two species, the initial flux across the membrane of $ZnHTar^{+}$ will be 432 times smaller than that of Zn^{2+} assuming zero concentration at the acceptor/membrane interface. Correspondingly, the ratio of Zn^{2+} to the neutral species ZnTar is 1.87 in the solution, and the flux of Zn^{2+} is 2289 times that of the neutral species. Besides, the absence of tartrate in the initial acceptor solution will lead to dissociation of $HZnTar^{+}$ or ZnTar once they enter the acceptor, further

slowing down the equilibration of these species (while favouring the attainment of the equilibrium for free Zn).

Measurements in the ethanolic medium demands longer equilibration times (Fig 4-5) than in aqueous medium. This extended equilibration time might be related to a slower permeation process in the membrane. Comparison with the predicted VMINTEQ concentrations (shown in Fig 4-5) is just to have an idea, as VMINTEQ does not consider the presence of ethanol. At equilibrium, the free Zn concentration measured with AGNES (at two gains, each with 2 different deposition times: Y=11.4, t_1=75s and t_1=100 s; Y=22.74, t_1=150 s and t_1=200 s) resulted in $[Zn^{2+}]_{AGNES}$= 6.50 ± 0.10 µmol L^{-1}, which agrees (within the experimental error) with $[Zn^{2+}]_{DMT}$= 7.3 ± 0.7 µmol L^{-1}.

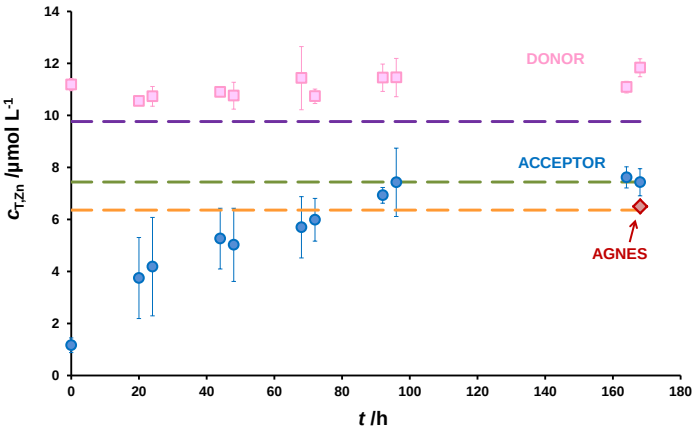

Figure 4-5. Evolution of total Zn concentrations with time in the donor (pink squares) and the acceptor solutions (blue circles) of the synthetic solution in ethanolic medium. The orange dashed line stands for the free zinc concentration predicted in the Donor by Vminteq – assuming aqueous solution- considering the measured total Zn concentration ($c_{T,Zn}$= 11.5 µmol L^{-1}). The green dashed line stands for the summation of free zinc and the positive complexes and the purple dashed line for the summation of free zinc and the neutral complexes. The red diamond marker corresponds to AGNES data. Other conditions for donor: $c_{T,KHTar}$= 0.011 mol L^{-1}, 13.5% ethanol, pH=3.422. Initial conditions for acceptor: $c_{T,NaNO3}$ = 0.1 mol L^{-1}, $c_{T,KNO3}$= 0.011 mol L^{-1}, pH=3.422 The error bars represent the standard deviation (n=4).

4.4.2 Analysis of real wine

To calculate the free concentration with eqn. 4-2), it is necessary to establish a suitable reference cation. In the following, various candidates are considered, starting with K, a typical choice.

The total concentration of K in the acceptor of the replicates with initially "just K" in the acceptor decreases with time, whilst that decrease is not observed in the "multimetal" acceptors (Fig 4-6). Trying to obtain an explanation of this change in the "just K" acceptor, it is necessary to point out that the concentrations of the rest of principal cations (Ca, Mg and Na) can only increase in the acceptor because of their initial absence in the acceptor and their tendency to an equilibration close to the concentrations of those cations in the donor (see Fig 4-7). Consequently, the required transference of Ca, Mg and Na from donor to acceptor has to be compensated with transference of K from the acceptor to the donor so as to keep electroneutrality. We conclude that K can be used as reference cation in the "multimetal" acceptor configuration, but not in the case of the "just K" configuration due to the requirement of a longer time to reach true equilibrium of all species. In fact, in these experiments of “just K”, the concentrations of Mg, Ca and Na in the acceptor after 200 hours are still increasing (see Fig 4-7). Notice that, in general (see Figs 4-6 and 4-8), the equilibration time determined is even slightly longer than those needed for synthetic alcoholic wine.

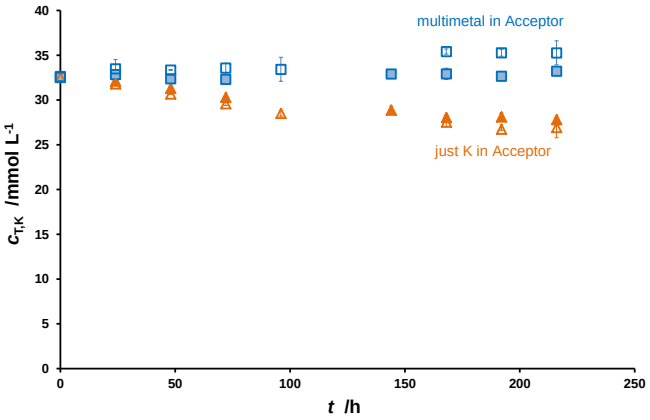

Figure 4-6. Plot of total concentration of K *versus* time in the acceptor for the four replicates of homogenization 1 (full markers) and homogenization 2 (empty markers) of wine. Orange triangle markers correspond to the acceptor solutions with just K and blue squares with K, Na, Mg and Ca ("multimetal").The error bars represent the standard deviation (n=2).

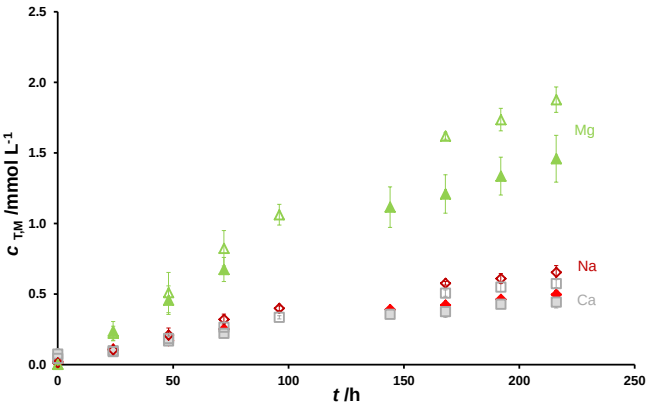

Figure 4-7. Plot of $c_{T,M}$ vs time in the acceptor (with “just K”) for the four replicates of homogenization 1 (full markers) and homogenization 2 (empty markers) of wine. The red diamond markers correspond to Na, green triangle markers to Mg and grey square markers to Ca. Initial conditions in the acceptor: $c_{T,K}$=33.1 mmol L^{-1}, pH=3.422.

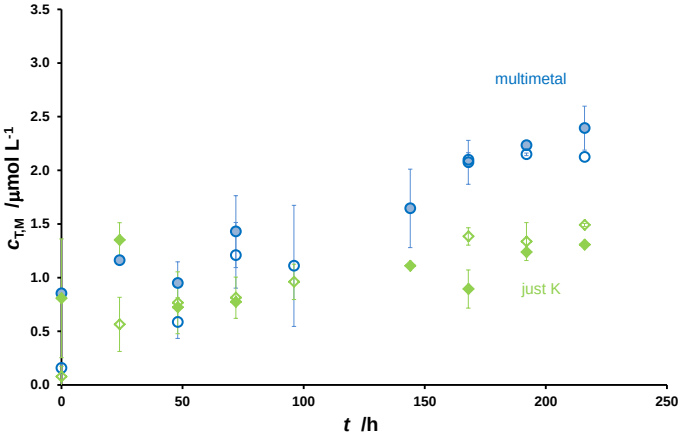

Figure 4-8. Plot of the total concentration of Zn *versus* time in the acceptors of homogenization 1 (full markers) and homogenization 2 (empty markers) of wine. The blue circle markers correspond to “multimetal” acceptors and the green triangle markers to ”just K” ones. Initial conditions in the acceptor: pH=3.422. The error bars represent the standard deviation (*n*=2).

Na concentration remains stable in the "multimetal" acceptor (see Fig 4-9). This indicates that its free concentration in the acceptor is very close to the free concentration in the donor solution, and both solutions have similar ionic strength. In such case, Na can also be used as reference cation.

At 216 hours $\frac{[K^+]_D}{[K^+]_A} \approx \frac{[Na^+]_D}{[Na^+]_A}$ in "multimetal", but not in "just K" acceptors.

This equality confirms the attainment of equilibrium for K^+ and Na^+ in "multimetal” conditions.

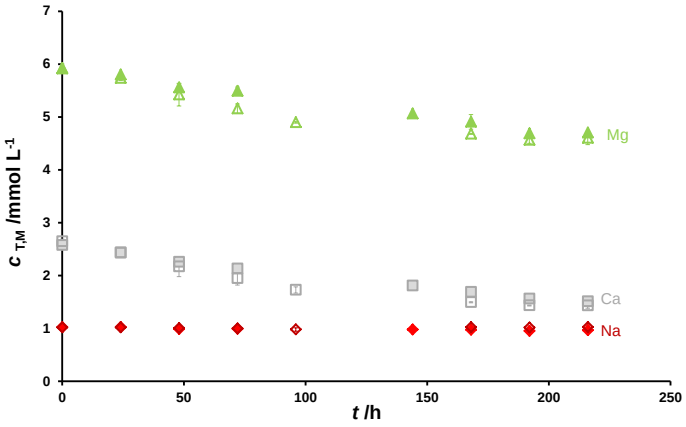

Figure 4-9. Plot of the total concentration of a metal M (such as Na, Mg and Ca) *versus* time in the acceptors for the four replicates of homogenization 1 (full markers) and homogenization 2 (empty markers) of wine. The red diamond markers correspond to Na, green triangle markers to Mg and grey square markers to Ca. The error bars represent the standard deviation (n=2).

Ca and Mg concentrations decrease with time in the "multimetal" acceptor (Fig 4-9). A hypothesis to explain this fact could be that these divalent cations are relevantly complexed in the wine (and not just free), so the free concentration in the acceptor is initially higher than in the donor, so that some transference of Ca and Mg to the donor is needed for equilibration. Due to the much larger volume of the donor, the change in the composition of the wine is negligible. Because of the large difference between the total and free concentration of Ca or Mg in the donor (of the order of the drop from the initial to equilibrium concentrations seen in Fig 4-9), none of them can be used as reference cation.

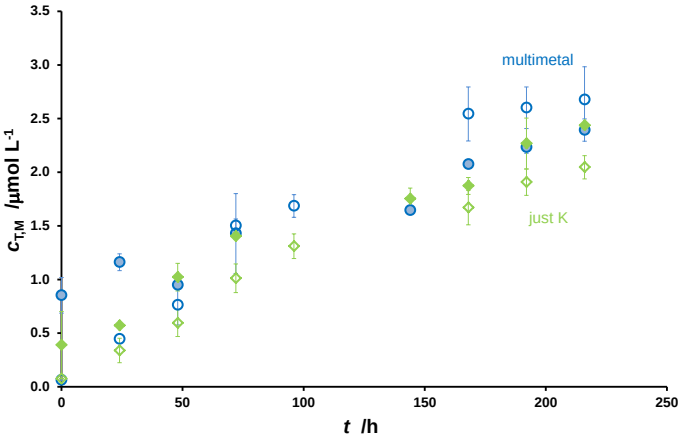

Figure 4-10. Plot of the total concentration of Fe vs time in the acceptor of homogenization 1 (full markers) and homogenization 2 (empty markers) of wine. The blue triangle markers correspond to “multimetal” acceptors and green square markers to ”just K” ones. Initial conditions in the acceptor: pH=3.422.The error bars represent the standard deviation (*n*=2).

The evolution of the trace analytes in the acceptor can be considered to have reached equilibrium also around 200 h (see Figs 4-8 and 4-10). When the equation (4-2) is applied (considering the average values of the ICP-MS for the total concentrations) for times longer than 150 h leads to results in Table 4-2. In accordance with what has been explained up to now, the safer [Zn^{2+}] is the one obtained in “multimetal” acceptors when taking K (or Na) as the reference cations. The average of these eight data (considering the 2 replicates at each homogenization) is 1.76 µmol L^{-1} which is in excellent agreement with the totally independent AGNES technique that yielded 1.7 ± 0.2 µmol L^{-1}. Reported free Zn concentrations in similar red wines (with AGNES) were within the same order of magnitude: 0.45 µmol L^{-1}(Companys et al., 2008) and 1.49 µmol L^{-1}(Chito et al., 2013). Computations of [Zn^{2+}] with equation (4-2) when using either Ca or Mg as reference ion (see table 4-2) are clear overestimations, though by a factor not larger than 2.5 (i.e. the order of magnitude is still correct). The use of "just K" acceptors (with Ca, Mg and Na away from equilibrium) produced either around 20% underestimation (acceptors homogenization 1), or around 8% overestimation (acceptors homogenization 2).

Table 4-2. Free Zn^{2+}, Fe^{3+}, Ca^{2+} and Mg^{2+} concentrations determined in the Raimat wine after the application of the correction equation (4-2). *n*=2 replicates. Bold figures indicate reliable determinations.

Acceptor/Sample	**Reference ion**	**[Zn^{2+}] /µmol L^{-1}**	**[Fe^{3+}] /µmol L^{-1}**	**[Ca^{2+}] /mmolL^{-1}**	**[Mg^{2+}] /mmolL^{-1}**
Acceptor "just K" homogenization 1	K	1.35±0.06	2.8±0.2	0.49±0.05	1.65±0.08
Acceptor "multimetal" homogenization 1	K	**1.78±0.05**	**1.81±0.09**	**1.2±0.2**	**3.7±0.2**
	Na	**1.70±0.03**	**1.69±0.06**	**1.11±0.04**	**3.2±0.1**
	Mg	2.54±0.02	3.09±0.06		
	Ca	3.39±0.07	4.8±0.2		
Acceptor "just K" homogenization 2	K	2.1±0.1	3.4±0.2	0.80±0.04	2.57±0.09
Acceptor "multimetal" homogenization 2	K	**1.81±0.09**	**1.86±0.05**	**1.04±0.07**	**3.3±0.2**
	Na	**1.8±0.1**	**1.81±0.06**	**1.08±0.04**	**3.4±0.1**
	Mg	2.9±0.3	3.7±0.3		
	Ca	4.1±0.4	6.4±0.5		

In the case of Fe, we consider that the relevant oxidation form is its trivalent state, given that the acceptor solution and the wine are in contact with the atmosphere. Similar reasonings (on the various acceptor solutions) to those expound for Zn apply also to Fe(III). The average of the most reliable data (those with K and Na as reference ion in equilibrated "multimetal" acceptors) is 1.79±0.08 µmol L^{-1}, which represents an 8.82% of free Fe(III) with respect to the total Fe content in the wine. Comparison with previous works (Ajlec and Stupar, 1989; Costa and Araujo, 2001; Pyrzynska, 2007) is hindered by the fact that there the speciation is considered between total Fe(II) and Fe(III) without distinguishing free and complexed fractions

of each oxidation state. Some Fe(II) (Danilewicz, 2016) could be still present in the wine at the equilibration time. Nevertheless, it will be probably mostly preserved in the form of strong complexes rather than free Fe(II), so that $[Fe^{2+}]$ in the acceptor can be assumed to be negligible in comparison with $[Fe^{3+}]$ given that the acceptor solution has no compounds capable to keep a redox cycle while the solution is open to the air. In any case, the current results about Fe(III) have to be taken as a first rough approximation.

The free concentrations of Ca and Mg in the wine can also be estimated taking K or Na as reference ion (see Table 4-2) in the configuration with "multimetal" acceptor. Their averages are 1.11± 0.09 mmol L^{-1} and 3.4± 0.3 mmol L^{-1}, respectively. They represent 40% of free Ca and 57% of free Mg in wine. The measured percentage of free Ca in this wine is in the range from 33 to 64% of ionised Ca found by (Cardwell et al., 1991) using an ion selective electrode in different kind of wines.

Here, the Cu free concentrations could not be accurately determined. The data indicate a level around 0.10 μmol L^{-1}. This concentration represents a 0.71% of the total Cu, lower than the free copper range of 3.3–31% reported in ref. (Wiese and Schwedt, 1997). But, the lack of a clear stabilization of the acceptor Cu concentration leads us to report it just as a very rough estimation. Future work could be devoted to tackle Cu speciation in wine using DMT technique.

4.5 Conclusions

In DMT measurements, it is critical to choose a suitable reference ion to determine the free metal concentration. In that sense, the measurement of cations in complex matrices (as wine in this chapter) is a good starting point to elaborate an appropriate acceptor composition of the non-analyte ions (or even the analytes). But, on the other hand, for practical reasons it could be easy to work with longer equilibration times rather than prepare an acceptor solution with a composition that is as close as possible to the real one.

Faster designs of DMT are needed to tackle some complex media (as wine and other food matrices). Despite the longer required equilibration times, DMT technique could give us the free metal concentrations in a sample of non-aqueous nature. The usual speciation programme (VMinteq) does not consider that kind of medium and

its aqueous predictions should be taken as just an approximation to the hydroalcoholic medium, but the electroanalytical technique AGNES could be use to compare the obtained results.

4.6 References

Ajlec,R., Stupar,J., 1989. Determination of Iron Species in Wine by Ion-Exchange Chromatography Flame Atomic-Absorption Spectrometry, *Analyst.* 114, pp. 137-142.

Ali,T.A., Mohamed,G.G., Farag,A.H., 2015. Electroanalytical Studies on Fe(III) Ion-Selective Sensors Based on 2-methyl-6-(4-methylenecyclohex-2-en-1-yl)hept-2-en-4-one Ionophore, *International Journal of Electrochemical Science* 10, pp. 564-578.

Bakker,E., Pretsch,E., 2007. Modern Potentiometry, *Angew. Chem. , Int. Ed.* 46, pp. 5660-5668.

Bradshaw,M.P., Prenzler,P.D., Scollary,G.R., 2002. Square-wave voltammetric determination of hydrogen peroxide generated from the oxidation of ascorbic acid in a model wine base, *Electroanal.* 14, pp. 546-550.

Cardwell,T.J., Cattrall,R.W., Mrzljak,R.I., Sweeney,T., Robins,L.M., Scollary,G.R., 1991. Determination of Ionized and Total Calcium in White Wine Using A Calcium Ion-Selective Electrode, *Electroanal.* 3, pp. 573-576.

Centineo,G., Rodriguez,J.A., Munoz,E. On-line isotope dilution analysis with the 7700 Series ICP-MS: Analysis of trace elements in high matrix samples. Agilent Publication 5990-9171EN. Agilent Publication 5990-9171EN. 2001.

Chito,D., Galceran,J., Companys,E., Puy,J., 2013. Determination of the Complexing Capacity of Wine for Zn Using the Absence of Gradients and Nernstian Equilibrium Stripping Technique, *J. Agric. Food Chem.* 61, pp. 1051-1059.

Chito,D., Weng,L., Galceran,J., Companys,E., Puy,J., van Riemsdijk,W.H., van Leeuwen,H.P., 2012. Determination of free Zn^{2+} concentration in synthetic and natural samples with AGNES (Absence of Gradients and Nernstian Equilibrium

Stripping) and DMT (Donnan Membrane Technique), *Sci. Total Envir.* 421-422, pp. 238-244.

Coetzee,P.P., van Jaarsveld,F.P., van Haecke,F., 2014. Intraregional classification of wine via ICP-MS elemental fingerprinting, *Food Chem.* 164, pp. 485-492.

Companys,E., Naval-Sanchez,M., Martinez-Micaelo,N., Puy,J., Galceran,J., 2008. Measurement of free zinc concentration in wine with AGNES, *J. Agric. Food Chem.* 56, pp. 8296-8302.

Costa,R.C.D., Araujo,A.N., 2001. Determination of Fe(III) and total Fe in wines by sequential injection analysis and flame atomic absorption spectrometry, *Anal. Chim. Acta* 438, pp. 227-233.

Cremazy,A., Leclair,S., Mueller,K., Vigneault,B., Campbell,P., Fortin,C., 2015. Development of an In Situ Ion-Exchange Technique for the Determination of Free Cd, Co, Ni, and Zn Concentrations in Freshwaters, *Aquat. Geochem.* 21, pp. 259-279.

Danilewicz,J.C., 2016. Fe(II):Fe(III) Ratio and Redox Status of White Wines, *American Journal Of Enology And Viticulture* 67, pp. 146-152.

Diaz-de-Alba,M., Galindo-Riano,M.D., Pinheiro,J.P., 2014. Lead electrochemical speciation analysis in seawater media by using AGNES and SSCP techniques, *Environ. Chem.* 11, pp. 137-149.

Domingos,R.F., Simon,D.F., Hauser,C., Wilkinson,K.J., 2011. Bioaccumulation and Effects of CdTe/CdS Quantum Dots on Chlamydomonas reinhardtii - Nanoparticles or the Free Ions?, *Environ. Sci. Technol.* 45, pp. 7664-7669.

Feldmann,J., Salaun,P., Lombi,E., 2009. Critical review perspective: elemental speciation analysis methods in environmental chemistry - moving towards methodological integration, *Environ. Chem.* 6, pp. 275-289.

Fu,Q., Qian,S., Li,N., Xia,Q., Ji,Y., 2012. Characterization of a New Zn2+-Selective Electrode Based on Schiff-base as Ionophore, *International Journal of Electrochemical Science* 7, pp. 6799-6806.

Galceran,J., Companys,E., Puy,J., Cecília,J., Garcés,J.L., 2004. AGNES: a new electroanalytical technique for measuring free metal ion concentration, *J. Electroanal. Chem.* 566, pp. 95-109.

Galceran,J., Huidobro,C., Companys,E., Alberti,G., 2007. AGNES: a technique for determining the concentration of free metal ions. The case of Zn(II) in coastal Mediterranean seawater., *Talanta* 71, pp. 1795-1803.

Galceran,J., Lao,M., David,C., Companys,E., Rey-Castro,C., Salvador,J., Puy,J., 2014. The impact of electrodic adsorption on Zn, Cd or Pb speciation measurements with AGNES, *J. Electroanal. Chem.* 722-723, pp. 110-118.

Gao,R., Temminghoff,E.J.M., van Leeuwen,H.P., van Valenberg,H.J.F., Eisner,M.D., van Boekel,M.A.J.S., 2009. Simultaneous determination of free calcium, magnesium, sodium and potassium ion concentrations in simulated milk ultrafiltrate and reconstituted skim milk using the Donnan Membrane Technique, *Int. Dairy J.* 19, pp. 431-436.

Gonzalvez,A., Armenta,S., Pastor,A., de la Guardia,M., 2008. Searching the most appropriate sample pretreatment for the elemental analysis of wines by inductively coupled plasma-based techniques, *J. Agric. Food Chem.* 56, pp. 4943-4954.

Gramlich,A., Tandy,S., Slaveykova,V.I., Duffner,A., Schulin,R., 2012. The use of permeation liquid membranes for free zinc measurements in aqueous solution, *Environ. Chem.* 9, pp. 429-437.

Gustafsson,J.P. Visual MINTEQ version 3.0. <www.lwr.kth.se/English/ Oursoftware/vminteq/index.htm>. 2010.

Ibanez,J.G., Carreon-Alvarez,A., Barcena-Soto,M., Casillas,N., 2008. Metals in alcoholic beverages: A review of sources, effects, concentrations, removal, speciation, and analysis, *J. Food Compos. Anal.* 21, pp. 672-683.

Jones,A.M., Xue,Y., Kinsela,A.S., Wilcken,K.M., Collins,R.N., 2016. Donnan membrane speciation of Al, Fe, trace metals and REEs in coastal lowland acid sulfate soil-impacted drainage waters, *Sci. Total Envir.* 547, pp. 104-113.

Lamaka,S.V., Taryba,M.G., Zheludkevich,M.L., Ferreira,M.G., 2009. Novel Solid-Contact Ion-Selective Microelectrodes for Localized Potentiometric Measurements, *Electroanal.* 21, pp. 2447-2453.

Parat,C., Pinheiro,J.P., 2015. ISIDORE, a probe for in situ trace metal speciation based on Donnan membrane technique with related electrochemical detection part 1: Equilibrium measurements, *Anal. Chim. Acta* 896, pp. 1-10.

Pesavento,M., Alberti,G., Biesuz,R., 2009. Analytical methods for determination of free metal ion concentration, labile species fraction and metal complexation capacity of environmental waters: A review, *Anal. Chim. Acta* 631, pp. 129-141.

Pohl,P., Sergiel,I., 2009. Evaluation of the Total Content and the Operationally Defined Species of Copper in Beers and Wines, *J. Agric. Food Chem.* 57, pp. 9378-9384.

Puy,J., Galceran,J., Cruz-Gonzalez,S., David,C.A., Uribe,R., Lin,C., Zhang,H., Davison,W., 2014. Metal accumulation in DGT: Impact of ionic strength and kinetics of dissociation of complexes in the resin domain, *Anal. Chem.* 86, pp. 7740-7748.

Pyrzynska,K., 2007. Chemical speciation and fractionation of metals in wine, *Chemical Speciation and Bioavailability* 19, pp. 1-8.

Quetel,C.R., Nelms,S.M., Van Nevel,L., Papadakis,I., Taylor,P.D.P., 2001. Certification of the lead mass fraction in wine for comparison 16 of the International Measurement Evaluation Programme, *Journal of Analytical Atomic Spectrometry* 16, pp. 1091-1100.

Rotureau,E., 2014. Analysis of metal speciation dynamics in clay minerals dispersion by stripping chronopotentiometry techniques, *Colloids Surf. A* 441, pp. 291-297.

Rousseva,M., Kontoudakis,N., Schmidtke,L.M., Scollary,G.R., Clark,A.C., 2016. Impact of wine production on the fractionation of copper and iron in Chardonnay wine: Implications for oxygen consumption, *Food Chem.* 203, pp. 440-447.

Tariba,B., 2011. Metals in Wine-Impact on Wine Quality and Health Outcomes, *Biological Trace Element Research* 144, pp. 143-156.

Temminghoff,E.J.M., Plette,A.C.C., van Eck,R., van Riemsdijk,W.H., 2000. Determination of the chemical speciation of trace metals in aqueous systems by the Wageningen Donnan Membrane Technique, *Anal. Chim. Acta* 417, pp. 149-157.

Weng,L.P., van Riemsdijk,W.H., Temminghoff,E.J.M., 2005. Kinetic aspects of donnan membrane technique for measuring free trace cation concentration, *Anal. Chem.* 77, pp. 2852-2861.

Wiese,C., Schwedt,G., 1997. Strategy for copper speciation in white wine by differential pulse anodic stripping voltammetry, potentiometry with an ion-selective electrode and kinetic photometric determination, *Fresenius J. Anal. Chem.* 358, pp. 718-722.

CHAPTER 5

Conclusions

This thesis has focussed on the analytical techniques AGNES and DMT to study metal speciation in different natural media, without the necessity of modifying the sample, which is one of the advantages of these techniques. The main conclusions can be summarized as:

- The existence of induced adsorption, where the analyte M^{n+} accumulates on the electrode surface via formation of a complex ML, does not disturb the equilibrium state reached at the end of the first stage of AGNES. Several titrations have been done in systems which show induced adsorption (Cd+ Polyacrilic Acid, CdI and Pb-Xylenol Orange) and the free metal concentration obtained by AGNES and the one given by the corresponding ISE electrode are in good agreement between them and with the theoretical data.

- Electrodic adsorption in the studied systems did not show a kinetic impact, as AGNES measurements did not require longer deposition times.

- A strategy has been developed to apply AGNES in a solution that contains a component which has the capacity of blocking the electrode surface, due to its adsorption or other irreversibility circumstances affecting the redox process. In the particular studied case, the strategy prescribes that AGNES procedure should be performed without stirring and using a deposition time up to 100 s, given that from that point on the blockage appears. The application of a very negative potential does not remove the blocking component from the electrode surface, so it is better to work with an HMDE electrode (as a renewed electrode surface is obtained with every new drop) than to work with a rotating disk electrode, a screen printed electrode or a microelectrode.

- In the case of the second stage of AGNES, the adsorption process does not affect the faradaic current (I_f) or charge (Q_f) as their value is independent from this phenomenon. But adsorption could affect the blank value by changing the structure of the double layer. Thus, it is better to work with an AGNES variant that does not required the blank subtraction or using a high

gain (*Y*) as in this way the capacitive current or charge would be negligible in front of the faradaic one.

- The electroanalytical technique AGNES could be used to discriminate between several complexation models by introducing the complexation constants in the database of the program VMinteq and comparing the theoretical free metal concentrations with the same data experimentally obtained by AGNES.

- In titrations of fixed amounts of $c_{T,Zn}$ and GSH while pH is varied, Ferretti and (especially) Krezel models yield free metal ion concentrations in good agreement with the corresponding ones obtained by AGNES. Ferretti's model just consider two more species than Krezel's ($Zn_2G_2H_{-1}^{3-}$ and $Zn_2G_2H_{-2}^{4-}$), but both species are just relevant at pH above 8. In fact, the main differences between these models arise in the pH region 7-8 caused by the different abundances of the species ZnG_2^{4-} and $ZnG_2H_2^{2-}$

- In the case of titrations at constant pH (7.5 and 8), while the $c_{T,Zn}$ is variable, a buffer was used. EPPS was selected given the lack of complexation between the metal and the buffer as seen in DPP experiments. Under these experimental conditions, the most suitable complexation models have been Ferretti's and Krezel's, in this order.

- For the speciation study of Zn in root extracts of *Hordeum Vulgare*, Ferretti's and Krezel's models have been used to obtain the theoretical free zinc concentration. But it has been shown that the free zinc concentration determined by AGNES is lower than the predicted ones. This fact has been attributed to the need of contemplating the existence of other ligands, such as other phytochelatins, in the complexation model of the extract.

- The determination of free Zn concentration in wine has been done by DMT and cross-validated with AGNES. Firstly, a synthetic solution composed by 13.5% ethanol, $c_{T,Zn}$= 1.16×10^{-5} mol L^{-1} and $c_{T,KHTar}$= 0.011 mol L^{-1} and adjusted to pH 3.422 has been studied. The free zinc concentration determined by AGNES is consistent with the predicted one. No impact of complexes was seen in DMT, given that, according to the prediction, the crossing of positive or neutral species such as $HZnTar^+$ or ZnTar would

have increased the total zinc concentration measured in the acceptor solution by more than 30%. For these specific concentration conditions and assuming a common diffusion coefficient for both species, the initial flux of $ZnHTar^{+}$ through the membrane is predicted to be 432 times smaller than the one corresponding to Zn^{2+} (considering zero concentration at the acceptor/membrane interface).

- The required equilibration time in DMT experiments is longer when working in ethanolic medium. It could be related to a slower permeation process in the membrane.

- For determining the free metal concentration with DMT, it is necessary to determine the most appropriate reference cation. In the case of acceptor solutions with just K, its concentration decreases with time while Mg, Ca and Na concentrations (arriving from the donor solution) are increasing even after 200h. As in the acceptor solution initially there is just K, when the other arriving positive cations arrive, some K from the acceptor is transferred to the donor in order to keep the electroneutrality. Because of the evolution on the concentration, "just K" acceptors are not optimum.

- On the other hand, a "multimetal" acceptor solution containing K, Na, Mg and Ca has also been used. Here the free Na and K concentration remain stable during the whole experiment pointing out that free Na and K concentration in the donor solution is similar to the corresponding in the acceptor, suggesting that both elements could be used as reference cations. On the other hand, Mg and Ca concentrations in the acceptor decrease, so that they could not be used as reference ions. One explanation is that those divalent elements are more complexed in the donor solution than expected, consequently the initial free concentration in acceptor solution is higher than in donor. Therefore, what is expected in this case is some transfer of Ca and Mg from acceptor to donor, but due to the large volume of the donor solution its composition remains essentially unaltered.

- The final free zinc concentration determined by DMT using K and Na as reference ions (in multimetal acceptors), 1.76 μmol L^{-1} is in good agreement with the corresponding one determined by AGNES, 1.7 μmol L^{-}

[1]. To determine Fe concentration, it has been considered that the relevant oxidation form is its trivalent state given that both, the acceptor solution and the real wine are in contact with the atmosphere. Finally, Cu concentration could not be determined due to the lack of stabilization in the acceptor solution.